



TÜBINGER GEOWISSENSCHAFTLICHE ARBEITEN (TGA)

Reihe C:
Hydro-, Ingenieur- und Umweltgeologie

Schriftleitung:
P. Grathwohl, G. Teutsch

Daniela Zamfirescu

Release and Fate of Specific Organic Contaminants at a Former Gasworks Site

TGA, C53, 2000

Release and Fate of Specific Organic Contaminants at a Former Gasworks Site

Daniela Zamfirescu

*Lehrstuhl für Angewandte Geologie
Institut für Geologie und Paläontologie
Eberhard-Karls-Universität Tübingen
Sigwartstraße 10
72076 Tübingen
Germany*

Herausgeber:

Institut und Museum für Geologie und Paläontologie
der Universität Tübingen
Sigwartstraße 10, D-72076 Tübingen

Schriftleitung der Reihe C:

Lehrstuhl für Angewandte Geologie
Prof. Dr. Peter Grathwohl & Prof. Dr. Georg Teutsch

Redaktion:

Dr. Mike Herbert

ISSN 0935-4948

*"There are more things in heaven and earth, Horatio,
Than are dreamt of in your philosophy."*

William Shakespeare

"I hate quotations. Tell me what you know. "

Ralph Waldo Emerson

Release and Fate of Specific Organic Contaminants at a Former Gasworks Site

Daniela Zamfirescu*

Abstract: In the 19th and 20th century, thousands of coal gasification plants were operating all over the world. Pipeline distribution of natural gas following World War II replaced manufactured gas as a major fuel; as a result manufactured gas production came to an end and determined widespread shutdown of gas plants. Soil and groundwater contamination by coal tars, very complex organic mixtures resulted as a byproduct of the dry distillation of coal, potentially exists at all former gasworks sites because of prior process operations and residual management practices. This lasted now up to more than one century and the contaminant release persists as the sources are still present. The complexity of groundwater contamination at former gasworks arises from the complex original composition of tars, but also from the biotic transformations undergone by organic compounds in the subsurface environment. This work focuses on 'Testfeld Süd', a former gas manufacturing plant located in the Neckar Valley in S-W Germany, which has been operating between 1870 and 1970. The main objective was the qualitative and quantitative assessment of groundwater contamination by site-specific organic chemicals. This included both investigations of the NAPL source(s) and of the plume(s) of dissolved contaminants. First the composition of coal tars from different locations in the field was determined. The three main compound classes assessed were monocyclic aromatic hydrocarbons (MAHs), polycyclic aromatic hydrocarbons (PAHs) and heterocyclic aromatic compounds. Some of them are known to be of serious toxicologic concern, but for the majority, possible health effects have not yet been assessed. Two main types of NAPLs have been spilled in the subsurface at the site: coal tars/tar oils in the area of the former tar distilleries and lighter distillation fractions in the area of the former benzene distilleries located further downstream. The initial composition of NAPLs was variable, but also contamination events occurred over almost one century at different points in time. The composition of the sources has changed during decades, mainly due to faster release of easy soluble compounds into the groundwater and enrichment of the less soluble ones in the organic mixtures. Compounds recalcitrant to biodegradation, such as acenaphthene, which persist in high concentrations in the aqueous phase, were found to be also enriched in aged NAPLs, probably by partitioning from the groundwater into the leached organic phase. Dissolution out of residual NAPL phase and desorption out of contaminated aquifer material or low permeability zones were identified as the most important release mechanisms of coal tar constituents into the groundwater. The maximum concentrations for dissolution out of residual phase monitored in column experiments in the laboratory were equal to the saturation concentrations and depend on the composition of the mixture. In most cases, dissolution out of residual phase takes place only within a short domain relative to the entire volume containing residual NAPL, explaining the extremely long periods of time needed for complete dissolution. Mass transfer zones longer than the contaminated domain are more advantageous for remediation purposes, as they allow higher mass fluxes for dissolution. Even if saturation is reached, measured concentrations depend on the observation scale. In small, homogeneous columns in the laboratory or locally in the field - e.g. individual sampling ports in multilevel wells - the measured concentration equals saturation. Average concentrations in multilevel wells were indeed in very good accordance with saturation concentrations for the organic mixture from the same location. In larger columns or in conventional, depth averaged groundwater samples, the observed concentration would be lower due to dilution effects, although saturation is locally attained. For desorption, the maximum concentrations in column expe-

* Dissertation an der Geowissenschaftlichen Fakultät der Universität Tübingen
Anschrift des Verfassers: Daniela Zamfirescu, Haselweg 28, 72076 Tübingen

riments were much lower than for dissolution out of residual phase. For a given contaminated volume, diffusion limited desorption plays a secondary role, as long as residual NAPL is present. However, release rates measured in column experiments cannot be extrapolated to field conditions without knowledge of the contamination history and the exact volume and geometry of the source. Field investigations (concentrations in multilevel wells, pumping tests) showed that, at least close to the source area, there are several different plumes. Sharp vertical concentration profiles may attenuate with increasing distance from the source. A further objective of this work was to characterise the behaviour of the most relevant compound classes in the contaminant plume, with special emphasis on substances recalcitrant to biodegradation. Over the entire distance assessed (ca 130 m from the source area), the plume is entirely anaerobic. Due to poor biodegradation, as the distance from the source area increases, there is an enrichment of O- and N-heterocyclic compounds in the plume relative to usually assessed tar constituents (PAHs and MAHs). Most of the investigated compounds undergo a first order decay process (linear decrease of concentration with distance in a semi-logarithmic plot). The half-life distance varied between 30 m for benzene and up to 200 m for alkyl-naphthalenes. With an estimated decay rate of only 0.1 % per day, dimethyl-benzofurans were the most recalcitrant of all compounds that could be identified with the available analytical method. Acenaphthene is degraded only within about 50 m downstream from the source area, then its concentration remains almost constant and very high (ca 180 µg/l) over a long distance. This behaviour of acenaphthene has been observed at numerous other former gasworks sites. It supports earlier findings that the biodegradation of acenaphthene under anaerobic conditions takes place only by cometabolism, e.g. with naphthalene, and comes to a standstill if the concentration of the easily biodegradable naphthalene drops under a certain threshold. It is not known how far the plume extends downstream at 'Testfeld Süd'.

Freisetzung und Verhalten spezifischer organischer Schadstoffe an einem ehemaligen Gaswerkstandort

Kurzfassung. An ehemaligen Gaswerkstandorten entstand über Jahrzehnte eine massive Verunreinigung vor allem durch Teer und Teerdestillate, sehr komplexe organische Gemische, die bis heute noch in erheblichen Mengen in den Untergrund vorliegen. Die Komplexität der Grundwasserkontamination beruht sowohl auf die toxischen, zum Teil kanzerogenen und mutagenen ursprünglichen Teerbestandteilen, als auch auf die komplizierten Umwandlungen dieser Stoffe infolge biologischer Abbauprozessen im Grundwasser. Ziel der vorliegenden Arbeit war die Identifizierung und Quantifizierung standortrelevanter organischer Schadstoffe im Grundwasser des 'Testfeld Süd', ein ehemaliger Gaswerkstandort im Neckartal. Im Schadensherd am 'Testfeld Süd' liegt eine in ihrer Zusammensetzung sehr komplexe, heterogen verteilte residuale Teerphase vor. Es handelt sich um Gemische organischer Stoffe, hauptsächlich monozyklische aromatische Kohlenwasserstoffe (MAK), polyzyklische aromatische Kohlenwasserstoffe (PAK) und hetrozyklische aromatische Verbindungen. Viele dieser Verbindungen (vor allem die Heterozyklen) sind in Routineanalysen an ähnlichen Standorten noch nicht untersucht worden. Aufgrund ihrer hohen Konzentrationen und Toxizität, sowie ihrer oft geringen Bioabbaubarkeit, stellen sie ein erhebliches Gefährdungspotential für das Grundwasser im Abstrom dar. Im Gelände wurden Teerphasenkörper identifiziert, die unterschiedliche Alterungsgrade aufweisen. Dieses ist sowohl durch technologisch bedingte unterschiedliche Zusammensetzung, aber auch durch zeitlich versetzte Versickerung, also unterschiedliche Verweilzeiten im Untergrund zurückzuführen. Nicht oder sehr schwer abbaubare Stoffe, wie zum Beispiel Acenaphthen, die im Grundwasser in konstant hohen Konzentrationen vorliegen, sind zum Teil auch in gealterten Teerphasen angereichert. Langzeit-Säulenversuche zur Bestimmung der lösungs- und desorptionsbedingten Emission aus kontaminiertem Aquifermaterial zeigten, daß die Lösung aus residualer Phase für die sich im Grundwasser einstellenden Konzentrationen maßgeblich ist. Die Desorption von Teerinhaltstoffen aus kontaminiertem Aquifermaterial bzw. der Eintrag aus Zonen geringer Durchlässigkeit werden von der Lösung aus residualer Teerphase vollständig überlagert. Die im Schadensherd im Multilevelmeßstellen ermittelten lokalen Konzentrationsmaxima stimmen mit den im Säuleneluat bei homogener Schadstoffverteilung bestimmten Sättigungskonzentrationen überein. Eine Übertragung der im Labor gemessenen Freisetzungsraten auf Feldmaßstab zur Grundwasser-Gefährdungsabschätzung ist nur möglich, wenn die Lage und Größe des kontaminierten Bereichs, die Kontaktoberfläche Teer/Wasser und die Grundwassergeschwindigkeit bekannt sind. Felduntersuchungen (tiefenhorizontierte Konzentrationsprofile, Immissionspumpversuche) deuten darauf hin, daß nahe am Schadensherd mehrere Schadstofffahnen vorhanden sind. Im Abstrom vom Schadensherd wurde das Verhalten einzelner Schadstoffklassen in der 'Hauptfahne' untersucht. Die Schadstofffahne am 'Testfeld Süd' ist im gesamten untersuchten Bereich (ca 130 m vom Schadensherd in Grundwasserfließrichtung) anaerob. Es wurde eine Anreicherung von O- und N-Heterozyklen im Vergleich zu routinemäßig quantifizierten Teerinhaltstoffen (PAK und BTEX) festgestellt, was auf ihre geringe Bioabbaubarkeit zurückzuführen ist. Der Bioabbau der meisten Verbindungen in der Fahne verläuft als Reaktion erster Ordnung. Die Halbwärtsstrecke lag zwischen ca 30 m für Benzol und 200 m für Alkyl-Naphthaline. Die Konzentrationen der Alkyl-Benzofurane blieben praktisch unverändert mit zunehmender Entfernung vom Schadensherd. Die Acenaphthen-Konzentration nimmt nur innerhalb der ersten 50 m vom Schadensherd geringfügig ab und bleibt dann im übrigen, bisher erfassten Verlauf der Fahne, konstant hoch (ca 180 µg/l). Dadurch werden neueste Untersuchungen zum Bioabbau vom Acenaphthen aus Kreosot bestätigt die belegen, daß dieses nur durch Kometabolismus in Gegenwart von Naphthalin oder Phenanthren abgebaut werden kann; selbst dann sind die Abbauraten nur gering. Damit könnte die auch an anderen Gaswerkstandorten festgestellte Persistenz von Acenaphthen im Grundwasser erklärt werden. Weil Naphthalin von allen PAK aufgrund der hohen Wasserlöslichkeit sehr schnell im Teer angereichert und biologisch abgebaut wird, kommt wahrscheinlich auch der Acenaphthenabbau rasch zum Erliegen. Die tatsächliche Länge der Schadstofffahne am 'Testfeld Süd' ist bisher noch nicht bekannt.

Acknowledgements

Financial support for this work was provided by the *German Research Foundation*, Priority Program 546: 'Geochemical Processes with Long Term Impact on Anthropogenically Affected Seepage- and Groundwater'.

My very special thanks go to my advisor, Prof. Dr. Peter Grathwohl, for his expertise, for his advice and suggestions, and for always being there for numerous discussions, which helped me keep straight time and time again. I also thank so much to Prof. Dr. Georg Teutsch, for his trust to start me off on this project and for his continuous support, which I very much appreciate.

I am grateful to all those who have initiated me into the 'spirit of Tübingen' and kindly supported me in many ways throughout the years, particularly Hansjörg Weiß, Annegret Walz, Sybille Kleineidam, Peter Merkel, Rainer Klein, Tom Schiedek, Elvira Lemp, Gerald Peschik, Thomas Wendel, Hermann Rügner, Christoph Schüth, Sigggi Kraft, Uli Maier, Jörg Danzer, Christina Eberhardt, Diana Loyek.

I would also like to thank to Anne Hartmann-Renz, Renate Seelig, Bernice Nisch and Renate Riehle for their technical assistance in the laboratory, as well as to Martin Herfort, Ingo Schettler, Jost Ries, Detlef Bösel, Thomas Holder, Wolfgang Kürner for the exchange of information and all the work at 'Testfeld Süd'.

Thanks to Gudrun and Volker and to all friends not named here, for their personal or professional involvement along the way!

And last but not least, a special thank to my parents, to Michi and Ilinca, to Puita and Romulus and to all those at home I cannot mention here by name, for their support and loving encouragement 'from a distance'!

Contents

Abbreviations

Notation

1. The Problem	1
1.1 Tar Contamination at Former Manufacturing Gas Plants	1
1.2 Research Objectives	2
2. The Field Site ‘Testfeld Süd’	3
3. Coal Tar Constituents	5
3.1 Chemical Composition of Coal Tar	5
3.2 Physical and Chemical Properties of Important Contaminants at Gasworks Sites	5
3.3 Toxicology of Coal Tar Constituents	8
3.4 Natural Attenuation of Coal Tar Constituents	14
4. Analysis of Coal Tar Constituents from Water Samples	16
4.1 Sample Handling	16
4.2. Instrumental Setup	17
4.3 Calibration without Reference Substances	18
5. Dissolution out of Residual NAPL Phase	20
5.1 Theory	20
5.1.1 Dissolution out of Complex Organic Mixtures at Equilibrium	20
5.1.2 Mass Transfer through Liquid Boundary Layers: Dissolution Kinetics from NAPLs	21
5.1.3 Mass Transfer Coefficients	22
5.1.4 Length of the Mass Transfer Zone (Saturation Length)	23
5.1.5 Retardation of the Dissolution Front	24
5.1.6 Possible Concentration-Time Profiles for Dissolution out of Residual NAPL Blobs	25
5.2 Materials and Methods	26
5.2.1 Coal Tar Samples from ‘Testfeld Süd’	26
5.2.2 Experimental Setup for Dissolution out of Residual NAPLs	26
5.2.3 Samples Used in Column Experiments for Dissolution	28
5.2.4 Analysis of PAHs from Contaminated Aquifer Material	28
5.3 Results and Discussion	28
5.3.1 Source Composition at the Site	28
5.3.2 Simulation of Equilibrium Dissolution out of Residual NAPL Phase from ‘Testfeld Süd’	33
5.3.3 Column Experiments with Disturbed Samples	36
5.3.4 Column Experiments with Undisturbed Samples	47
5.3.5 Conclusions	49
6. Diffusion Limited Desorption	51
6.1 Theory	51
6.1.1 Desorption out of Spherical Grains and Aggregates	51
6.1.2 Desorption out of Layers of Low Permeability	52
6.2 Materials and Methods	52
6.2.1 Experimental Setup	52
6.2.2 Samples Used in Column Experiments for Desorption	53
6.2.3 Analysis of PAHs from Contaminated Aquifer Material	53

6.3 Results and Discussion	54
6.3.1 Desorption out of Spherical Grains and Aggregates	54
6.3.1.1 Column Experiments with Undisturbed Samples	54
6.3.1.2 Column Experiments with Disturbed Samples	58
6.3.1.3 Conclusions	61
6.3.2 Desorption out of Layers of Low Permeability	63
6.3.2.1 Experimental Results	63
6.3.2.2 Conclusions	63
7. The Plume at ‘Testfeld Süd’	65
7.1 PAH and MAH	65
7.1.1 Multilevel Wells	65
7.1.2 The Plume Downgradient: B28-B42-NT01	67
7.2 Substituted PAH and Heteroaromatic Compounds in B28-B42-NT01	67
7.2.1 Point Measurements	67
7.2.2 Plumes Differentiation and Estimation of Mass Fluxes Using Pumping Tests	69
7.3 Relative Distribution of Various Compound Classes in the Plume	72
8. Quantitative Evaluation of Intrinsic Bioremediation at ‘Testfeld Süd’	75
8.1 Theory	75
8.2 Materials and Methods	76
8.3 Results and Discussion	76
8.3.1 Decay Rates in the Plume	76
8.3.2 Extrapolation of Concentrations Towards the Source Area	79
8.4 Conclusions	81
9. Summary	82
References	85
Appendices	91

Abbreviations

<i>Ace</i>	- Acenaphthene
<i>Ace-d10</i>	- Decadeutero-Acenaphthene
<i>Ant</i>	- Anthracene
<i>Any</i>	- Acenaphthylene
<i>BaA</i>	- Benzo(a)anthracene
<i>BaP</i>	- Benzo(a)pyrene
<i>BbF-BkF</i>	- Benzo(b)fluoranthene, Benzo(k)fluoranthene
BCF	- bioconcentration factor
<i>Benz</i>	- Benzene
<i>Bf</i>	- Benzofuran
<i>BghiP</i>	- Benzo(g,h,i)perylene
<i>Bph</i>	- Biphenyl
BTEX	- generic for <u>B</u> enzene, <u>T</u> oluene, <u>E</u> thylbenzene and <u>X</u> ylenes
<i>Bth</i>	- Benzothiophene
<i>Carb</i>	- Carbazole
<i>Chr</i>	- Chrysene
<i>Chr-d12</i>	- Dodecadeutero-Chrysene
<i>DahA</i>	- Dibenzo(a,h)anthracene
<i>Dbf</i>	- Dibenzofuran
<i>1,2-Dichlorobenzene-d4</i>	- Tetradeutero-1,2-Dichlorobenzene
<i>DimetBph</i>	- Dimethylbiphenyl
<i>DimetNap, DimethylNap</i>	- Dimethylnaphthalene
<i>DimetPhe</i>	- Dimethylphenanthrene
DNAPL	- <u>D</u> ense <u>N</u> on- <u>A</u> queous <u>P</u> hase <u>L</u> iquids
EC ₅₀	- effect concentration fifty
EPA	- Environmental Protection Agency
<i>EtBenz</i>	- Ethylbenzene
<i>EtNap</i>	- Ethylnaphthalene
<i>Fln</i>	- Fluorene
<i>Fth</i>	- Fluoranthene
<i>Ina</i>	- Indane
<i>Indeno</i>	- Indeno(1,2,3-cd)pyrene
<i>Ine</i>	- Indene
<i>IsoPb</i>	- Isopropylbenzene
LC ₅₀	- lethal concentration fifty
LD ₅₀	- lethal dose fifty
LfU	- Landesanstalt für Umweltschutz
LNAPL	- <u>L</u> ight <u>N</u> on- <u>A</u> queous <u>P</u> hase <u>L</u> iquids
MAH, MAHs	- <u>M</u> onocyclic <u>A</u> romatic <u>H</u> ydrocarbon(s)
<i>MetAnt</i>	- Methylanthracene
<i>MetBf</i>	- Methylbenzofuran
<i>MetBth</i>	- Methylbenzothiophene
<i>MetDbf</i>	- Methyl dibenzofuran
<i>MethylIne</i>	- Methylindene
<i>MetFln</i>	- Methylfluorene
<i>1-MetNap</i>	- 1-Methylnaphthalene
<i>2-MetNap</i>	- 2-Methylnaphthalene
<i>Nap</i>	- Naphthalene
<i>Nap-d8</i>	- Octadeutero-Naphthalene
NAPL, NAPLs	- <u>N</u> on- <u>A</u> queous <u>P</u> hase <u>L</u> iquid(s)
PAH, PAHs	- <u>P</u> olycyclic <u>A</u> romatic <u>H</u> ydrocarbon(s)
<i>Pb</i>	- Propylbenzene
<i>Pery</i>	- Perylene

<i>Pery-d12</i>	- Dodecadeutero-Perylene
<i>Phe</i>	- Phenanthrene
<i>Phe-d10</i>	- Decadeutero-Phenanthrene
<i>Pyridine-d5</i>	- Pentadeutero-Pyridine
<i>Py</i>	- Pyrene
<i>1,2,3-Tmb</i>	- 1,2,3-Trimethylbenzene
<i>1,2,4-Tmb</i>	- 1,2,3-Trimethylbenzene
<i>1,3,5-Tmb</i>	- 1,3,5-Trimethylbenzene
<i>Tol</i>	- Toluene
<i>TrimetBph</i>	- Trimethylbiphenyl
<i>TrimetNap, TrimethylNap</i>	- Trimethylnaphthalene
<i>TrimetThiophene</i>	- Trimethylthiophene
VOC	- <u>V</u> olatile <u>O</u> rganic <u>C</u> ompounds
<i>o-Xyl</i>	- ortho-Xylene
<i>p-Xyl</i>	- para-Xylene

Notation

Dimensions: L = length, M = mass, T = time.

A	- total (absolute) area of the residual blobs [L^2]
A_0	- specific interfacial area NAPL-water (i.e. the surface area NAPL/water per unit volume of porous medium) [$L^2 L^{-3}$]
c	- concentration of a solute in the mobile (aqueous) phase [$M L^{-3}$]
c_0	- aqueous concentration at the source [$M L^{-3}$]
c_{eq}	- equilibrium solute concentration in aqueous phase [$M L^{-3}$]
$c_{sat,i}$	- saturation concentration of a compound i for dissolution out of a mixture [$M L^{-3}$]
$c_{sat,i}^{t-1}$	- saturation concentration of component i at time step $(t-1)$ [$M L^{-3}$]
$c(x)$	- concentration as a function of distance [$M L^{-3}$]
d	- characteristic length (mean grain diameter) [L]
d_s	- density of the dry solids [$M L^{-3}$]
D_a	- apparent diffusion coefficient ($D_a = D_e / \alpha$) [$L^2 T^{-1}$]
D_{aq}	- aqueous diffusion coefficient of the component i [$L^2 T^{-1}$]
f_i	- mass fraction of the component i in the NAPL (mass i per mass NAPL) [-]
F_{max}	- the maximum contaminant flux due to desorption [$M M^{-1} T^{-1}$]
f_{oc}	- fraction of natural organic carbon [-]
g	- total concentration of the n components in the mixture [wt %]
g_i	- concentration of the component i in the tar [wt %]
k	- first order overall attenuation rate [T^{-1}]
k_{diss}	- mass transfer coefficient for dissolution [$L T^{-1}$]
K_d	- distribution coefficient between solids and water at equilibrium [$L^3 M^{-1}$]
K_{ow}	- octanol/water partition coefficient [-]
m	- number of water soluble components in the organic mixture [-]
m_i	- mass of the component i in the organic phase [M]
$m_{i,(el+ex)}$	- total mass of the component i (leached plus extracted) [M]
m_{sample}	- the dry mass of the aquifer material [M]
m_{tar}	- total mass of the organic phase [M]
m_{tar}^t	- total mass of the organic phase at time step t [M]
mm_i^t	- mass of solute in the organic phase at time step t [M]
mw_i^t	- mass of solute in the aqueous phase at time step t [M]
M_{eq}	- total mass of a substance sorbed in a sample at equilibrium [$M M^{-1}$]
M_i	- molar weight of the component i [$M mole^{-1}$]
\overline{M}_{tar}	- the average molar weight of the NAPL [$M L^{-3}$]
n	- even number of equal time intervals for numerical integration (Simpson) [-]
n_i	- the number of moles of component i in a mixture [-]
n_i^t	- number of moles of component i in the organic phase at time step t [-]
n_{tar}^t	- number of moles of tar at time step t [-]
r	- radial distance [L]
r_b	- average blob radius [L]
Re	- Reynolds number [-]
R_i	- retardation factor of the dissolution front for component i [-]
S^0	- NAPL residual saturation (NAPL volume per volume of the porous medium) [-]
Sc	- Schmidt number [-]
Sh	- Sherwood number [-]
Sh'	- modified Sherwood number [-]
$S_{w,i}$	- water solubility of the pure compound i [$M L^{-3}$]

$S_{w,i}^{scl}$	- aqueous solubility of the subcooled liquid i [$M L^{-3}$]
t	- time [T]
t_e	- contact (equilibration) time [T]
T	- actual temperature of the system [$^{\circ}C$]
T_m	- melting temperature of the pure crystalline substance [$^{\circ}C$]
v_a	- linear water flow velocity [$L T^{-1}$]
v_x	- the linear groundwater velocity (in longitudinal direction) [$L T^{-1}$]
V_w^t	- water volume exchanged during one time step [L^3]
x	- depth, distance in the flow direction [L]
$x_{0,5}$	- half life distance (distance travelled during the half-life time) [L]
X_s	- length of the mass transfer zone [L]

Greek Symbols

α	- capacity factor of the porous medium ($\alpha = \varepsilon + K_d \rho$) [-]
α_{ion}	- ionisation degree [-]
α_x	- longitudinal dispersivity [L]
χ_i	- mole fraction of the component i in a mixture [-]
χ_i^t	- mole fraction of the component i in a mixture at time step t [-]
δ	- thickness of the stagnant water film [L]
ε	- intraparticle porosity [-]
γ_i	- activity coefficient of the component i in an organic mixture [-]
η_w	- dynamic viscosity [$M L^{-1} T^{-1}$]
λ	- first order decay rate [T^{-1}]
ν_w	- cinematic viscosity of water [$L^2 T^{-1}$]
θ	- NAPL-filled porosity [$L^3 L^{-3}$]
ρ	- bulk density ($\rho = (1-\varepsilon) \rho_s$) [$M L^{-3}$]
ρ_{tar}	- density of the NAPL (tar) [$M L^{-3}$]
ρ_w	- water density [$M L^{-3}$]

1. The Problem

1.1 Tar Contamination at Former Manufactured Gas Plants

Prior to the widespread use of natural gas, combustible gas manufactured from coke, coal and oil served in Europe and North America as the major gaseous fuel for urban heating, lighting and cooking for at least one century (LUTHY et al., 1994). The procedure for production of gas from coal was already developed at the end of the 17th century. The first company selling gas was founded in the United Kingdom in 1802 (first gas lighting in Redruth, Cornwall 1792, first commercial gas lighting in Birmingham 1805). In 1830 Britain had 200 town gas plants. In Denmark the first manufactured gas plant was established 1853 (DYREBORG, 1996). In Germany, coal-tar organic chemical industry emerged in 1860-1870 and 1880-1890 coal tar was recognized as a recoverable by-product. In the first decade of the 20th century, coal-tar benzene served as 'motor spirit' automobile and aviation fuel (HATHEWAY, 1997).

In the 19th and 20th century, coal gasification plants were operating all over the world - an estimate of over 1,000 in Germany (more than 100 in Baden-Württemberg) (PYKA, 1994), 125 sites in Denmark, 3,000 in the U.K., and 56 sites in Ontario, Canada (LUTHY et al., 1994; DYREBORG, 1996; JOHANSEN, 1996). In the United States alone there are from 21,300 to 32,600 coal tar contaminated sites. Out of these only about 1,500 reported to US EPA (*Brown's Directory of North American Gas Plants, from 1887*), the rest are former plants at rail yards producing compressed illuminating gas for use in rail cars (100-200), gas plants at military posts, yards and stations, arsenals and munitions plants (150-250), institutional gas machines (5,000-10,000), gas fuel supply units for industrial plants (11,000-15,000), coke works producing coke without recovery of by-products (2,000-4,300), and tar distilleries (200-400).

In the 1920s petrol cracking put pressure on coal-tar industry. Pipeline distribution of natural gas following World War II replaced manufactured gas as a major fuel and as a result manufactured gas production came to an end

between 1950-1960 in the US, in the 1970s in Germany. North Sea natural gas discoveries between 1970-1980 dampened manufactured gas production in Britain and determined widespread shutdown of gas plants (HATHEWAY, 1997).

Today, most of the equipment at former gasworks sites has been removed, except for subsurface structures such as pipelines, tanks and pits. Soil and groundwater contamination potentially exists at all former gasworks sites because of prior process operations and residual management practices.

Residuals produced from the volatile component of bituminous coal consist of ammonia liquors, ash and clinker, tar, a variety of complex organic fractions resulting during the distillation process of coal tar, coke. Some tar was used on site or sold, but was often disposed on site in tar wells, sewers or pits (LUTHY, 1994; PYKA 1994; MERKEL, 1996; NELSON et al.; 1996, LOYEK, 1998). This led to a severe contamination of the subsurface environment which lasted now up to more than a century and the contaminant release persists as the sources are still present.

Even though during the last decades major efforts have been made in order to understand and describe the transport processes and fate of coal tar constituents in groundwater, these mainly focused on a relatively small number of compounds. The effectiveness of conventional remediation techniques is very low as applied to former gasworks sites and the costs are very high.

Since the mid nineties the concept of 'natural attenuation' defined as 'the biodegradation, dispersion, dilution, sorption, volatilisation, and/or chemical or biochemical stabilisation of contaminants to effectively reduce their toxicity, mobility or volume to levels that are protective of human health and the ecosystem' (NYER and DUFFIN; 1997; OTTEN et al., 1998) gained growing attention as alternative intrinsic cleanup process at contaminated sites. However, the requirement that the contaminated groundwater should have travelled a certain distance down-gradient for allowing natural attenuation to deplete concentrations down to acceptable limits might not be fulfilled when potential receptors are

located close to the contaminant source. This is often the case at former manufactured gas plants, which are always located in urban areas (SCHIEDEK et al., 1998). Another limitation which should always be taken into account is that in most cases there is very sparse knowledge about the nature and toxicity of metabolites resulted during transformation of coal tar constituents initiated by microorganisms. There is evidence that there is only a slight decrease in the toxicity of coal-tar contaminated groundwater despite biodegradation that reduced most of the known organic contaminants (MÜLLER et al., 1991). Because biodegradation may lead to more toxic, more mobile or recalcitrant products (KROPP et al., 1994; GRIFOLL et al., 1994; SELIFONOV et al., 1998; U.S EPA, 1999), alone the fact that the primary tar constituents can no more be detected is hence not necessarily an indication of remediation.

1.2 Research Objectives

The main objective of this work was an evaluation of the nature and extent of groundwater contamination by specific organic compounds at a former manufacturing gas plant ('Testfeld Süd') in South Germany.

Special research focus was on:

1. Identification of the most important contaminants in the groundwater at the site.
2. Characterisation of the residual phase causing the subsurface contamination. An exact localisation and complete characterisation of the contamination sources is not possible. On the other hand, the composition and geometry (localisation, spatial distribution) of the sources has to be known in order to quantify the concentrations as well as the fluxes of the contaminants in the groundwater at the site.

For these reasons, the composition of coal tars from different locations in the field was determined. The information gained should clarify whether or not there are major differences between source composition at different locations in the field and if the spatial distribution of sources relative to each other could influence the

concentrations expected in the groundwater (saturation concentrations).

3. Identification of the main release mechanisms of site specific organic chemicals out of residual NAPL phase and contaminated aquifer material using column experiments; determination of contaminant release rates and their relative importance for groundwater contamination (e.g. dissolution vs. desorption); comparison of the results of column experiments using disturbed and undisturbed samples with the contaminant distribution in the groundwater at the source.

4. Characterisation of the plume with respect to the fate of the most relevant compound classes, mainly monocyclic aromatic hydrocarbons (MAH), polycyclic aromatic hydrocarbons (PAH) and heterocyclic aromatic compounds, with special emphasis on substances recalcitrant to biodegradation.

Since the early eighties the site was subject of investigations mainly done by the 'Geologisches Landesamt Baden - Württemberg' and some consulting companies, all using a traditional approach for determination of hydraulic parameters and some standard chemical analyses generally used to evaluate the degree of groundwater contamination.

2. The Field Site 'Testfeld Süd'

The former gasworks site investigated is located in the Neckar Valley in S-W Germany. The contaminated quaternary aquifer is highly heterogeneous and consists of typical fluvial deposits with medium grained gravel intersected by sandy and silty lenses. The 3 to 4 m deep aquifer is covered by 1 to 4 m thick alluvial loam (clay and silt) topped by some 2 to 4 m thick anthropogenic fill (e.g. demolition debris). Clays of the Middle Keuper underlain by Muschelkalk are forming the almost impermeable substratum (REICHERT et al., 1998).

In some areas there is some influx of mineral water from the deeper confined groundwater system into the alluvial aquifer. The former gasworks site is located about 1 km upstream from the medicinal and mineral water springs in Stuttgart-Bad Cannstatt and Stuttgart-Berg. The water influx from the western Keuper hills into the aquifer is not significant. The entire contaminated area is artificially sealed (roads, buildings, etc.), so that there is practically no significant recharge from the surface.

Transmissivity ranges between 4.7×10^{-5} and $1.2 \times 10^{-2} \text{ m}^2/\text{s}$ and the average porosity is 0.15. The prevailing groundwater flow direction is parallel to the Neckar, from South to North/North-West with a mean flow velocity of about 2.4 m/d (GEOLOGISCHES LANDESAMT BADEN-WÜRTTEMBERG, 1989, 1992; JUNGBAUER UND PARTNER, 1993; BÖSEL, 1998; HERFORT, 1999).

The former gas works (Fig. 2.1) operated between 1870 and 1970. 1875 the gas production was 15.5 million m^3 per year and was constantly increased, e.g. to 148 million m^3 per year in 1952 (JUNGBAUER UND PARTNER, 1993). Gas manufacturing as well as processing of the by-products by distillation were performed for 50 to 100 years in various facilities, many interconnected by underground pipelines, and spread on site over a total area of about 20,000 m^2 . Tar was also disposed on site in pits. During World War II the site was bombed repeatedly, culminating 1944 with burning and practically total destruction.

The variety of organic mixtures separated by distillation is the primary factor determining the complex contamination of the underground. Given the initial location of individual facilities on site, it appears that the main contamination with high molecular, tar-like organic mixtures is concentrated around the tar pits and former tar distillation facilities in the southern area of the site. Further downstream there are probably some additional sources of lighter hydrocarbons, in the area of the benzene distilleries. But even in this area, some DNAPL was found at the bottom of the aquifer (in B55 and B56), possibly supporting the supposition that due to extensive war damage, these NAPL sources were virtually spread over the entire area. This makes it practically impossible to map out exactly the contamination sources at 'Testfeld Süd'.

Today, the structures at the surface formerly associated with gas manufacturing have been removed. This is probably not the case for all underground facilities such as e.g. pipelines. The site is owned by the towns department of works and it serves primarily for the distribution of natural gas, which is stored on site in liquid form at very low temperatures in a huge underground tank (Fig.2.1). The natural gas tank which is about 10 m deep and has 100 m in diameter is constituting a seriously perturbation for the groundwater flow.

The site has been subject of extensive groundwater monitoring, mainly performed by the Geological Survey of the Land Baden-Württemberg. On site there are a great number of conventional groundwater wells; most of them are however located in the source area. In many of these wells, there is some separate NAPL phase, and the concentrations of compounds dissolved in the groundwater are equal to the saturation concentrations for dissolution out of organic mixtures. Only a limited number of groundwater wells are located downstream in the plume area.

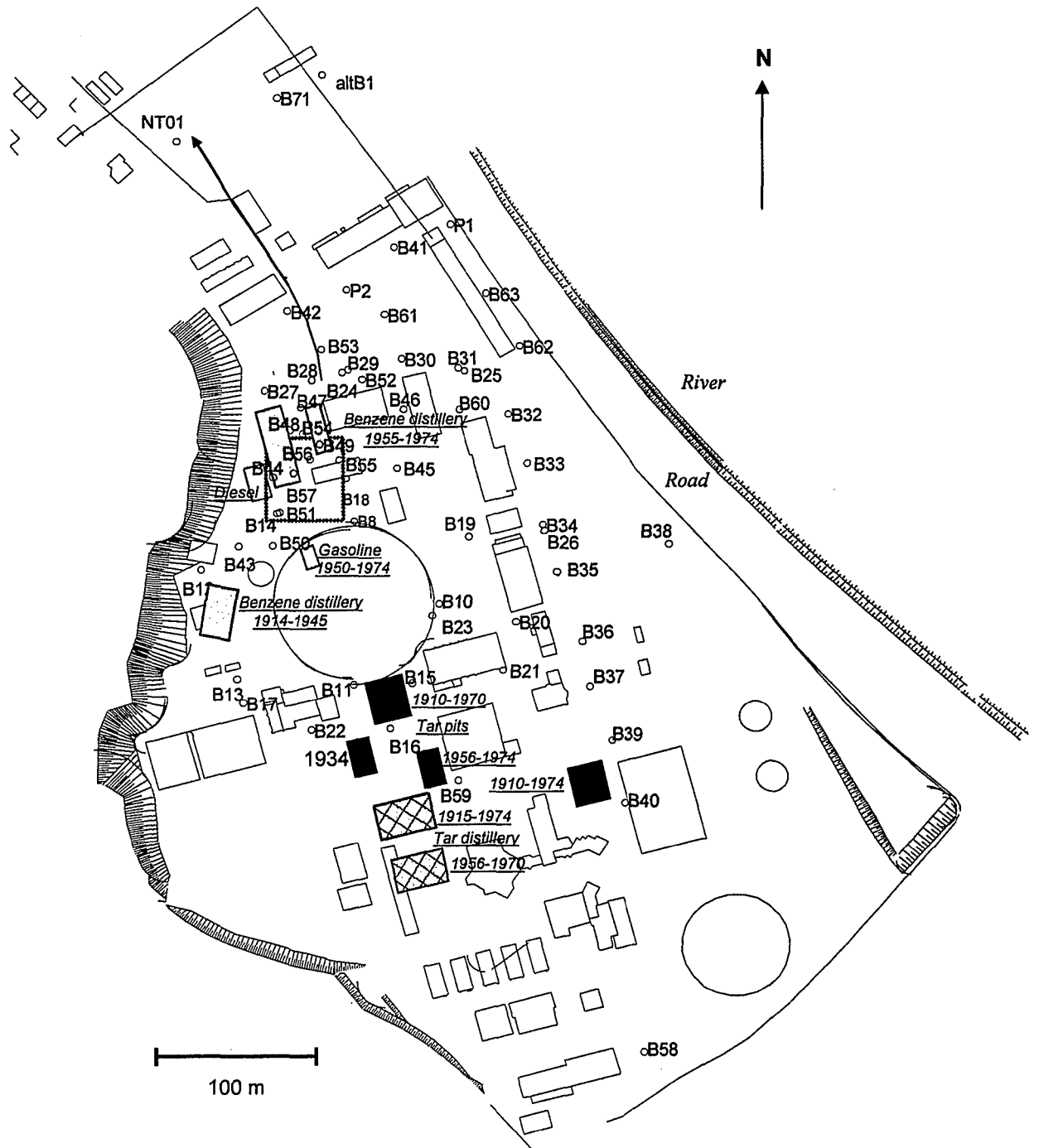


Fig. 2.1: The former gas works site 'Testfeld Süd': location of the main known sources of contamination (filled rectangles) and the available groundwater monitoring wells. The dotted rectangle marks the area of the groundwater wells equipped with multilevel packers; the arrow shows the prevailing groundwater flow direction in the plume area as determined in tracer tests. Both the tar distillation and disposal facilities (located in the upstream area) and the former benzene distilleries (downstream from the fluid gas storage tank - marked by the circle - situated in the northern area of the tar processing facilities) are major sources for the groundwater contamination by residual NAPLs with different composition. The exact amount and spatial distribution of NAPLs in the underground is not known (the filled rectangles are indicating only the approximate location of individual facilities on site). It is assumed that the source area extends from the former tar pits in the south to the benzene distilleries in the north (area with multilevel wells). The gas tank itself (ca 100 m diameter, 10 m deep) does not contaminate the groundwater, but is seriously complicating the groundwater flow conditions. This study focuses on the emission out of various sources into the groundwater and on the distribution and fate of specific contaminants in the resulting plume. Some compounds in the plume reach the well NT01, but it is not known how far the plume extends further downstream. According to tracer tests, the wells B28, B42 and NT01 nearly follow the centre line of the main plume.

3. Coal Tar Constituents

3.1 Chemical Composition of Coal Tar

The Anglo-American literature dealing with the environmental hazard of former manufactured gas plants does not always distinguish between 'coal tar' and 'creosote'. In most cases the latter even replaces the former or is sometimes considered to be a distillation product of it. Sometimes it is distinguished between 'creosote' and 'coal tar creosote' (e.g. FOWLER et al., 1993).

According to NENITESCU (1966), creosote is obtained out of by-products of the dry distillation of wood (mainly beech) by extraction with sodium hydroxide, followed by acid precipitation and distillation. Creosote is a high boiling (200-220 °C) phenolic oil. As the name says, creosote consists mainly of a mixture of higher phenols, such as *creosole* (methylphenol) and phenolic ethers, such as *creosole* (the methyl ether of 1,2-dihydroxy-5-methylbenzene). It is 'creosote' that was used for wood preservation.

Coal tar results as a by-product (3-4 wt %) of the dry distillation of coal at 900-1000 °C (maybe the confusion between coal tar and creosote arises from the fact that both are by-products of some similar distillation process). The composition of coal tar can vary with the origin of the coal and the gasifier design and operating conditions. The constituents of high-temperature-coal-tar (mainly aromatic hydrocarbons, most of them polycyclic) are then separated by sequential distillation. The first distillation step yields the so called tar oils - light oil (80-170 °C, 1.4-5.8 %), medium oil (170-240 °C, 3.5-12 %), heavy oil (240-270 °C, 10-12 %), anthracene oil (270-370 °C, 12-27 %) - and pitch as a residuum (50-60 %) (NENITESCU, 1966; PYKA, 1994; LOYEK, 1998). Out of each of these fractions, various aromatic compounds are separated by further distillation, using in many cases devices located on site.

The content of phenolic compounds in any of these fractions and in high-temperature-coal-tar as well is much lower than in creosote (as defined before). However, if coal is distilled at lower temperatures (ca 500 °C), the coal tar yield is higher (up to 12 %) and its composition is different. Initially, low-temperature coal tar

does not contain benzene, toluene, naphthalene and anthracene, but contains higher alkanes and cycloalkanes (e.g. hexahydrofluorene) and high amounts of phenols (20-50 %). Further, the low-temperature-coal-tar vapours undergo combustion processes which yield important amounts of hydrogen which partially reduces the phenols to aromatic hydrocarbons (e.g. phenol to benzene). During combustion, unsaturated hydrocarbons react with ammonia or hydrogen sulphide, forming heterocycles with nitrogen or sulphur (NENITESCU, 1966). Coal tar also contains heteroaromatic compounds with oxygen in the π -cyclic system. The ratio of N:S:O in coal tar is approximately 7:2:1 and is very similar to that in shale oil (JOHANSEN, 1996).

Any of the above mentioned fractions and residues produced during coal gasification and subsequent fractionation of by-products virtually consist sources of subsurface contamination at former gas manufacturing plants. A high variability in source composition results therefore from the gas production process alone.

In the present work, the terms 'coal tar' and 'tar oils' are used generically for gasworks wastes.

3.2 Physical and Chemical Properties of Important Contaminants at Gasworks Sites

As mentioned above, coal tars are very complex organic mixtures consisting of tens of thousands of compounds. The complexity of groundwater contamination at former gasworks arises from the complex original composition of tars, but also from the biotic transformations which organic compounds undergo in the subsurface environment.

In this thesis, three main compound classes are addressed: polycyclic aromatic hydrocarbons, monocyclic aromatic hydrocarbons and heterocyclic aromatics. Some polar organics presumed to be biodegradation products of tar constituents have also been detected at the site and have been included in this study.

Characteristic for the chemicals investigated is the extremely wide range of physico-chemical properties. For the main compounds investigated, they are listed in Table 3.1. However, for many substances, especially alkyl-

derivatives, there are often no physico-chemical data in the literature. In such cases, the octanol-water partition coefficients have been estimated from K_{ow} values of compounds with similar structure, using following empirical rules (after SCHWARZENBACH et al., 1996):

- the introduction one methyl group in the molecule increases the $\log K_{ow}$ by 0.4-0.5 log units (i.e. a factor of 3 in K_{ow});
- one OH group lowers the $\log K_{ow}$ by 0.67 log units (a factor of 4.7 in K_{ow});
- two H atoms increase the $\log K_{ow}$ by 0.26 log units (a factor of 1.8 in K_{ow}).

The properties of the 16 EPA PAH have been described in detail by PYKA, 1994; MERKEL, 1996; LOYEK 1998. From *Naphthalene* to *Indeno(1,2,3-cd)pyrene* the octanol-water partition coefficient increases by 4, the water solubility by 6 orders of magnitude. K_{ow} s of most compounds listed in Table 3.1 are comparable to or lower than the one of *Naphthalene*, the most soluble EPA PAH. The amount of higher PAHs (4 ring and more) released by dissolution out of organic phase is not very high as their subcooled liquid solubilities are lower than 1-2 mg/l and their contribution to the composition of coal tar is rarely higher than 1 wt %. Additionally, due to

their high sorption capacity, most of them are immobilized in sediments after relatively short distances and are consequently less relevant for groundwater contamination. However, for aged contamination, their saturation concentration might increase as the organic phase is enriched with low solubility compounds due to advanced dissolution of the well soluble ones.

In contrast to the PAHs, monocyclic aromatic hydrocarbons (MAH) have higher water solubilities. Their relative amount in coal tars is rather low, but at former gasworks they also occur as separate distillation mixtures or even as pure phase. Consequently, close to the source they occur in groundwater at considerably higher concentrations than PAHs.

Hydrocarbon molecules are lipophilic, therefore at equilibrium between water and any organic phase they partition preferentially into the organic phase. If in the molecule some carbon atoms are replaced by heteroatoms (nitrogen, oxygen or sulphur) the polarity increases and these compounds have much higher affinity for the aqueous environment (higher water solubility) than PAHs and monocyclic aromatics.

Table 3.1: Physico-chemical properties of the main organic compounds identified and quantified at 'Testfeld Süd'. Data compiled from ^a Verschueren (1996); ^b Mackay and Shiu (1981); ^c Lyman et al. (1990); ^d Johansen (1996); ^e Sims and Overcash (1983); ^f Walther and Luthy (1984); ^g Lyman et al. (1990); ^h U.S. National Library of Medicine, Hazardous Substances Database; ⁱ ChemFinder; ^j Aldrich Handbuch Feinchemikalien 1996-1997; ^k Environmental Science Center of Syracuse Research Corporation (SRC), Experimental log K_{ow} database.

Substance	Molar Weight [g/mol]	Melting Point [°C]	Boiling Point [°C]	Vapour Pressure [mm Hg] at 25°C	Aqueous Solubility [mg/l] at 25°C	Subcooled Liquid Solubility [mg/l]	$\log K_{ow}$ ^k
(1)	(2)	(3)	(4)	(5)	(6)	(7)	(8)
Polycyclic aromatic hydrocarbons (16 EPA)							
Naphthalene	128	80.6 ⁱ	218 ⁱ	4.92 · 10 ⁻² ^h	30 ^b	119.2	3.37
Acenaphthylene	152	93.5-94.5 ⁱ	265 ⁱ	2.9 · 10 ⁻² ^h	16.1 ^f	84.5	4.07
Acenaphthene	154	95 ⁱ	279 ⁱ	2 · 10 ⁻² ^h	3.47 ^b	20	4.33
Fluorene	166	116 ⁱ	295 ⁱ	1.3 · 10 ⁻² ^h	1.98 ^b	18.1	4.18
Phenanthrene	178	99.5 ⁱ	340 ⁱ	6.8 · 10 ⁻⁴ ^h	1.29 ^b	8.32	4.46
Anthracene	178	217.5 ⁱ	340 ⁱ	1.96 · 10 ⁻⁴ ^h	0.07 ^b	6.38	4.45
Fluoranthene	202	110.8 ⁱ	375 ⁱ	6 · 10 ⁻⁶ ^h	0.26 ^b	2.11	5.33
Pyrene	202	156 ⁱ	404 ⁱ	6.85 · 10 ⁻⁷ ^h	0.14 ^b	2.72	5.32
Benzo(a)anthracene	228	159.8 ⁱ	437.6 ⁱ	5 · 10 ⁻⁹ ^h	0.014 ^b	0.33	5.61
Chrysene	228	255.8 ⁱ	448 ⁱ	6.3 · 10 ⁻⁹ ^h	0.002 ^b	0.44	5.61
Benzo(b)fluoranthene	252	167 ⁱ	357 ⁱ	5 · 10 ⁻⁷ ^h	0.0012 ^b	0.035	6.57
Benzo(k)fluoranthene	252	215.7 ⁱ	480 ⁱ	5 · 10 ⁻⁷ ^h	0.00055 ^b	0.035	6.84
Benzo(a)pyrene	252	176.5 ⁱ	495 ⁱ	5 · 10 ⁻⁷ ^h	0.0038 ^b	0.14	6.04
Dibenzo(a,h)anthracene	278	266 ⁱ	524 ⁱ	1 · 10 ⁻¹⁰ ^h	0.0005 ^b	1.66	5.97
Indeno(1,2,3-cd)pyrene	276	162.5 ⁱ	536 ⁱ	1 · 10 ⁻¹⁰ ^h	0.062 ^b	0.13	7.66
Benzo(g,h,i)perylene	276	278.3 ⁱ	500 ⁱ	1 · 10 ⁻¹⁰ ^h	0.00026 ^b	0.027	7.23

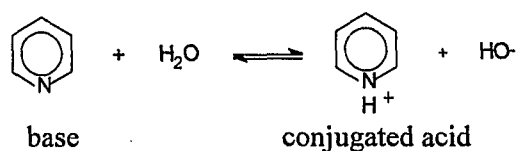
Table 3.1 (continued)

(1)	(2)	(3)	(4)	(5)	(6)	(7)	(8)
<u>Other PAH</u>							
Indane	118	-51 ⁱ	176.5 ⁱ	#	100 ^g	liquid	3.18
Methylindanes	132	#	#	#	#	-	3.68*
Dimethylindanes	146	#	#	#	#	-	4.18*
Indene	116	-35 ^a	182 ^a	1.1 ^h	300 ^g	liquid	2.92
Methylindenes	130	#	#	#	#	-	3.42*
Dimethylindenes	156	#	#	#	#	-	3.92*
1-Methylnaphthalene	142	-22 ^a	240-243 ^a	#	28.5 ^h	liquid	3.87
2-Methylnaphthalene	142	34-36 ^a	241-242 ^a	#	25.4 ^h	31.7	3.86
Dimethylnaphthalenes	156	#	263 ^a	#	#	-	4.36*
Ethylnaphthalene	156	#	251-260 ^j	#	#	-	4.36*
Trimethylnaphthalenes	170	#	285 ⁱ	#	#	-	4.86*
<u>Monocyclic aromatic hydrocarbons</u>							
Benzene	78	5.5 ^a	80.1 ^a	95.2 ^h	1770 ^b	liquid	2.13
Toluene	92	-95.1 ^a	110.8 ^a	22 ^a	515 ^b	liquid	2.73
o-Xylene	106	-25 ^a	144 ^a	8.84 ^h	175 ^b	liquid	3.12
p-Xylene	106	13 ^a	138.4 ^a	6.6 ^h	185 ^b	liquid	3.15
Ethylbenzene	106	-95 ^a	136.2 ^a	9.53 ^h	152 ^b	liquid	3.15
Propylbenzene	120	-100 ^a	159 ^a	2.5 ^a	55 ^b	liquid	3.69
Isopropylbenzene	120	-96 ^a	152.7 ^a	3.2 ^h	50 ^b	liquid	3.66
1,2,3-Trimethylbenzene	120	<-15 ^a	176 ^a	#	75 ^b	liquid	3.66
1,2,4-Trimethylbenzene	120	-57 ^a	169 ^a	#	57 ^b	liquid	3.63
1,3,5-Trimethylbenzene	120	-52.7 ^a	164.7 ^a	#	50 ^b	liquid	3.42
<u>Heterocyclic aromatic compounds</u>							
Thiophene	84	-30-(-38) ⁱ	84 ⁱ	79.7 ^h	3600	liquid	1.81
Trimethylthiophene	126	#	#	#	#	-	3.31*
Benzofuran	118	<-18 ⁱ	173-175 ^a	0.44 ^h	220 ^d	liquid	2.67
Methylbenzofurans	132	#	197-198 ⁱ	#	#	-	3.17*
Dimethylbenzofurans	146	#	#	#	#	-	3.67*
Dibenzofuran	168	83-84 ⁱ	285 ⁱ	4.4 · 10 ⁻³ ^h	4.75 ^d	17.6	4.12
Methyldibenzofuran	182	#	#	#	#	-	4.62*
Bezothiophene	134	30-33 ⁱ	221 ^d	#	130 ^d	162.1	3.12
Carbazole	167	240-248 ⁱ	354-355 ⁱ	1.37 · 10 ⁻⁶ ^h	1.2 ^d	199.2	3.71
Acridine	179	108 ⁱ	346 ⁱ	1.35 · 10 ⁻⁴ ^h	#	-	3.48
Xanthene	182	101-102 ⁱ	310-312 ⁱ	#	#	-	4.73*
Thioxanthene	198	#	#	#	#	-	-
<u>Other (presumably metabolites)</u>							
Methylindanol	148	#	#	#	#	-	2.98*
Tetramethylindanone	188	#	#	#	#	-	4.48*
Methylnaphthol	158	64-66 ⁱ	#	#	#	-	3.16
Dihydro-trimethyl-naphthalenone	186	#	#	#	#	-	3.86*
Acridone (Acridinone)	195	>300 ⁱ	#	#	#	-	3*
Methylquinolinol	159	#	#	#	#	-	1.5

* roughly estimated

no data

Nitrogen-containing heterocycles are neutral bases, their reaction with water, described by the basicity constant pK_b , results in the formation of a cation:



(3.1)

The formation of the base by release of a proton by the conjugated acid is described by the acidity constant pK_a , where

$$pK_a + pK_b = pK_w \quad (3.2)$$

$K_w = [H^+][HO^-]$ is the ionic product of water, $pK_w = -\log K_w = 14$ at 25° C. K_w changes with temperature, the pH of neutrality is 7 at exactly 25 °C (STUMM and MORGAN, 1996).

From Eq. 3.2 it follows that the stronger an acid is (low pK_a), the weaker its conjugate base (high

pK_b), while the stronger the base (low pK_b), the weaker its conjugate acid (high pK_a). pK_a is a measure of the strength of an acid relative to the acid/base pair H_3O^+/H_2O . The value of pK_a tells at which hydrogen ion activity, expressed by the pH , the acid is present in equal parts in the dissociated (ionic) and non-dissociated (molecular) forms. For nitrogen-heterocycles of environmental interest, the acidity constant pK_a is between 5 and 7.

The ionisation degree α_{ion} is the fraction of molecules present in ionized form at a given temperature. It can be calculated from the pK_a and is pH dependent (SCHWARZENBACH, 1996):

$$\alpha_{ion} = \frac{1}{1 + 10^{(pH - pK_a)}} \quad (3.3)$$

At $pH = pK_a$, $\alpha_{ion} = 0.5$. If the pH value increases by 1 the ionisation degree α_{ion} decreases by almost a factor of 10 (Table 3.2).

Table 3.2: Influence of pH on the ionisation degree α_{ion} of Nitrogen-containing heterocyclic compounds

Substance	pK_a	α_1 (at $pH=7$)	α_2 (at $pH=8$)	α_1 / α_2
Quinoline	4.92	0.0082	0.0008	9.8
2-Methyl-quinoline	5.83	0.0633	0.0067	9.4
3-Methyl-quinoline	5.67	0.0447	0.0047	9.5
4-Methyl-quinoline	5.20	0.0156	0.0016	9.8
Acridine	5.68	0.0457	0.0048	9.5

Biodegradation, which implies some oxidation reactions, always leads to more polar substances. With the exception of hydroxyquinolines, metabolites have higher aqueous solubilities than the parent compounds (JOHANSEN, 1996; CHANG et al., 1998).

Due to their polarity, the identification of heteroaromatic compounds as well as of metabolites of coal tar constituents fails if routine analytical methods and concentration methods (e.g. solvent extraction using common organic solvents such as cyclohexane) applicable for hydrocarbons are used.

3.3 Toxicology of Coal Tar Constituents

A lot of national and international organisations are involved in reviewing or evaluating data pertaining to the possible hazards posed by industrial chemicals (Appendix I). Their work is

concerned with animal toxicology and human health and often includes an evaluation of ecotoxicological data and environmental effects.

In spite of the great number of chemicals registered, there are still a lot which may be present at former industrial sites (including former gasworks), but have not been yet identified or subject of toxicological evaluation. Given the complexity of the sources of contamination (complicated mixtures of substances), even after decades of research at contaminated sites, the exact characterisation of the contaminant sources is rarely completed.

Coal tars and tar oils are such an example. The only contaminants so far considered of concern and monitored in routine analyses at former gasworks sites are PAHs (16 EPA), BTEX and sometimes phenols. Tar constituents such as e.g. heterocyclic aromatic compounds have been subject of more detailed investigation only at a few field sites world wide: Borden (Canada), Pensacola, Wyoming, Seattle and Saint Louis (U.S.), Ringe, Holte, Federicia, Trige and Østre (Denmark) (JOHANSEN, 1996; DYREBORG, 1996). At the same time it is well known that generally an increase in alkyl substitution and/or heteroatom substitution into the aromatic ring increases the toxicity of the compound (VERSCHUEREN, 1996). Up to now, alkylated PAHs and heterocyclic aromatic compounds have not been included in routine groundwater analysis.

Although a detailed description of toxicological properties is not the subject of this work, some short comments are made concerning the selection of compounds to be considered in analysis.

In general, toxicological effects determined in animals are extrapolated to humans. These effects are most often indicated as the number of test animals in which the applied dose induces a certain effect after a certain period of administration (e.g. lethal dose fifty, LD_{50}). However, there is a lot of uncertainty in the extrapolation itself (which is sometimes not even possible from strain to strain of the same species) and the value alone in fact provides no information without the knowledge of the course (slope) of the dose-effect curve - substances with different toxicity may have for instance the same LC_{50} (EISENBRAND and METZLER, 1994).

There is even evidence that high doses of e.g. endocrine disruptors may cause less damage than a lower dose (CANADIAN WWF, 1998). This kind of inverted dose-response curve means that testing some compounds at high doses and extrapolation back to lower doses would miss effects that would show up at low doses. In other words, for giving evidence about a certain compound, some additional information to a single value (e.g. LC₅₀) is needed. In most cases, even in extensive databases such information is not contained. Further, there is a lot of doubt among the research community whether such tests are at all justified from both scientific and ethic point of view (U.S. NATIONAL SOCIETY OF MEDICAL RESEARCH).

The key parameters generally considered besides acute toxicity are some chronic toxicity such as structural or organ damage, outright loss of fertility, mutagenic effect and cancer. Persistence in the environment and ability to bioaccumulate must also be taken into account.

But 'kill-you-dead' poisons and cancer causing chemicals are not the only concern. Even modern, sophisticated testing for chemical safety is bound to miss long term impacts such as e.g. hormone disrupting effects. Unless the effects are physically apparent or severe, hormone disfunction inducing behavioural changes, altered immune response, infertility may not be noticed and cannot be detected by usual toxicity tests. Subtle, delayed effects come out decades after the exposure or even in next generations. Among the known or suspected hormone disruptors are dioxins and furans, some pesticides, higher phenols and phthalates. Substances with similar structures as *Benzofuran*, *Dibenzofuran* and their alkyl isomers are coal tar constituents and are found in groundwater at tar contaminated sites; with the exception of *Benzofuran* which is known to cause cancer, the effects of the others on wildlife and humans were not assessed so far.

A further challenge in estimating the toxic potential of contaminants, especially at former gasworks sites, is that not only the contaminant sources are complex organic mixtures, but also the contaminated groundwater contains hundreds of dissolved substances and there is evidence that for mixtures of compounds with the same (or similar) mode of action, effects are completely concentration additive (VERHAAR et al. 1995). Research on the effect of mixing four pesticides show that the effect of the mixture can be up to orders of magnitude stronger than the chemical acting individually (CANADIAN WWF, 1998). That means that failure to identify and quantify most compounds may lead to serious underestimation of groundwater toxicity. It must be recognized that in real life chemicals act in mixture and that it has to be done more than toxicology tests with individual substances.

In conclusion, toxicological data should be interpreted with caution. A comparison of the toxic effect of a set of chemicals may be done only if it refers to the same species and the test was conducted under the same conditions (duration, mode of administration, etc.). An extrapolation to humans may not always be legitimate. Testing only at levels of organization of the individual species provides no information directly related to ecological consequences of the release of a hazardous chemical. For these reasons, (semi)quantitative evaluation of the ecological and health impact of chemicals is in most cases a very difficult task; in some cases the lack of immediate cause-effect evidence does not necessarily exclude more subtle long-term effects.

Table 3.3 shows a compilation of toxicological data for contaminants found at the site 'Testfeld Süd'. For other substances mentioned in this study but not included in Table 3.3 there were no toxicity data available. A complete list of the substances identified and quantified in the field at 'Testfeld Süd' is shown in Appendix II.

Table 3.3: Manmade sources, toxicity and carcinogenicity of selected contaminants of concern at former gasworks sites, other than 16 EPA PAHs minus *Naphthalene* (alphabetical order). Data from ^a the International Agency for Research on Cancer (IARC, see Appendix 1), ^b Occupational Health and Safety - Material Safety Data Sheets, ^c NTP Chemical Repository (Radian Corporation, Aug. 29, 1991), ^d CA-EPA Office of Environmental Health Hazard Assessment, ^e Verschuieren, ^f Merck Safety Data Sheets, ^g Johansen, ^h U.S. National Library of Medicine, Hazardous Substances Data Bank. LC₅₀ (lethal concentration fifty) [mg/l]: a concentration that, when administered by the respiratory route, is expected to kill 50 % of the test animals; LD₅₀ (lethal dose fifty) [mg/kg body weight/day]: that dose-rate which would cause death in 50 % of the test animals; EC₅₀ (effect concentration fifty): expresses acute toxicity in *Daphnia* as the effective average concentration causing swimming inability in half of the test animals after a certain time; BCF (bioconcentration factor): the ratio of concentration of the chemical between organism (certain tissue) and the exposure water measured at equilibrium.

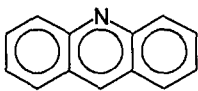
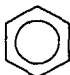
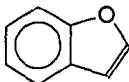
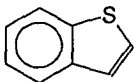
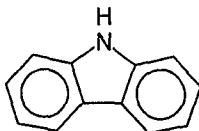
Substance / Structure (1)	Properties (2)
<u>Acridine</u> <u>(Dibenzopyridine)</u> 	Manmade sources ^e : - in airborne coal tar emissions: 8.4 mg/g of sample or 300 µg/m ³ of air; - in coke oven emissions: 32-173 µg/g of sample; - in coal tar: 9.2 mg/g of sample - in wood preservative sludge: 3.5 g/l of raw sludge Carcinogenicity: - human carcinogen (group 1) ^a Toxicity: - terratogenic ^g - fish: toxic at 5 mg/l ^g - <i>Daphnia</i> : toxic at 0.7 mg/l, 1.7 mg/l immobilization concentration IC ₅₀ ^g - 2.9 mg/l 24 h LC ₅₀ in <i>Daphnia pulex</i> ^g - BCF ^g 120-126 in <i>fathead minnow (Pimephales promelas)</i> , 30 in <i>Daphnia</i>
<u>Benzene</u> 	Manufacturing sources ^e : - petroleum refinery, solvent recovery plant, coal tar distillation, coal tar processing, coal coking Carcinogenicity: - carcinogenic to humans (group 1) ^{a,f} Toxicity: - known to cause developmental toxicity, reproductive toxicity ^g - <i>Daphnia</i> : 680 mg/l EC ₅₀ ^g
<u>Benzofuran</u> <u>(Coumarone)</u> 	Manmade sources ^e : - in gasoline exhaust: <0.1-2.8 ppm Carcinogenicity: - possibly carcinogenic to humans (group 2B) ^a - known to cause cancer ^f Toxicity ^b : - 500 mg/kg intraperitoneal, <i>mouse</i> LD ₅₀ - 7 g/kg/14 days intermittent oral, rat LD ₅₀
<u>Benzothiophene</u> 	Manmade sources ^e : - constituent of coal tar creosote: 0.1 wt % Carcinogenicity: not available Toxicity : - fish: 13.6 mg/l 96 h LC ₅₀ in <i>guppy (Poecilia reticulata)</i> ^b - <i>Daphnia</i> : 64 mg/l EC ₅₀ ^g - algae: 10000 mg/l EbC ₅₀ (population growth) in <i>green algae</i> ^b - 1,700 mg/kg acute oral, rat LD ₅₀ ^f - >2,000 mg/kg acute dermal, rat LD ₅₀ ^f - BCF(residue) 750 µg/l 50 weeks in <i>water flea (Daphnia magna)</i> 1,800 µg/l ^b
<u>Carbazole</u> 	Manmade sources ^e : - constituent of coal tar creosote: 0.1 wt % Carcinogenicity: - animal limited evidence, not classifiable as to carcinogenicity to humans (group 3) ^a - known to cause cancer ^d Toxicity : - >5,000 mg/kg oral, rat LD ₅₀ ^b - 200 mg/kg intraperitoneal, <i>mouse</i> LD ₅₀ ^b

Table 3.3 (continued)

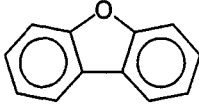
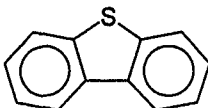
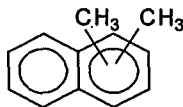
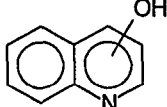
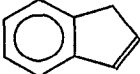
(1)	(2)
	<ul style="list-style-type: none"> - fish: 1 mg/l 48 h LC₅₀ in <i>striped mullet (Mugil cephalus)</i> ^g - invertebrate: 39 mg/l 48 h EC₂₀ (biomass) <i>ciliate protozoa (Tetrahymena thermophila)</i> ^b - <i>mosquito fly (Culex) larvae</i>: 0.1 mg/l (in acetone) 24 h LC₇ ^g 5 mg/l (in ethanol) 24 h LC₉ ^g 0.05 mg/l (in ethanol) 24 h LC₀ ^g - BCF 115 (wet weight) in <i>Daphnia pulex</i> ^g 108 in <i>Daphnia magna</i> ^g
<p><u>Dibenzofuran</u></p> 	<p>Manmade sources:</p> <ul style="list-style-type: none"> - constituent of coal tar creosote: 0.1 wt % ^g - 1 % in coal tar ^f <p>Carcinogeny:</p> <ul style="list-style-type: none"> - not classifiable as to carcinogeny to humans ^f <p>Toxicity:</p> <ul style="list-style-type: none"> - mutagenic (sister chromatid exchange in <i>hamster ovary</i> 10 mg/l) ^b - fish: 1.8 mg/l 96 h LC₅₀ in <i>flathead minnow (Pimephales promelas)</i> ^g 1.8 mg/l 96 h LC₅₀ in <i>guppy</i> ^b - invertebrates: 1.31 mg/l LC₅₀ in <i>opossum shrimp (Mysidopsis bahia)</i> - algae: 1.5 mg/l 96 h EC₅₀ (photosynthesis) in <i>diatom. (Skeletonema costatum)</i>
<p><u>Dibenzothiophene</u></p> 	<p>Manmade sources ^g:</p> <ul style="list-style-type: none"> - constituent of coal tar creosote: 0.1 wt % - in coal tar: 1.6 g/kg - in carbon black: 50 mg/kg <p>Carcinogeny:</p> <p>not available</p> <p>Toxicity:</p> <ul style="list-style-type: none"> - <i>Daphnia</i>: 0.5 mg/l EC₅₀ ^g
<p><u>Dimethylnaphthalene</u></p> 	<p>Manmade sources ^g:</p> <ul style="list-style-type: none"> - constituent of coal tar creosote: 4 wt % 2,3-dimethylnaphthalene, 4 wt % 2,6-dimethylnaphthalene; - in coal tar fumes: 1.6 wt % (no specific isomer) - 2,000 mg/l in Kuwait crude oil (sum of dimethylnaphthalenes) - 3,600 mg/l in S. Louisiana crude oil (sum of dimethylnaphthalenes) <p>Carcinogeny:</p> <p>not available</p> <p>Toxicity ^b:</p> <ul style="list-style-type: none"> - fish: 5.1 mg/l 24 h LC₅₀ in <i>sheepshead minnow (Cyprinodon variegatus)</i> - invertebrates: 0.08 µg/l 24 h LC₅₀ in <i>brown shrimp (Panaeus aztecus)</i> - <i>Daphnia pulex</i>: 1.28 mg/l 48 h EC₅₀ (1,3-dimethylnaphthalene) <p>BCF (1,3-dimethylnaphthalene) in <i>oysters (Crassostrea virginica)</i>:</p> <p>8,400 after 2 days of exposure 36,000 after 4 days of exposure</p>
<p><u>Hydroxyquinoline</u></p> 	<p>Carcinogeny:</p> <ul style="list-style-type: none"> - not classifiable as to carcinogeny to humans (group 3) ^a <p>Toxicity:</p> <ul style="list-style-type: none"> - 1.5 mg/l EC₅₀ (nitrification inhibition) ^g
<p><u>Indene</u></p> 	<p>Manufacturing sources ^g: petroleum refining, coal processing</p> <p>Manmade sources ^f:</p> <ul style="list-style-type: none"> - average concentration in coal tar: 1 wt % <p>Carcinogeny:</p> <p>not available</p> <p>Toxicity:</p> <ul style="list-style-type: none"> - human ^f: by analogy between chemical structure and toxicological effects of related chemicals, inhalation of indene vapors can be expected to cause irritation of mucous membranes; use of indene-coumarone resins contaminated with traces of monomers (indene and benzofuran) can cause allergic dermatitis

Table 3.3 (continued)

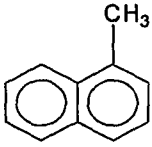
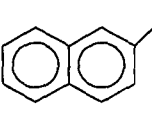
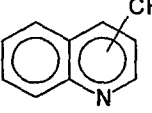
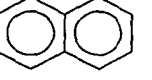
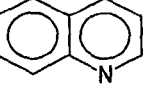
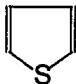
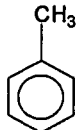
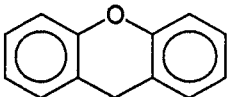
(1)	(2)
<p><u>1-Methylnaphthalene</u></p> 	<p>- fish: 39 mg/l 1 h LC₅₀ (static bioassay) in <i>fathead minnow</i> 14 mg/l 24 h, 48 h, 72 h and 96 h LC₅₀ (static bioassay) in <i>fathead minnow</i>^g</p> <p>Manufacturing sources^e: petroleum refining, coal processing</p> <p>Man-caused sources^e:</p> <ul style="list-style-type: none"> - constituent of coal tar creosote 7 wt % - in coal tar fumes: 0,7 wt % - 2,000 - 4,000 mg/l in diesel fuel - 500 mg/l in Kuwait crude oil - 800 mg/l in S. Louisiana crude oil <p>Carcinogenicity: no data</p> <p>Toxicity^e:</p> <ul style="list-style-type: none"> - fish: 39 mg/l 1 h LC₅₀ (static bioassay) in <i>fathead minnow</i> 9 mg/l 24 h, 48 h, 72 h and 96 h LC₅₀ (static bioassay) in <i>fathead minnow</i> - 8.4 mg/l 48 h LC₅₀ (static bioassay) in <i>brown trout</i>, yearlings - BCF 129 in <i>Coho salmon</i>
<p><u>2-Methylnaphthalene</u></p> 	<p>Manmade sources^e:</p> <ul style="list-style-type: none"> - constituent of coal tar creosote 11 wt % - in coal tar pitch fumes: 1 wt % - 3,500 - 9,000 mg/l in diesel fuel - 700 mg/l in Kuwait crude oil - 900 mg/l in S. Louisiana crude oil <p>BCF 23,500 after 4 weeks in bile of <i>rainbow trout</i>, 40-300 in other tissues</p>
<p><u>Methylquinoline</u></p> 	<p>Manmade sources^e:</p> <ul style="list-style-type: none"> - constituent of coal-tar creosote 0.05 wt % 2-methylquinoline, 0.05 wt % 4-methylquinoline <p>Carcinogenicity: not available</p> <p>Toxicity^e:</p> <ul style="list-style-type: none"> - 26 mg/l (2-methylquinoline) 96 h LC₅₀ in embryos of <i>South African clawed frog</i> - invertebrates (ciliates): 400 mg/l (2-methylquinoline), 625 mg/l (6-methylquinoline), 226 mg/l (8-methylquinoline) 24 h LC₁₀₀ in <i>Tetrahymena pyriformis</i> - <i>Daphnia magna</i>: 11 mg/l (6-methylquinoline) 48 h LC₅₀
<p><u>Naphthalene</u></p> 	<p>Manmade sources^e:</p> <ul style="list-style-type: none"> - in coal tar pitch fumes: 0.9 wt % - in emissions from open burning of scrap rubber tires: 486-816 mg/kg of tire - in commercial coal tar: 150 mg/kg - constituent of coal tar creosote: 11 wt % - 350-1,500 mg/l in diesel fuel - 400 mg/l in Kuwait crude oil, S. Louisiana crude oil <p>Carcinogenicity: - causes cancer</p> <p>Toxicity:</p> <ul style="list-style-type: none"> - 8 mg/l 24 h LC₅₀, 6.1 mg/l 96 h LC₅₀ in <i>Pimephales promelas</i>^g - <i>Daphnia</i>: 23 mg/l EC₅₀^g <p>BCF 13,000 after 4 weeks in bile of <i>rainbow trout</i>, 40-300 in other tissues</p>
<p><u>Quinoline</u> <u>(Benzo(b)pyridine)</u></p> 	<p>Manmade sources^e:</p> <ul style="list-style-type: none"> - constituent of coal tar creosote: 0.1 wt %; the same for isoquinoline <p>Carcinogenicity: - known to cause cancer^d - mutagenic</p> <p>Toxicity :</p> <ul style="list-style-type: none"> - 26 mg/l 96 h LC₅₀ in embryos of <i>South African clawed frog</i> (<i>Xenopus laevis</i>); 6,5 mg/l for dimethylquinoline^g - <i>Daphnia</i>: 29 mg/l EC₅₀^g - BCF 8 in <i>fathead minnow</i> (<i>Pimephales promelas</i>)^g

Table 3.3 (continued)

(1)	(2)
<p><u>Thiophene</u></p> 	<p>Carcinogenity: no data</p> <p>Toxicity: - human ^f: causes skin irritation, may induce sensitization responses - 100 mg/kg intraperitoneal, mouse LD₅₀ ^g - <i>Daphnia</i>: 320 mg/l EC₅₀ ^h</p>
<p><u>Toluene</u></p> 	<p>Carcinogenity:ⁱ - animal limited evidence, unclassifiable as carcinogenic to humans (group 3)^a</p> <p>Toxicity: - known to cause reproductive toxicity ^d</p>
<p><u>Xanthene (Dibenzopyran)</u></p> 	<p>Manmade sources: - in coal tar pitch fumes: 1.1 wt %</p> <p>Carcinogenity: not available</p> <p>Toxicity: not available</p>

Compounds usually quantified at former manufacturing gas plants such as non-alkylated PAHs and some BTEX have been omitted from Table 3.3. *Benzene*, *Toluene* and *Naphthalene* are listed for comparison purposes. Among the 10 monocyclic aromatic hydrocarbons monitored at the site, with the exception of *Benzene* and *Toluene*, there are also other compounds known as terratogenic or causing reproductive toxicity: *Isopropylbenzene*, *Xylenes*, *Ethylbenzene*. To date there is no detailed information available about the effects of *trimethylbenzenes* on human health.

The carcinogenic potential of PAHs has been subject of detailed research. PAHs are frequently not carcinogenic *per se*, but may become so due to metabolic transformations in mammal cells (it is distinguished between the 'parent, proximate or ultimate carcinogenic compound'). PAHs molecules with a 'bay-region' have the highest carcinogenic potential. Their carcinogenic effect is induced by attachment of diol groups, followed by epoxide formation in the 'bay-region' during metabolic transformations (KÄSTNER et al. 1993). Among the 16 EPA PAHs, up to now *Naphthalene*, *Pyrene*, *Benzo(a)anthracene*, *Benzo(a)pyrene* and *Dibenzo(a,h)anthracene* are known to cause cancer, while *Fluoranthene* is not carcinogenic itself, but amplifies the carcinogenity of *Benzo(a)pyrene*. The carcinogenic potential of the others is not completely elucidated yet, although not excluded. The substitution of some H atoms in a PAH molecule by alkyl (e.g. methyl) groups increases the carcinogenic

potential, whereas hydroxy-PAHs are among the most carcinogenic substances at all (KÄSTNER et al. 1993). Hydroxy-PAHs also result during biodegradation in aquatic environments. For alkyl-derivatives of PAHs, the toxicity is highly dependent on the position of the alkyl chain, e.g. 1- and 9-*Methyl-Phenanthrene* are proved to be mutagenic, while the other isomers of position are not (ROSENKRANZ et al., 1991).

No PAHs beyond the 16 EPA, nor their oxidized derivates are monitored in routine groundwater investigations so far.

In Table 3.4 Minimal Risk Levels (MRL) according to the U. S. Agency for Toxic Substances and Disease Registry (ATSDR, see Appendix I) are listed for some groundwater contaminants identified at 'Testfeld Süd'. The MRL is an estimate of the daily human exposure to a hazardous substance that is likely to be without appreciable risk of adverse non-cancer health effects over a specified duration of exposure. These substance specific estimates are used by ATSDR health assessors and other responders to identify contaminants and potential health effects that may be of concern at hazardous waste sites. MRLs are not intended to define clean-up or action levels for ATSDR or other Agencies.

MRLs are derived for acute (1-14 days), intermediate (15-364 days) and chronic (365 days and longer) exposure durations, and for the oral and inhalation routes of exposure. ATSDR does not use serious health effects (irreparable

damage to the liver or kidneys, or birth defects) as basis for establishing MRLs. Exposure to a

level above the MRL does not mean that adverse health effects will occur.

Table 3.4: Minimal Risk Levels (MRLs) according to the U. S. Agency for Toxic Substances and Disease Registry (ATSDR), updated January 1998

Substance	Route	Duration	MRL	Endpoint
Benzene	inhalation	acute	0,05 ppm*	immunological
		intermediate	0,004 ppm	neurological
Toluene	inhalation	acute	3 ppm*	neurological
		chronic	1 ppm*	neurological
	oral	acute	0,8 mg/kg/day	neurological
		intermediate	0,02 mg/kg/day	neurological
m-Xylene	oral	intermediate	0,6 mg/kg/day	hepatic
p-Xylene	oral	acute	1 mg/kg/day	neurological
Xylenes, total	inhalation	acute	1 ppm*	neurological
		intermediate	0,7 ppm*	development
		chronic	0,1 ppm*	neurological
	oral	intermediate	0,2 mg/kg/day	renal
Naphthalene	inhalation	chronic	0,002 ppm*	respiratory
		acute	0,05 mg/kg/day	neurological
	oral	intermediate	0,02mg/kg/day	hepatic
Methyl-Naphthalene	oral	chronic	0,07 mg/kg/day	respiratory
Acenaphthene	oral	intermediate	0,6 mg/kg/day	hepatic
Fluorene	oral	intermediate	0,4 mg/kg/day	hepatic
Anthracene	oral	intermediate	10 mg/kg/day	hepatic

* vol. vapour phase concentration

3.4. Natural Attenuation of Coal Tar Constituents

The concept of 'natural attenuation' covers all physical, chemical and biological processes that help to reduce the concentration of dissolved contaminants in a groundwater plume, such as dispersion, dilution, sorption, volatilisation, biological and chemical degradation. It is now recognized that the major process that influences the contamination pattern in the groundwater is biological degradation (GIDDINGS et al., 1985; MÜLLER et al., 1989; MCALISTER and CHANG, 1994; JOHANSEN, 1996; DYREBORG, 1996).

In spite of the numerous biodegradation studies performed especially during the last decade with typical groundwater contaminants, this very complex process is still far from being entirely understood.

As the coal tar constituents are concerned, most studies focused so far on MAH and PAH and little is known about heterocyclic aromatic compounds. Many microbiological studies focus on the isolation of bacteria capable to metabolise various individual coal tar constituents and eventually attempt to identify the metabolic pathways (e.g. EATON and NITTEAUER, 1994; HADDOCK and GIBSON,

1995; GRIFOLL et al., 1995; LANTZ et al., 1997; SCHMID et al., 1997; RHEE et al., 1998; GIEG et al., 1996; SATO et al., 1997; STUART-KEIL et al., 1998; DUTTA et al. 1998; TSAO et al., 1998; TAY et al., 1998; HAMMER et al., 1998). Most of these studies are performed in the laboratory with individual substances and only rarely deal with a combination of contaminants.

Other researchers determined biodecay rates at laboratory scale using various experimental setup, as well as at field scale (e.g. CHRISTENSEN et al., 1994; FOWLER et al., 1993; ACTON AND BARKER, 1992; NIELSEN et al., 1995, LEVINE et al., 1997; KIM et al., 1995; COHEN et al., 1995; SALANITRO, 1993; BUSCHEK and ALCANTAR, 1995; CHERRY et al., 1996).

The persistence of a contaminant is not exclusively related to its chemical structure, but also depends on other factors such as accessibility, redox conditions, concentration, presence of other substrate and type of microorganisms (MACKENBROCK et al., 1994; ALEXANDER, 1995; JOHANSEN, 1996; DYREBORG, 1996). For this reason, the results of biodegradation studies - both identification of metabolic pathways and determination of

conditions of the experiment and can sometimes even be contradictory. Additionally, in order to evaluate the migration of dissolved contaminants at real field sites, the basic degradation processes in mixtures and the different interactions among the compounds (cometabolism, toxic effects), as well as the redox conditions in the aquifer must be known. During the last years, it has been shown that some coal tar constituents inhibit the biodegradation of others. For coal tar constituents, the observed order of toxicity/inhibition was heterocycles > phenols > PAHs (LANTZ et al., 1997; JOHANSEN, 1996; DYREBORG, 1996; ARCANGELI, 1996).

Similar to other processes affecting the dissolved contaminants in aquifers, the rates at which biodegradation proceeds are typically scale dependent in nature. The problem of scaling up biodegradation rates obtained in the laboratory to the field scale is not solved, new methods of measurement and quantification have to be developed for field conditions.

In this study, apparent biodecay rates will be evaluated using point-concentrations for various compounds found in the plume at 'Testfeld Süd'.

4. Analysis of Coal Tar Constituents from Water Samples

4.1 Sample Handling

The water samples from the field and the column effluents were handled similarly.

Three main classes of compounds have been quantified from water samples in this work: volatile organic compounds, 16 EPA PAHs as well as alkylated derivatives and some more polar compounds (mainly heterocycles).

The **volatile organic compounds (VOC)** (*Benz*, *Tol*, *o-Xyl*, *p-Xyl*, *Et-Benz*, *trimethylbenzenes*, *Ina*, *Ine* and *Bf*) have been analysed directly from water, without prior concentration, using a Purge and Trap device (Tekmar 3000) coupled to a HP 6890 GC-MS (method described further). For the first groundwater samples from the field *Benz*, *Tol*, *Et-Benz*, *o-Xyl*, *p-Xyl* were analysed by a headspace GC (Carlo Erba) with an FID detector. Because the reproductibility was not very good probably mainly due to the sampling procedure (headspace vials frequently unsealed) and also because other substances were quantified additionally to these five BTEX, the volatile compounds were then measured only by Purge and Trap GC-MS. *Fluorobenzene* and *1,2-Dichlorobenzene-d4* in methanol (2000 µg/ml) were used as an internal standard (EPA 524, Supelco). Compared to headspace GC/FID, further advantages of Purge and Trap GC-MS are the much lower detection limit (about three orders of magnitude) and the possibility to identify unknown substances using the mass spectrometer. Because in this method no prior concentration/conservation by solvent extraction is required, the volatile compounds had to be analysed immediately after sampling, in order to minimise losses due to degassing and/or biodegradation during storage. This sometimes causes difficulties when a large number of samples has to be analysed within relatively short time.

The **16 EPA PAHs** were extracted from water samples using cyclohexane as a solvent (10 ml solvent usually containing 10 µl of internal standard for 600-800 ml water) and measured using a HP 5890 GC-MS. The internal standard (Restek) was a solution of 200 mg/l *Nap-d8*,

Ace-d10, *Phe-d10*, *Chr-d12*, *Pery-d12* in cyclohexane.

In addition to the analysis of the more 'traditional' compounds (BTEX and PAHs), some new compounds have been measured in groundwater samples down-stream from the source. A special focus was on **heterocyclic aromatic hydrocarbons**. Because many of these are polar due to the presence of one or more heteroatoms in the aromatic cycle (see also Chapter 3.2), they cannot be assessed by traditional liquid/liquid extraction when unpolar organic solvents are used. A method developed by JOHANSEN (1996) was used in this work for trace analysis of heteroaromatic compounds in groundwater. He used dichloromethane as a solvent and found for heterocycles a maximum extraction efficiency at pH = 8. The optimised method of JOHANSEN was here performed as follows: The pH of the water sample was adjusted to 8 using a 10 M KOH solution. Ca 900 ml of sample (groundwater) were extracted three times with 50 ml dichloromethane in a separating funnel. A solution of *Pyridine-d5* (4403.9 µg/ml) and *Nap-d8* (4447.5 µg/ml) in dichloromethane was used as an internal standard (*Pyridine* is a N-heterocyclic compound). The combined dichloromethane extract (150 ml) was concentrated by vacuum rotary evaporation to ca 5 ml and further under a slow stream of N₂ to 200-500 µl. The concentrated extracts were analysed by GC-MS. There was poor reproductibility of the *Pyridine-d5* peak, most probably due to partial loss during concentration of the extracts and eventually due to decomposing in the GC capillary column (this phenomenon has been observed by JOHANSEN and also in this work for N-heterocyclic tar constituents such as *Quinoline*). Therefore, for quantification only *Nap-d8* was used as an internal standard (calibration discussed further). Similarly to *Pyridine-d5*, some volatile compounds initially dissolved in the groundwater have surely been lost during solvent evaporation.

Because the dichloromethane-extraction is expensive, extremely time-consuming, susceptible to sample losses and uses large amounts of toxic solvent, in the future it will have to be replaced by other concentration

methods (e.g. solid phase micro-extraction). Especially for N-heterocycles and oxygenated metabolites, JOHANSEN (1996) also observed adsorption effects in the column or injection port and decomposition in the GC column, and proposed therefore to replace the GC-MS by LC-MS analysis.

4.2 Instrumental Setup

The main parameters for the analysis of volatile compounds, 16 EPA PAHs and polar compounds are summarised in Table 4.1 to 4.3.

In this work, the Purge and Trap method was used for the concentration of volatile substances (mainly *Benz*, *Tol*, *EtBenz*, *Xylenes*, *Trimethylbenzenes*, *Ina*, *Ine* and *Bf*), which have been routinely measured in groundwater and column effluent samples. All these were available as pure compounds.

Because during pumping tests in the plume at 'Testfeld Süd' the target compounds mentioned above were not anymore detectable, but others such as alkyl-*Benzofurans*, *Methyl-Benzothiophene* as well as alkyl-*Ine* and alkyl-*Ina* were present in high concentrations (for some comparable to *Ace*), these were also quantified from chromatograms obtained by Purge and Trap GC-MS (Scan mode); because they were not available as pure substances, the non-alkyl-derivatives listed above were used for calibration.

Table 4.1: Parameters for analysis of volatile aromatics (VOC) by Purge and Trap GC-MS. This method (Scan mode) was also used for the quantification of heterocycles, *Ina*- and *Ine*-derivatives from emission pumping tests.

Purge and Trap Autosampler (Tekmar 3000)	
Sample amount:	25 ml
Purge time:	11 min
Carrier:	Helium 5.0
Gas flux:	50 ml/min
Trap:	Supelco Carboxpack C&B
Desorption temperature:	225 °C
Desorption time:	4 min
GC-MS (HP 6890)	
Injector	
Temperature:	250 °C
Carrier:	Helium 5.0
Split ratio:	10:1
Column	
Type:	HP 5.5 % Phenyl-Methyl-Siloxan
Film thickness:	0.25 µm
Int. diameter:	0.25 mm
Length:	60 m

Table 4.1 (continued)

Oven (temperature program)		
	$T_0=40\text{ °C}$	$t_0=4\text{ min}$
$R_1=10\text{ °C/min}$	$T_1=90\text{ °C}$	$t_1=8\text{ min}$
$R_2=8\text{ °C/min}$	$T_2=250\text{ °C}$	$t_2=2\text{ min}$
Detector (MSD)		
Temperature:	315 °C	
Mode:	Scan/Selected Ion Mode (SIM)	

Table 4.2: Parameters for GC-MS analysis of the 16 EPA PAH

GC-MS (HP 5890)		
Injector		
Temperature:	250 °C	
Carrier:	Helium 5.0	
Split ratio:	10:1	
Column		
Type:	Restek	XTI-5,5% Diphenyl-, 95% Dimethyl-polysiloxan
Film thickness:	0.25 µm	
Int. diameter:	0.25 mm	
Length:	30 m	
Oven (temperature program)		
	$T_0=65\text{ °C}$	$t_0=4\text{ min}$
$R_1=10\text{ °C/min}$	$T_1=270\text{ °C}$	$t_1=10\text{ min}$
$R_2=10\text{ °C/min}$	$T_2=310\text{ °C}$	$t_2=6.5\text{ min}$
Detector (MSD)		
Temperature:	315 °C	
Mode:	SIM	

Table 4.3: Parameters for GC-MS analysis of polar compounds

GC-MS (HP 5890)		
Injector		
Temperature:	250 °C	
Carrier:	Helium 5.0	
Split ratio:	10:1	
Column		
Type:	HP 5.5 % Phenyl-Methyl-Siloxan	
Film thickness:	0.25 µm	
Int. diameter:	0.25 mm	
Length:	60 m	
Oven (temperature program)		
	$T_0=40\text{ °C}$	$t_0=5.5\text{ min}$
$R_1=5\text{ °C/min}$	$T_1=47\text{ °C}$	$t_1=3\text{ min}$
$R_2=6\text{ °C/min}$	$T_2=100\text{ °C}$	$t_2=1\text{ min}$
$R_3=8\text{ °C/min}$	$T_3=160\text{ °C}$	$t_3=2\text{ min}$
$R_4=8\text{ °C/min}$	$T_4=200\text{ °C}$	$t_4=2\text{ min}$
$R_5=8\text{ °C/min}$	$T_5=270\text{ °C}$	$t_5=5\text{ min}$
Detector (MSD)		
Temperature:	315 °C	
Mode:	SIM	

4.3 Calibration without Reference Substances

This work was initially focused on the 16 EPA PAHs, plus an extended list of more volatile aromatic hydrocarbons and *Bf*. These were identified in the NAPLs from the site and in the groundwater as well.

The tar analyses showed however, that there are also other, more polar constituents, mainly heterocyclic, present in relatively large amounts. Initially, the aim was to see if they are also present in the plume downstream. The groundwater samples taken from the plume centre-line (wells B28-B42-NT01) were extracted with dichloromethane as described in Chapter 4.1. Based on the results of the tar analyses on one hand, and on the other hand imposed by which substances were at all available in pure form, a set of 10 compounds was chosen as target compounds for calibration: *Bf*, *Ina*, *Ine*, *TetrahydroNap*, *1-MetNap*, *2-MetNap*, *Bph*, *Dbf* and *Carb*. These covered also a relatively wide range of K_{ow} -values. For calibration, a solution of those in dichloromethane was prepared in a concentration of around 1000 $\mu\text{g/ml}$. *Nap-d8* was used as internal standard.

The GC-MS analyses of the dichloromethane extracts showed that in the groundwater there were a lot of other substances that would normally not be assessed.

This impediment can partially be overcome. Concentrations of compounds of environmental interest that are not available in pure form can be estimated by calibration with substances with similar properties (BELLER et al., 1995;

JOHANSEN, 1996). The similarity of properties refers to the value of K_{ow} , respectively to the retention time in the GC column. Sometimes, substituted derivatives are calibrated with the parent (non-substituted) compound (JOHANSEN, 1996), e.g. *Methyl-Bf* with *Bf*. This was the method used for the groundwater samples taken during pumping tests analysed by Purge and Trap (results in Chapter 7).

Even if the absolute concentration values obtained by this method are not exact, they are still useful if their attenuation in the plume is an issue in terms of relative concentrations and can be used for the evaluation of biodecay rates (Chapter 8).

Table 4.4 shows an overview of the compounds quantified in the plume (results in Chapter 7, Table 7.3) and the compounds used for calibration, based on their similar K_{ow} , respectively on the similar retention time.

According to this, the calibration was also in this case performed with similar substances available (the 10 listed above) with similar properties. To test for the error resulting from working either with retention times or with K_{ows} , these two methods were compared for the sum of the analysed compounds in 9 groundwater samples. As expected, the error was concentration dependent (greater for lower concentrations), but within acceptable limits (0.2 to 10.2 %). Because for many compounds the K_{ow} values were empirically estimated (taking into account the compound structure), concentrations were finally calculated by calibration with substances with similar retention time.

Table 4.4: Calibration without reference substances for substituted PAH, heterocycles and presumed metabolites

Substance (Nb of Isomers)	Retention time [min]	K_{ow} [-]	Calibrated with: (function of R.T.)	Calibrated with: (function of K_{ow})
<u>Calibration Mix</u>				
Benzofuran	10.07	2.67	-	-
Indane	21.25	3.18	-	-
Indene	22.58	2.92	-	-
Tetrahydro-Naphthalene	22.87	3.49	-	-
Benzothiophene	26.93	3.12	-	-
1-Methyl-Naphthalene	29.34	3.87	-	-
2-Methyl-Naphthalene	29.77	3.86	-	-
Biphenyl	31.26	3.98	-	-
Dibenzofuran	34.21	4.12	-	-
Carbazole	40.42	3.71	-	-
<u>Substances in the analysed groundwater</u>				
<u>Alkyl-PAH</u>				
Methyl-Indane	24.12	3.68	Carbazole	Tetrahydro-Naphthalene
Methyl-Indene (2)	25.81	3.42	Tetrahydro-Naphthalene	Tetrahydro-Naphthalene
	26	3.42		
Dimethyl-Indene (6)	28.05	3.92	Biphenyl	Benzothiophene
	28.21	3.92		
	28.28	3.92		
	28.34	3.92		
	28.54	3.92		
	28.59	3.92		
Dimethyl-Naphthalene (3)	32.63	4.36	Dibenzofuran	Biphenyl
	32.71	4.36		
	33.4	4.36		
Ethyl-Naphthalene	31.71	4.36	Dibenzofuran	Biphenyl
Trimethyl-Naphthalene (5)	34.30	4.86	Dibenzofuran	Dibenzofuran
	34.41	4.86		
	34.74	4.86		
	35.08	4.86		
	35.61	4.86		
<u>Heterocycles</u>				
Methyl-Benzofuran (3)	24.44	3.17	Indane	Tetrahydro-Naphthalene
	24.56	3.17		
	24.71	3.17		
Dimethyl-Benzofuran (2)	27.18	3.67	Carbazole	Benzothiophene
	27.36	3.67		
Dibenzofuran	34.21	4.12	Dibenzofuran	Dibenzofuran
Methyl-Dibenzofuran (2)	36.59	4.62		
	36.93	4.62		
Acridine	36.79	3.48	Tetrahydro-Naphthalene	Dibenzofuran
Xanthene	41.45	4.73	Dibenzofuran	Carbazole
Thioxanthene	41.04	?	Dibenzofuran	
<u>Oxidation products</u>				
Methyl-Indanol / - Indanone (3)	31.29	2.98	Indene	Biphenyl
	31.34	2.98		
	31.90	2.98		
Tetramethyl-Indanone	33.50	4.48	Dibenzofuran	Biphenyl
Methyl-Naphthol (2)	35.93	3.16	Benzothiophene	Dibenzofuran
	36.07	3.16		
Acridinone	35.42	3	Benzothiophene	Carbazole
Methylquinolinol/-quinolinone	39.17	1.5		Carbazole
	39.75	1.5		
	39.98	1.5		

5. Dissolution out of Residual NAPL Phase

5.1 Theory

5.1.1 Dissolution out of Complex Organic Mixtures at Equilibrium

The dissolution out of a mixture is described by Raoult's law which states that the saturation concentration of a substance at equilibrium depends on the molar fraction of that substance in the mixture (detailed discussion by LOYEK, 1998):

$$c_{sat,i} = \chi_i \cdot \gamma_i \cdot S_{w,i} \quad (5.1)$$

with:

$$\chi_i = \frac{n_i}{\sum_{i=1}^m n_i} \quad (5.2)$$

$c_{sat,i}$ is the equilibrium (saturation) concentration of an individual compound i for dissolution out of a complex organic mixture [$M L^{-3}$], χ_i the mole fraction of the component i in the mixture [-], γ_i the activity coefficient of the component i in the organic mixture [-], $S_{w,i}$ the water solubility of the pure compound i [$M L^{-3}$], n_i the number of moles of component i in the mixture and m the total number of components in the mixture.

The activity coefficient in the organic mixture, describing the deviation of the component i from the ideal behaviour, is in many cases unity or very close to 1.

For compounds which in their pure form are crystalline solids at ambient temperature, but exist in the mixture as a liquid at the same temperature (e.g. many PAHs), $S_{w,i}$ in Eq (5.1) must be replaced by the aqueous solubility of the subcooled liquid. After LANE and LOEHR (1992), the subcooled liquid solubility can be calculated as:

$$\log S_{w,i}^{scl} = \log S_{w,i} + 0.01 \cdot (T_m - T) \quad (5.3)$$

with $S_{w,i}^{scl}$ the aqueous solubility of the subcooled liquid [$M L^{-3}$], $S_{w,i}$ the aqueous solubility of the pure crystalline substance [$M L^{-3}$], T_m the melting temperature of the pure

crystalline substance [$^{\circ}C$] and T the actual temperature of the system [$^{\circ}C$].

For simplification, in dissolution calculations it is often assumed that the composition of the mixture remains unchanged as the dissolution process advances, and hence that the saturation concentrations do not change during time. This simplification, combined with a limited number of compounds for which the concentration in the mixture has been analysed (usually only 16 EPA PAHs), may lead to an erroneous course of calculated saturation concentrations during time.

Assuming a certain volume of porous medium contaminated with residual NAPL of known composition, the change of the saturation concentrations of individual compounds from the mixture due to advancing dissolution can be simulated. It is assumed that the dissolution out of residual phase takes place at equilibrium and the concentration of each component in the aqueous phase at any time and at any point in the water within the contaminated volume is equal to the saturation concentration calculated according to Raoult's law. The density and average molar weight of the NAPL are assumed to remain constant during dissolution.

For each time step t (number of pore volumes exchanged), it is accounted for the change in tar composition due to dissolution and the actual saturation concentration can be calculated.

The mass of component i transferred into the aqueous phase from $t-1$ to t is given by:

$$mw_i^t = V_w^t \cdot c_{sat,i}^{t-1} \quad (5.4)$$

V_w^t is the water volume exchanged from $t-1$ to t [L^3] and $c_{sat,i}^{t-1}$ the saturation concentration of component i , assumed to be constant during one time step [$M L^{-3}$].

The mass of the component i remained in the organic phase after the actual time step is then:

$$mm_i^t = mm_i^{t-1} - mw_i^t \quad (5.5)$$

and the number of moles of component i in the organic phase:

$$n_i^t = \frac{mm_i^t}{M_i} \quad (5.6)$$

with M_i - the molar weight of component i [M mole⁻¹].

The total mass of the organic phase left after the time step t is:

$$m_{tar}^t = m_{tar}^{t-1} - \sum_{i=1}^m mw_i^t \quad (5.7)$$

m is the number of water soluble components in the organic mixture.

The number of moles of tar left after the time step t is then:

$$n_{tar}^t = \frac{m_{tar}^t}{M_{tar}} \quad (5.8)$$

At this point, the saturation concentrations are recalculated from the new tar composition. The new mole fraction of the component i is:

$$\chi_i^t = \frac{n_i^t}{n_{tar}^t} \quad (5.9)$$

and, according to Raoult's law, the new saturation concentration used for the calculations at the next time step ($t+1$) is:

$$c_{sat}^{t+1} = \chi_i^t \cdot S_{w,i} \quad (5.10)$$

where $S_{w,i}$ is the water solubility of the component i (for solids: the subcooled liquid solubility) [M L⁻³].

5.1.2 Mass Transfer through Liquid Boundary Layers: Dissolution Kinetics from NAPL Blobs

The mass flux of a chemical species across an interface between two phases results from differences between the chemical potentials of that species in the two phases. For dissolution out of a organic mixture, the maximum (equilibrium) concentration of any species is given by Raoult's law (Eq. 5.1).

Assuming that there is no chemical reaction and no mass accumulation at the interface between the organic and the aqueous phase, the inter-phase mass transfer process involves diffusion through the bulk organic phase toward the interface and diffusion and convection/dispersion away from the interface

into the bulk aqueous phase. At the interface, the concentration ratio of the species in the two phases at equilibrium is given by its NAPL/water partition coefficient. In chemical engineering, this process has been traditionally described by the stagnant two-film model and this also applies for dissolution out of residual NAPL. The model approximates the tar-water interface by introducing two films adjacent to the interface, one in the organic, the other in the aqueous phase (stagnant water film).

The molecules passing from the organic into the aqueous phase have to overcome successively the resistance to diffusion located in each film - resistance in series. The rate of the overall mass transfer is therefore controlled by the highest resistance to diffusion.

The resistance to diffusion in the organic film is given by the ratio between the film thickness and the diffusion coefficient of the species in the organic phase. The resistance to diffusion in the stagnant water film equals the ratio between the film thickness and the aqueous diffusion coefficient, multiplied by the partition coefficient of the species between the organic and the aqueous phase. Since tar and tar oil constituents are hydrophobic, their partition coefficient between NAPL and water is much greater than 1. Because the diffusion coefficients in the two phases are roughly similar, from the definition of the resistance in each film it results that the resistance to mass transfer in the water film is much higher than in the organic film, so that the latter can be neglected (at least at early times).

With these considerations, the rate of inter-phase mass transfer during dissolution out of a NAPL into water can be approximated by a single-resistance, linear-driving-force model, with the resistance entirely located in the stagnant water film (GRATHWOHL, 1998; LOYEK, 1998). According to Fick's 1st law, the mass flux F of a compound dissolving out of a organic mixture (blobs or ganglia trapped in a porous medium) and passing a stagnant water film of thickness δ is given by :

$$F = \frac{D_{aq}}{\delta} (c_{sat} - c_i) \quad (5.11)$$

D_{aq} is the aqueous diffusion coefficient of the component i [L² T⁻¹], δ the thickness of the

stagnant water film [L], c_{sat} the saturation concentration of component i for dissolution out of the mixture [M L⁻³] and c the concentration of the component i in the mobile (aqueous) phase [M L⁻³].

5.1.3 Mass Transfer Coefficients

The mass transfer coefficient for dissolution k_{diss} [L T⁻¹] is:

$$k_{diss} = \frac{D_{aq}}{\delta} \quad (5.12)$$

The film thickness δ , and hence k_{diss} cannot be measured directly. δ depends on various physical parameters of the mobile and the immobile phase (water viscosity and water density, linear flow velocity, NAPL density and well as NAPL residual saturation, grain diameter and porosity of the porous medium).

In porous media, the overall mass flux due to dissolution furthermore depends on the total volume and interfacial area of the NAPL. For spherical NAPL blobs, the specific interfacial area NAPL-water (i.e. the surface area NAPL/water per unit volume of porous medium) A_0 [L² L⁻³] is given by:

$$A_0 = \frac{3 \cdot \theta}{r_b} \quad (5.13)$$

where θ is the NAPL-filled porosity [L³ L⁻³] and r_b the average blob radius [L].

In reality, only a fraction of A_0 is accessible for mass transfer into the flowing water. This parameter is again not directly measurable.

For dissolution of pools (extensively investigated by LOYEK, 1998), the specific interfacial area NAPL-water is much lower than for blobs, leading to much longer overall duration for complete dissolution.

In chemical engineering, the mass transfer coefficient for transport through liquid boundary layers is calculated using the Sherwood number Sh , a dimensionless parameter relating interface mass transport resistances to molecular mass transport resistances:

$$Sh = \frac{k_{diss} \cdot d}{D_{aq}} \quad (5.14)$$

d is a characteristic length, usually set equal to the mean grain diameter [L].

This equation does not explicitly account for the effective, specific interfacial area for dissolution. For the calculation of dissolution rates accounting also for the interfacial area, a modified Sherwood number Sh' has been defined:

$$Sh' = \frac{k_{diss} \cdot A_0 \cdot d^2}{D_{aq}} \quad (5.15)$$

The Sherwood number has traditionally been calculated from empirical equations typically based on the Gilland-Sherwood correlation, of the type (WELTY et al., 1969):

$$Sh = a + b \cdot Re^m \cdot Sc^n \quad (5.16)$$

Re is the Reynolds number [-], Sc the Schmidt number [-] and a , b , m , and n are empirical constants.

E.g. for laminar flow in packed beds FITZER et al. (1995) found:

$$Sh = 1.9 \cdot Re^{0.5} \cdot Sc^{0.33} \quad (5.17)$$

POWERS et al. (1994) derived following empirical correlation for dissolution of naphthalene spheres:

$$Sh = 36.8 \cdot Re^{0.654} \quad (5.18)$$

Many similar equations have been obtained by various authors for the modified Sherwood number for dissolution of NAPL blobs or ganglia trapped in porous media (compilation in GRATHWOHL, 1997). As Sh' also accounts for the NAPL properties relevant for the mass transfer, these correlations also contain the NAPL-filled porosity θ . MILLER et al. (1990) for example found:

$$Sh' = 12 \cdot Re^{0.75} \cdot Sc^{0.5} \cdot \theta^{0.6} \quad (5.19)$$

The dimensionless Re number relating the inertial forces to the viscous forces (or the flow velocity to the momentum velocity) is given by:

$$Re = \frac{v_a \cdot d}{v_w} \quad (5.20)$$

with:

$$v_w = \frac{\eta_w}{\rho_w} \quad (5.21)$$

where v_a is the linear water flow velocity [$L T^{-1}$], ρ_w the water density [$M L^{-3}$], η_w the dynamic viscosity [$M L^{-1} T^{-1}$] and ν_w the cinematic viscosity of water [$L^2 T^{-1}$].

For water flow through natural porous media (linear flow velocities of few meters per day) Re is usually less than 1 (GRATHWOHL, 1998).

The dimensionless Sc number relating the diffusivity of momentum to the diffusivity of mass is defined as:

$$Sc = \frac{v_w}{D_{aq}} \quad (5.22)$$

For many organic compounds in water, Sc may be considered as constant and is approximately equal to 2600 (GRATHWOHL, 1998).

Each of the empirical equations presented above has the disadvantage that it applies only for the exactly defined system it has been derived for. Most of them do not account for the heterogeneity of the porous media and of the NAPL distribution. For natural systems, mass transfer due to dissolution can only be roughly approximated, as the most parameters needed for these correlations are not exactly known and some parameters have to be approximated.

5.1.4 Length of the Mass Transfer Zone (Saturation Length)

As the groundwater passes a region contaminated by residual NAPL blobs, the aqueous concentration of the component i increases due to mass transfer normal to the flow direction according to:

$$\frac{c_i}{c_{sat,i}} = 1 - \exp\left(\frac{-k_{diss} \cdot A_0 \cdot x}{v_a}\right) \quad (5.23)$$

with c_{sat} the saturation concentration of component i for dissolution out of the mixture [$M L^{-3}$], c_i the concentration of the component i in the mobile (aqueous) phase [$M L^{-3}$], k_{diss} the mass transfer coefficient [$L T^{-1}$], A_0 the specific interfacial area NAPL/water [$L^2 L^{-3}$], v_a the linear water flow velocity [$L T^{-1}$] and x the distance in the flow direction [L].

If the concentration in the aqueous phase is close to zero, the overall flux (Eq. 5.11) linearly depends on the components concentration at the interface and the aqueous concentration increases linearly with the flow distance x :

$$\frac{c}{c_{sat}} = \frac{k_{diss} \cdot A_0 \cdot x}{v_a} \quad (5.24)$$

The length of the mass transfer zone X_s [L], defined as the distance in the flow direction after which the water gets saturated with the component i is obtained from Eq. (5.24) for $c/c_{sat}=1$ (GRATHWOHL, 1998):

$$X_s = \frac{v_a}{k_{diss} \cdot A_0} \quad (5.25)$$

With Eq. (5.25), the length of the mass transfer zone X_s can be estimated after calculating ($k_{diss} \cdot A_0$) from the modified Sherwood number Sh' using empirical correlations as shown above. X_s represents the shortest distance in the flow direction after which maximum (saturation) concentration may be expected in the water. Within the mass transfer zone, the aqueous concentration is lower than saturation (allowing mass transfer). If the observation scale is greater than the length of the mass transfer zone, equilibrium is reached and the measured concentration equals the saturation concentration. Because k_{diss} is a function of the aqueous diffusion coefficient D_{aq} which for many compounds is almost constant ($5 \cdot 10^{-10} m^2/s$ at $10^\circ C$, the average groundwater temperature) and does not depend on other compound-specific parameters, it results that the length of mass transfer zone for dissolution is almost the same for any tar constituent.

At small scale (laboratory) and common hydraulic gradients, saturation is achieved after relatively short distances (in the range of centimetres) (GRATHWOHL, 1998; WEIB, 1998). Under field conditions, the distance after which the water passing the domain contaminated by residual blobs or ganglia gets saturated is variable and longer (in the range of meters) than in column experiments. This is also due to aquifer heterogeneity and heterogeneous distribution of the organic phase, leading to 'dissolution fingering' (MAYER and MILLER, 1996; IMHOFF and MILLER, 1996; IMHOFF et al., 1996).

Fig. 5.1 shows the variation of the saturation length as a function of the mean grain diameter (as it results using different correlations for the calculation of the mass transfer coefficient), for a residual saturation of 0.1 and a linear flow velocity of 14.8 m/d (these values apply for the column experiments with disturbed aquifer material which will be discussed further).

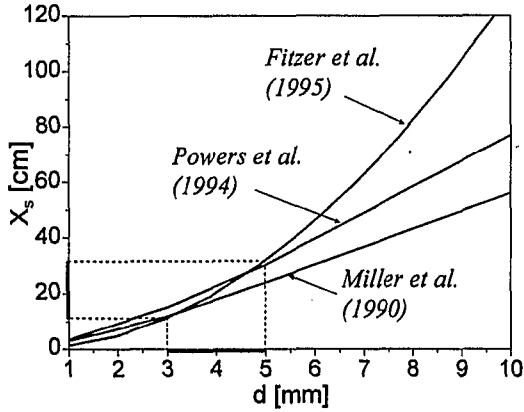


Fig. 5.1: Variation of the saturation length X_s with the mean grain diameter resulting from different correlations for the modified Sherwood number (FITZER - Eq. (5.17), POWERS et al. - Eq. (5.18) and MILLER et al. - Eq. (5.19)). The calculations were made for a residual saturation $S^0 \approx 0.1$; $v_a = 14.8$ m/d, $D_{aq} = 5 \cdot 10^{-10}$ m²/s. For grain diameters of 3-5 mm, the saturation length is in the range of 10-30 cm.

The saturation length increases for high flow velocities e.g. due to steep hydraulic gradients – forced (e.g. during classic remediation techniques such as ‘pump and treat’) or natural (locally encountered at some sites, e.g. ‘Testfeld Süd’ - BÖSEL, 1998; HERFORT, 1999). Such a case is advantageous in terms of duration for complete dissolution, as long as this occurs at non-equilibrium, i.e. not at maximum gradients (aqueous concentrations lower than saturation).

5.1.5 Retardation of the Dissolution Front

For NAPL blobs, the retardation factor of the dissolution front for the species i can be defined as the ratio between the overall mass of the component i (dissolved in the pore water plus contained in the NAPL) and the mobile mass (dissolved in the pore water) in a certain volume of contaminated (GRATHWOHL, 1998):

$$R_i = \frac{c_{sat,i} \cdot (1 - S^0) + f_i \cdot \rho_{tar} \cdot S^0}{c_{sat,i} \cdot (1 - S^0)} \quad (5.26)$$

$c_{sat,i}$ is the saturation concentration of the compound i for dissolution out of the mixture [M L⁻³], S^0 the initial NAPL residual saturation [-] (NAPL volume per volume of the porous medium), f_i the mass fraction of component i in the NAPL [-] (mass i per mass NAPL) and ρ_{tar} the density of the NAPL (tar) [M L⁻³].

The retardation factor of the dissolution front advancing through the contaminated domain in the flow direction is compound-specific. As it is a function of the saturation concentration of the component, according to Raoult’s law, it depends on its aqueous solubility and on the concentration (molar fraction) of the component in the NAPL. Because the dissolved mass of a given component is much smaller than the mass present in the NAPL, the term $c_{sat} (1 - S^0)$ in the numerator of Eq.(5.26) is much smaller than $(f_i \rho_{tar} S^0)$ and may be neglected. The retardation factor R [-] can be then approximated by:

$$R_i = \frac{f_i \cdot \rho_{tar} \cdot S^0}{c_{sat} \cdot (1 - S^0)} \quad (5.27)$$

If the mass fraction f_i of the species i in the tar is expressed as a function of the molar fraction χ_i ($f_i = \chi_i M_i / M_{tar}$) and considering that the saturation concentration of the component i is by definition equal to its aqueous solubility $S_{w,i}$ times the molar fraction χ_i in the NAPL, Eq. (5.27) becomes:

$$R_i = \frac{1}{S_{w,i}} \cdot \frac{M_i}{M_{tar}} \cdot \rho_{tar} \cdot \frac{S^0}{1 - S^0} \quad (5.28)$$

From the last equation it results that the retardation factor of the dissolution front for component i is inverse proportional to its aqueous solubility. This means that, when they are dissolving out of the same NAPL, the dissolution front of compounds with higher saturation concentration (e.g. Nap) advances faster in the flow direction than the front of the less soluble ones (e.g. Py). Since for the most tar constituents relevant for dissolution, the ratio M_i / M_{tar} is between 0.6 and 1.1, it follows that the contribution of this ratio to the value of

R_i is relative close to unity and Eq. (5.28) simplifies to:

$$R_i \cong \frac{\rho_{tar}}{S_{w,i}} \cdot \frac{S^0}{1-S^0} \quad (5.28 a)$$

Because the density of many NAPLs is very close to 1 kg/l, for very low residual saturation ($S^0 < 0.1$) we get finally to a very simple approximation for the retardation factor:

$$R_i \cong \frac{S^0}{S_{w,i}} \quad (5.28 b)$$

with both the NAPL density and the aqueous solubility expressed in kg/l or equivalent.

The retardation factor of the dissolution front equals the number of pore volumes that have to

be exchanged for complete removal of the residual component i (remediation time) by dissolution from the residual phase.

5.1.6 Possible Concentration-Time Profiles for Dissolution out of Residual NAPL Blobs

During dissolution out of residual NAPL blobs, the concentration in the water leaving the area contaminated with residual phase are determined not only by the composition of the organic phase, but also depend on the hydrodynamic conditions in the contaminated domain. Assuming some homogeneous distribution of the NAPL blobs (no dilution) and neglecting the hydrodynamic dispersion, the following situations may be encountered (Fig. 5.2):

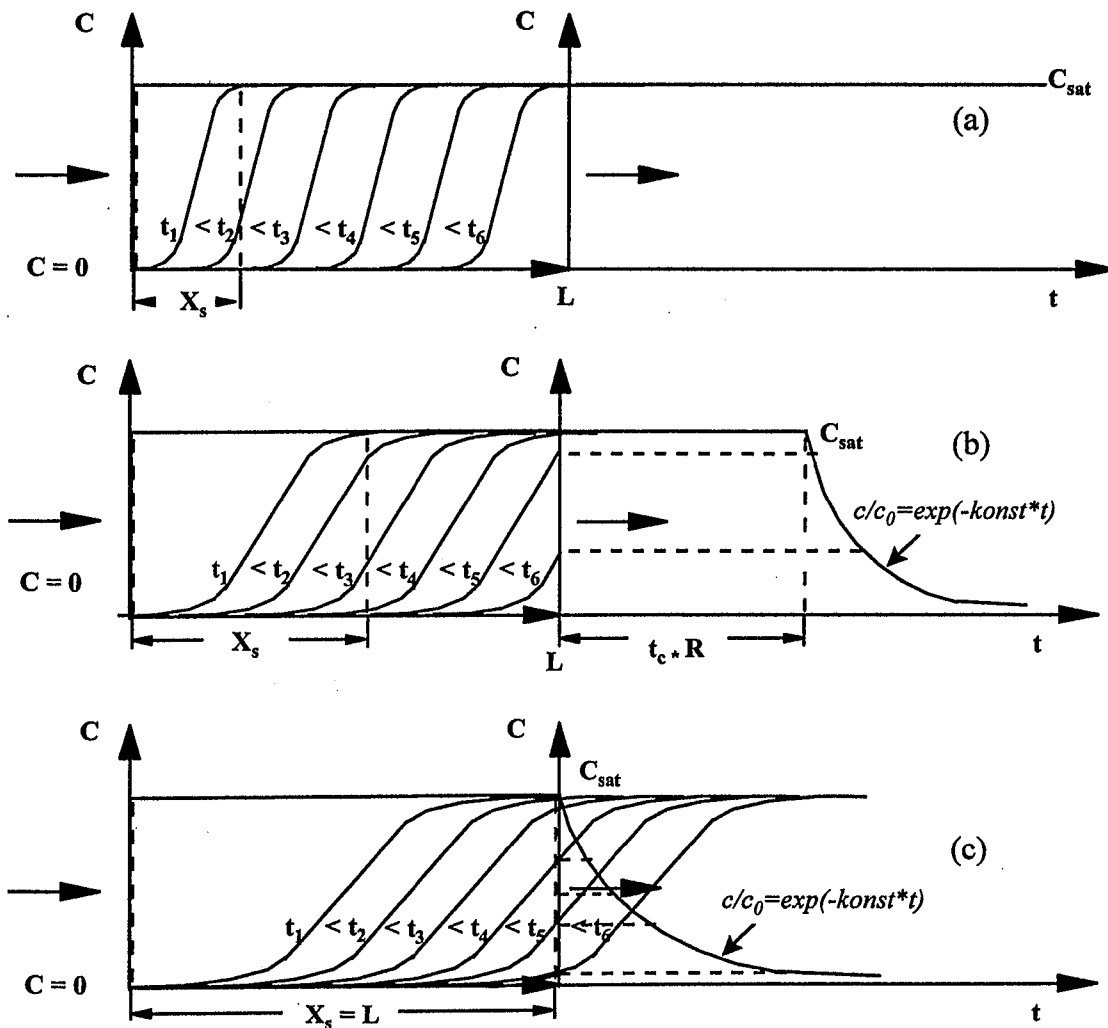


Fig. 5.2: Possible concentration profiles at the column outlet (end of the domain containing residual NAPL blobs) as a function of the length of the mass transfer zone X_s compared with the length L of the contaminated domain, assuming a homogeneous porous medium, homogeneous distribution of the blobs and no hydrodynamic dispersion (these conditions may apply quite well in small scale column experiments with disturbed samples).

- (a): If the length of the mass transfer zone is less than the length of the column, the concentration in the leachate equals the saturation concentration and remains constant over long time periods. The factor $t_c \cdot R$ (t_c - contact time in the column, R - retardation factor of the dissolution front) is longer than the duration of the experiment. This is most often the case for 'usual' hydraulic gradients (common groundwater velocities) and common monitoring time periods.
- (b): If the mass transfer zone X_s is long enough, but still shorter than the column (higher linear flow velocities than in the previous case), for each compound, the concentration in the leachate remains constant and equal to c_{sat} until the dissolution front exits the column. From this point, the concentration in the column decreases exponentially. The duration with constant c_{sat} is given by the product $t_c \cdot R$; it depends on the residual saturation S^0 and is compound-specific.
- (c): With further increasing linear flow velocities, the saturation length becomes as long as the column. Only at t_0 (beginning of the experiment), the concentration is close to c_{sat} , and then it decreases exponentially. There is no concentration plateau, since the contact time in the column is equal to the contact time in the mass transfer zone. If the saturation length X_s becomes to exceed the length of the column (contaminated domain) L , dissolution equilibrium is not attained. The decrease in concentration is still exponential, but the observed maximum (initial) concentration is always lower than saturation. For this reason, if the aim of the experiment is to determine saturation concentrations for dissolution out of residual phase, it is important to design column experiments such as the length of the mass transfer zone is not longer than the contaminated domain. Otherwise the saturation concentrations are not achieved in the column effluent. If the mass transfer zone is not longer than the column, but the concentration observed initially is lower than the equilibrium concentration, then the mass loss is very probably due to biodegradation (provided no sorption occurs and there is no dilution in the system).

5.2 Materials and Methods

5.2.1 Coal Tar Samples from 'Testfeld Süd'

Prior to be analysed, the tar samples from the field were centrifugated in order to separate eventual amounts of water. The samples from the bottom of the aquifer (e.g. B55) also contained some solids mobilised during sampling; these could not be separated from the liquid organic phase.

The NAPL composition and the saturation concentrations of individual constituents in water have been determined by extraction with cyclohexane, respectively dialysis (methods also described by PYKA, 1996; LOYEK, 1998).

About 0.2 g tar have been extracted at dark under continuous shaking for two weeks with 40 ml cyclohexane in air-tight headspace glasses. After extraction, the insoluble fraction was separated by centrifugation. 100 μ l extract were diluted with 4 ml cyclohexane, spiked with 5 μ l of an internal PAHs standard (200 mg/l *Nap-d8*, *Ace-d10*, *Phe-d10*, *Chr-d12*, *Pery-d12* in cyclohexane, Restek) and analysed by GC-MS.

For the determination of saturation concentrations, ca 4 g tar were inserted into dialysis tubing (Spectra/Por 6, Roth, cut-off ca 1000 Dalton, 12 mm \varnothing , 10 mm long) and equilibrated with distilled water (ca 300 ml) at dark over several weeks. For the analysis of the 16 EPA PAHs, ca 100 ml of the saturated water were extracted with 10 ml cyclohexane containing 10 μ l internal PAHs-standard 200 mg/l (Restek). The more volatile compounds were extracted with pentane containing 2000 μ g/ml *Fluorobenzene* and *1,2-Dichlorobenzene-d4* in methanol as an internal standard (EPA 524, Supelco). The extracts were analysed by GC-MS as described in Chapter 4 for extracts from water samples.

5.2.2 Experimental Setup for Dissolution out of Residual NAPLs

The contaminant release (emission) out of disturbed and undisturbed aquifer material from the site by dissolution out of residual phase was quantified in the laboratory using long-term column experiments with disturbed and

undisturbed samples. These allow to achieve maximum concentration gradients between the immobile and the mobile phase by constant exchange of the pore water in the column.

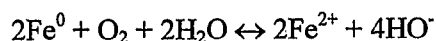
In all samples from the field, the matrix was very heterogeneous, consisting of gravels, sand and silty aggregates.

The disturbed samples (ca 600 g) were homogenised, inserted in glass columns (6 cm Ø) under water saturated conditions (in order to avoid captured air) between two filter layers (quartz sand with 1-2 mm grain diameter) and leached with distilled water using the methodology described by WEIB (1998). The effective length of the sample between the two quartz sand layers was about 12 cm.

Additionally, undisturbed samples were leached similarly to the disturbed ones, using the PVC drilling liners (ca 10 cm Ø, 40 to 100 cm long) as a column (Fig. 5.3). The liners were sealed by using tight inlet/outlet fittings and PTFE tape. The rest of the experimental setup (stainless steel tubing, fittings, pump, etc.) was the same as for the disturbed samples. The linear flow velocity in the undisturbed samples was 2 m/d.

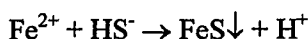
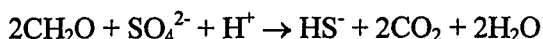
In the experiments for dissolution out of undisturbed material, the aqueous oxygen content was lowered to almost 0 mg/l by passing the water through an iron filing filter before entering the contaminated column. An indication of redox processes was the formation of a black precipitate (sulfides) in the column, possibly indicating some anaerobic degradation of the organic compounds. The chemical processes in the column associated with the increased iron content in the influent water could be described as follows:

By passing the water through the iron filing filter prior to entering the column, the oxygen concentration decreased to almost zero as a result of the rapid corrosion of iron predominantly by reaction with dissolved oxygen (JOHNSON and TRATNYEK, 1995):



The water entering the column was loaded with ferrous ions. Iron precipitated as sulfide during the microbial induced sulfate reduction of

dissolved hydrocarbons (CHRISTENSEN et al., 1994):



The presumption that iron precipitated in the column as sulfides was supported by the fact that at the end of the leaching experiment, when the aquifer material removed from the column came in contact with atmospheric oxygen, the black precipitate became orange-reddish as the Fe-sulfide was oxidised to iron hydroxide and sulfate ions.

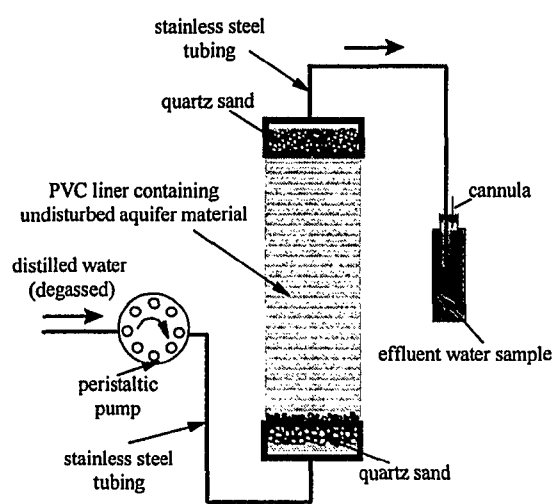


Fig. 5.3 Experimental design of column tests with undisturbed aquifer material (in PVC liners).

At the end of the experiment, the aquifer material was extracted for the determination of the amount of contaminants left in the solids after leaching. After all solids were removed and the outlet fittings and tubing were cleaned, the empty liner was leached for several days with clean water in order to determine the eventual background concentrations in the leachate caused by desorption out of the liner material (PVC). The background was set equal to the maximum concentration in the leachate from the empty liner. For the undisturbed samples, the concentrations measured in the column effluent have been corrected by the determined background.

The material removed from the top and the bottom of the liner in order to be replaced by the filter sand was homogenized, inserted into a glass column and leached at the same time with the undisturbed sample using degassed water at a linear flow velocity of 2 m/d. The

concentrations of PAH and BTEX were monitored in the column leachate.

The effluent water from columns containing both disturbed or undisturbed samples was collected in glass vials containing cyclohexane as a solvent trap for the PAH analysis, respectively in air-tight headspace vials for the analysis of volatile compounds. The great amount of water used during the long duration of the experiments (in average 3 months for each column) did not permit to collect the entire leachate. The sampling interval was shorter during the first days of each experiment, (to assess as good as possible e.g. eventual concentration peaks), and was longer at later times (of the order of days), when no significant variations in concentration were expected. The cyclohexane extracts have been analysed by GC-MS, and the more volatile substances were purged directly from the aqueous samples and also analysed by GC-MS (see further methods for GC-MS and Purge and Trap GC-MS analysis).

5.2.3 Samples Used in Column Experiments for Dissolution

All samples for the column experiments - disturbed and undisturbed - were taken at 'Testfeld Süd' from the saturated zone during drilling of the wells which were afterwards equipped with multilevel groundwater sampling systems. These wells are located immediately at the downstream border of the source area (Fig. 2.1). In some samples NAPL was present as a residual phase (e.g. in B55, B49), in others tar constituents (mainly PAHs) were sorbed into the aquifer material (e.g. in B56). Table 5.1 gives an overview of the column experiments which will be discussed in Chapter 5.3.

Table 5.1: Samples used in column tests and corresponding linear velocities for the quantification of contaminant release by dissolution out of residual NAPL blobs (results in Chapter 5.3). The sample names are those of the corresponding groundwater wells (see Fig.2.1).

Sample (well)	Depth [m]	Type	Linear flow velocity [m/d]
B55	4.5 - 5	disturbed	14.8
B55	5 - 5.5	disturbed	14.8
B49	7 - 7.7	undisturbed	2 m/d, 5 m/d, 0.7 m/d
B49	7 - 7.7	disturbed	2 m/d

5.2.4 Analysis of PAHs from Contaminated Aquifer Material

Because of the difficulty to obtain representative samples, the contaminant content in the solids (sorbed or residual phase) was determined by solvent extraction only at the end of the leaching experiments. The aquifer material from the columns B55C1 and B55C2 (discussed in Chapter 5.2) have been extracted using acetone and cyclohexane as a solvent using a method recommended by LfU Baden-Württemberg, as described by WEIB, 1998. At least for aged samples, this method proved to be not very effective, especially for higher molecular compounds, leading to considerable error in the mass balance in column experiments (see Chapter 5.2); in the desorption experiments it was replaced by hot-methanol extraction (see Chapter 6). The PAHs in the cyclohexane extracts were analysed by GC-MS as described in Chapter 4 for water samples.

5.3 Results and Discussion

5.3.1 Source Composition at the Site

As already mentioned, the source of subsurface contamination at 'Testfeld Süd' is very complex, mainly due to the contamination history and specific site situation as outlined in the following:

- a variety of distillation plants and by-products disposal facilities spread over an area of about 200,000 m²;
- many different organic distillation fractions resulting from the gas production and the subsequent by-product processing;
- individual facilities being operated over different time intervals between 1870-1970, leading to different ages of the underground spills (20 to 100 years);
- a network of underground structures such as tanks or pipelines connecting the individual facilities;
- extensive and repeated war damage.

After several sampling campaigns at 'Testfeld Süd', some organic phase could be taken into the laboratory and analysed. The tar oil samples were taken from the following groundwater wells: B15, B16, B50, B55 and B56. In the first three wells, the organic phase was floating on the groundwater table, whereas the tar oils in B55 and B56 are denser than water and were

pumped from the bottom of the aquifer when the wells have been set up, as well as during groundwater multilevel sampling.

Because of the numerous compounds quantified and the long duration of the analyses, only one parameter (i.e. for each tar sample either the saturation concentration or the wt %) was determined experimentally for individual compounds; the other was calculated according to Raoult's law (saturation concentrations from wt % or vice versa).

For the determination of the PAH content, all coal tar samples excepting the one from B55 were extracted with cyclohexane as described earlier (Chapter 4). The cyclohexane extracts were analysed by GC-MS for the 16 EPA PAHs. From this analyse, the concentration of the quantified compounds (wt %) in coal tar was directly obtained. The saturation concentrations were calculated from Raoult's law, assuming for the organic phase (tar) an average molar weight of 250 g/mole and $\gamma_i=1$:

$$c_{sat,i} = S_{w,i} \cdot \chi_i = S_{w,i} \cdot \frac{\frac{m_i}{M_i}}{\frac{m_{tar}}{M_{tar}}} \quad (5.29)$$

where m_i denotes the mass of the component i in the organic phase [M] and m_{tar} the total mass of the organic phase [M].

The saturation concentrations of 10 monocyclic aromatics, *Ina*, *Ine* and *Bf*, as well as for the 16 EPA PAH from B55 were determined using the dialysis method described in Chapter 5 (the saturated water from the tar sample B55 was extracted with cyclohexane and the extract was analysed for PAH as described in Chapter 4.1). For the more volatile compounds (MAHs, *Ina*, *Ine* and *Bf*), the saturated water samples resulted from the dialysis experiment were extracted with pentane and analysed by GC-MS. For some heterocyclic compounds saturation concentrations were also quantified. The coal tar composition (wt %) for B55 was then calculated according to Raoult's law using the measured saturation concentrations:

$$g_i = \frac{c_{sat,i}}{S_{w,i}} \cdot \frac{M_i}{M_{tar}} \times 100 \quad (5.30)$$

g_i is the concentration of the component i in the tar [wt %].

Table 5.2 shows the saturation concentrations of PAHs, MAHs and heterocycles determined for the organic phases from the site. In Table 5.3 the compositions of NAPLs from 'Testfeld Süd' expressed in wt % are compared with those measured for the 16 EPA PAH by LOYEK (1998) for a 'fresh' commercial tar ('Rütgers').

Table 5.2: Saturation concentrations for NAPLs from 'Testfeld Süd' (all determined by dialysis, except for PAHs from B15, B16, B50 and B56 - calculated from wt % knowing the aqueous solubilities of the pure substances (for solids, the subcooled liquid solubility) and assuming for tar an average molar weight of 250 g/mol).

Tar Sample →		B15 *	B16 *	B50 *	B23 *	B56 **	B55 **	Rütgers-tar Sat. Conc. [µg/l] (measured, LOYEK 1998)
Substance (Molar weight [g/mole])↓	Aqueous Solubility [µg/l]	Sat. Conc. [µg/l]	Sat. Conc. [µg/l]	Sat. Conc. [µg/l]	Sat. Conc. [µg/l]	Sat. Conc. [µg/l]	Sat. Conc. [µg/l]	
Nap (128)	119,200 ^{scl}	22,695	27,989	27,152	22,159	3,149	466	24,640
Any (152)	84,500 ^{scl}	1,023	1,339	1,214	146	66.7	18.7	#
Ace (154)	20,000 ^{scl}	585	658	278	4,933	33.7	1,359	29
Fln (166)	18,100 ^{scl}	456	524	607	1,770	43.8	482	240
Phe (178)	8,320 ^{scl}	277	334	469	626	25.0	286	230
Ant (178)	6,380 ^{scl}	40.5	48.7	55.2	70.8	3.41	3.08	40
Fth (202)	2,110 ^{scl}	16.8	20.4	22.4	10.1	0.940	8.79	26
Py (202)	2,720 ^{scl}	14	17.2	16.3	4.84	0.707	8.27	16
BaA (228)	330 ^{scl}	0.658	0.788	0.313	n.d.	0.004	n.d.	2.1
Chr (228)	440 ^{scl}	1.02	1.30	0.521	n.d.	0.01	n.d.	1.8
BbF-BkF (252)	350 ^{scl}	0.116	0.145	0.019	1.93	n.d.	n.d.	0.8
BaP (252)	140 ^{scl}	0.141	0.119	0.017	n.d.	n.d.	n.d.	< 0.3
Indeno (276)	1,660 ^{scl}	0.040	0.048	n.d.	n.d.	n.d.	n.d.	< 0.3
DahA (278)	130 ^{scl}	n.d.	n.d.	n.d.	n.d.	n.d.	n.d.	< 0.3
BghiP (276)	27 ^{scl}	0.010	0.011	n.d.	n.d.	n.d.	n.d.	< 0.4
Ina (118)	100,000	355	360	553	368	1.54	106	#
Ine (116)	300,000	9,958	10,288	8,184	1,255	17.5	11.2	#
1-MetNap (142)	28,500	539	551	592	390	10.7	117	#
2-MetNap (142)	31,700 ^{scl}	1,584	1,593	1,671	1,998	23.9	1,661	#
Bph (154)	130,000 ^{scl}	648	1.99	450	1,269	18.8	1,568	#
Benz (78)	1,770,000	5,853	5,633	7,541	132	38.4	62.6	#
Tol (92)	515,000	5,683	5,848	4,198	176	19.8	15.5	#
EtBenz (106)	152,000	920	993	599	185	4.27	58.9	#
p-Xyl (106)	185,000	3,120	3,287	3,500	543	12.1	120.8	#
o-Xyl (106)	175,000	1,050	1,107	1,191	237	5	47.4	#
IsoPb (120)	55,000	6.08	6.40	12.4	4.96	n.d.	2.56	#
Pb (120)	50,000	7.40	7.66	7.84	2.39	n.d.	0.780	#
1,3,5-Tmb (120)	75,000	2,424	2,512	4,194	614	1.87	145	#
1,2,4-Tmb (120)	57,000	411	423	637	107	3.13	15.6	#
1,2,3-Tmb (120)	50,000	129	133	210	37.5	2.08	6.16	#
Bf (118)	220,000	116	119	65.2	14.5	6.32	27.1	#
Bth (134)	162,100 ^{scl}	1,276	1,310	1,092	590	11.6	93.9	#
Dbf (168)	17,600 ^{scl}	668	656	342	1,820	3.19	1,841	#
Carb (167)	199,200 ^{scl}	246	261	139	58.9	n.d.	n.d.	#

*tar oil sample from top of the aquifer (floating on the groundwater table); ** tar oil sample from bottom of the aquifer; n.d.- not detected; # - not determined; scl - subcooled liquid

All analysed tar oil samples show lower PAH contents than the fresh 'Rütgers'-tar, but it may be assumed that the initial composition of tar oils at the time when the spills occurred, respectively when the organic phase was disposed, was not very different from one location to another and probably similar to that of a commercial coal tar. This probably applies for tars disposed in pits.

It is not possible to determine whether the tar oils found downgradient (B55, B56) have been spilled at that location (Fig. 2.1) or originate

from sources located up-gradient and have migrated slowly as separate phase in the groundwater flow direction.

In the samples from B15, B16 and B50, the PAH content is quite similar and dominated by *Nap*. The wells B15 and B16 are located at the border of the same coal tar pit (presumably at least ca 20 m³), where tar has been disposed from 1910 to 1970. Therefore it was expected that the two tar oil samples would be similar, which is the case for the most analysed compounds.

Table 5.3: Composition of tar oils from 'Testfeld Süd', in wt % (determined for PAH by direct extraction of the tars with cyclohexane, for all other compounds as well as for PAHs from B23 and B55 calculated from saturation concentrations obtained in dialysis experiments). In brackets: standard deviation where multiple determination available.

Tar Sample → Substance ↓	B15 *	B16 *	B50 *	B23 *	B56**	B55 **	Rütgers-tar Weight % (LOYEK 1998)
	Weight %	Weight %	Weight %	Weight %	Weight %	Weight %	
Nap (128)	9.73 (± 0.080)	12 (± 0.184)	11.6 (± 0.056)	9.50	1.35	0.200	12.3 (± 0.08)
Any (152)	0.737 (± 0.004)	0.963 (± 0.038)	0.874 (± 0.003)	0.105	0.048	0.013	1.88 (± 0.02)
Ace (154)	1.80 (± 0.025)	2.03 (± 0.047)	0.859 (± 0.010)	15.2	0.104	4.19	0.084 (± 0.0006)
Fln (166)	1.68 (± 0.039)	1.93 (± 0.053)	2.23 (± 0.064)	6.51	0.161	1.77	1.46 (± 0.01)
Phe (178)	2.37 (± 0.029)	2.86 (± 0.038)	4.02 (± 0.018)	5.36	0.214	2.44	4.44 (± 0.02)
Ant (178)	0.452 (± 0.018)	0.544 (± 0.006)	0.616 (± 0.005)	0.790	0.038	0.034	0.75 (± 0.01)
Fth (202)	0.642 (± 0.004)	0.782 (± 0.008)	0.856 (± 0.009)	0.388	0.036	0.337	2.10 (± 0.1)
Py (202)	0.417 (± 0.002)	0.510 (± 0.005)	0.484 (± 0.006)	0.144	0.021	0.246	1.28 (± 0.06)
BaA (228)	0.182 (± 0.003)	0.218 (± 0.001)	0.087 (± 0.0005)	n.d.	0.0012	n.d.	0.76 (± 0.05)
Chr (228)	0.211 (± 0.006)	0.269 (± 0.007)	0.108 (± 0.001)	n.d.	0.0019	n.d.	0.74 (± 0.06)
BbF-BkF (252)	0.167 (± 0.046)	0.209 (± 0.048)	0.028 (± 0.0004)	2.78	n.d.	n.d.	1.00 (± 0.06)
BaP (252)	0.101 (± 0.005)	0.086 (± 0.021)	0.013 (± 0.002)	n.d.	n.d.	n.d.	< 0.3
Indeno (276)	0.034 (± 0.003)	0.041 (± 0.002)	n.d.	n.d.	n.d.	n.d.	< 0.3
DahA (278)	n.d.	n.d.	n.d.	n.d.	n.d.	n.d.	< 0.3
BghiP (276)	0.043 (± 0.003)	0.047 (± 0.002)	n.d.	n.d.	n.d.	n.d.	< 0.3
Sum 16 EPA PAH	18.5	22.4	21.8	40.8	1.975	9.24	26.8
Ina (118)	0.168	0.168	0.261	0.174	0.00073	0.0016	#
Ine (116)	1.54	1.59	1.27	0.194	0.0027	0.00004	#
1-MetNap (142)	1.22	1.25	1.34	0.886	0.024	0.265	#
2-MetNap (142)	3.60	3.62	3.80	4.54	0.054	3.77	#
Bph (154)	0.307	0.001	0.213	0.602	0.009	0.743	#
Other PAH (non- 16 EPA)	6.84	6.63	6.88	6.4	0.09	4.78	-
Benz (78)	0.103	0.099	0.133	0.002	0.0007	0.000035	#
Tol (92)	0.406	0.418	0.300	0.013	0.0014	0.00003	#
EtBenz (106)	0.257	0.277	0.167	0.052	0.0012	0.000039	#
p-Xyl (106)	0.715	0.753	0.802	0.125	0.0028	0.00006	#
o-Xyl (106)	0.254	0.268	0.289	0.057	0.0012	0.00027	#
IsoPb (120)	0.006	0.006	0.012	0.005	n.d.	0.00005	#
Pb (120)	0.007	0.007	0.007	0.002	n.d.	0.000014	#
1,3,5-Tmb (120)	2.33	2.41	4.03	0.589	0.0018	0.0029	#
1,2,4-Tmb (120)	0.346	0.356	0.537	0.090	0.0026	0.00027	#
1,2,3-Tmb(120)	0.083	0.085	0.134	0.024	0.0013	0.00008	#
Sum 10 MAH	4.5	4.7	6.4	0.959	0.013	0.004	-
Bf (118)	0.025	0.025	0.014	0.003	0.0013	0.002	#
Bth (134)	0.526	0.001	0.450	0.243	0.0047	0.039	#
Dbf (168)	4.49	4.41	2.30	12.2	0.021	12.4	#
Carb (167)	16.4	17.5	9.30	3.94	n.d.	n.d.	#
Sum heterocycles Weight % all compounds determined	21.4	21.9	12.1	16.4	0.027	12.4	- 26.8 (only 16 EPA)

* tar oil sample from top of the aquifer; ** tar oil sample from bottom of the aquifer; n.d.- not detected; # - not determined

The other four tar samples were taken from sources located further down-gradient (in groundwater flow direction). Interestingly, it can be noticed that the longer the distance from B16 to the sources down-gradient, the more advanced the dissolution process of the tar oils is. Due to their much lower MAH and

heterocycles content, it can be concluded that the tar oils from B55 and B23 are obviously more aged (leached) than B15, B16 and B50. From B16/B15 to B23/B55 the content of *Dbf* (the less soluble of the quantified heterocycles) increases, whereas that of the more soluble *Bf* decreases. The same applies e.g. for *Nap* versus

Flu or *Phe*. Due to their great water solubility, the overall concentration of MAHs, *Ine* and *Ina* decreases dramatically in depleted samples.

An interesting behaviour shows *2-MetNap* which has a relative high and constant concentration in the analysed samples.

The tar oil sample from B56 yields extremely low saturation concentrations compared to any other sample. This organic phase has been accidentally mobilised by pumping after the well B56 was set up. The tar was therefore mixed with sediment particles and some water. Although most of the water has been separated by centrifugation prior to the analyse, the organic phase extracted with cyclohexane was mixed with an unknown amount of solids which could not be separated and exactly determined. The same holds for the tar sample from B55. The extracted mass of PAHs refers to the total amount of organic phase plus sediments and leads therefore to lower saturation concentrations of individual compounds (lower wt %).

Although it is difficult to draw conclusions without knowing the initial composition of the NAPL and the exact time of the spills, the expectation is confirmed that during the dissolution process, the more soluble compounds were depleted, whereas the less soluble ones were enriched in the organic phase. The immediate consequence of this behaviour is that the saturation concentrations for dissolution of lower soluble substances out of a mixture increase with time as their concentration (molar fraction) in the mixture increases (Raoult's law). The tar composition varies within the mass transfer zone; whether or not the variation would be measured in the water leaving the area with residual NAPL depends on the length of the mass transfer zone relative to the length of the domain containing residual tar blobs (as outlined in Chapter 5.1.5 with the retardation factor for the dissolution front).

However, there are two facts that apparently are in contradiction with this statement: the extremely high amount of *Ace* in the tar samples from B23 and B55 and the relatively high MAH content, especially *trimethylbenzenes*, in B50.

A possible explanation could be the following: when a substance partitions between two phases (e.g. tar oil and water), the direction of mass transfer depends on the direction of the concentration gradient: the mass flux is oriented from higher concentration towards lower concentration. If some coal tar comes in contact with water in which the concentration of a substance is lower than its saturation concentration out of the tar, there will be some mass transfer (dissolution) out of the mixture into the water until saturation is attained. The actual concentration in the water cannot exceed the saturation concentration out of the mixture. However, there may be imagined a situation in which the organic phase comes in contact with water already containing one of the components of the mixture at a higher concentration than its saturation concentration out of that mixture. The sense of mass transfer is then opposite, out of the water into the mixture, and the organic phase will be enriched with that substance until the saturation concentration out of it equals the concentration in the water. Only when the former exceeds the latter, dissolution of that compound out of the mixture can take place again.

Such a behaviour may apply for *Ace* at 'Testfeld Süd'. This PAH has a relatively high water solubility and, as it will be shown later, it occurs in groundwater at very high concentrations (thousands of $\mu\text{g/l}$ close to the sources and hundreds of $\mu\text{g/l}$ throughout the plume). A typical behaviour of *Ace* observed at all former gas manufacturing plants is its persistence in groundwater due to poor biodegradation (see also Chapter 7 and 8). The aqueous concentrations of *Ace* are therefore high over hundreds of meters distance down-gradient from the first source (area with tar pits) and possibly exceed saturation concentrations out of some aged organic phase encountered downstream at 'Testfeld Süd' (as in B55 or B23). During time, some tar downstream will be enriched in *Ace* due to lack of driving force for dissolution. *Ace* can be released again only if its saturation exceeds the concentration in the by-passing groundwater. Such an organic phase is then acting like a 'deposit' (sink) for *Ace*. The location of individual tar-oil bodies relative to the groundwater flow direction may therefore influence their dissolution behaviour in the

field (this scenario assumes that contaminants are biodegraded only in the aqueous phase.)

A similar effect is eventually responsible for the relatively high amounts of *trimethylbenzenes* in the organic phase from B50: this well is located downstream close to one of the former benzene distilleries at the site where massive MAHs contamination is present (Fig. 2.1).

5.3.2 Simulation of Equilibrium Dissolution out of Residual NAPL Phase from 'Testfeld Süd'

The aim of the following calculations was to verify if and how saturation concentrations are influenced by the variation of tar oil composition as dissolution advances, if not only the 16 EPA PAHs, but also four other polycyclic aromatics, ten monoaromatic hydrocarbons and four heterocycles are taken into account (see also Table 5.2 and 5.3).

The calculations were made for four tar samples from 'Testfeld Süd' (B15, B50, B23 and B55 - see wells location in Fig. 2.1) and for the 'Rütgers' tar-oil, for the latter only the 16 EPA PAHs content being available (data from LOYEK, 1998).

For the simulation of the dissolution out of residual phase, following assumptions have been made:

- the soluble fraction of the organic phase contains only the analysed compounds (Table 5.2 and 5.3), the rest is insoluble and its mass remains constant during time;
- the dissolution out of residual phase takes place at equilibrium and the concentration of each component in the aqueous phase at any time and at any point in the water within the contaminated domain is equal to the saturation concentration calculated according to Raoult's law;
- the tar oil composition at $t=0$ is the one listed in Table 5.3;
- the calculations were made for 100 m³ contaminated aquifer material (25 m² contaminated cross-section normal to the groundwater flow direction), assuming an effective porosity of 0.15 and an initial residual saturation of 2 %; the groundwater velocity is 2 m/d (after BÖSEL 1999, the average value of the water velocity obtained

from tracer tests at 'Testfeld Süd' is 2.25 m/d);

- for the residual organic phase an average molecular weight of 250 g/mole and a density of 1,200 kg/m³ were assumed, both constant during dissolution.

In this simplified case it has not been accounted for the exact geometry of the contaminated domain; in real cases of contamination in the field, the time necessary for complete dissolution depends not only on the total contaminated volume, but also on the length in flow direction containing residual organic phase (because the length of mass transfer zone for dissolution is as great as maximum tens of centimeters, the longer the distance in flow direction where groundwater gets in contact with the residual phase, the longer the time needed for dissolution). Due to the geometry of geological structures, NAPL spills would probably extend rather horizontally (rather „long and flat“ than „short and high/deep“).

For each time step t (number of pore volumes exchanged), it was accounted for the change in tar composition due to dissolution and the actual saturation concentration was recalculated at each step, according to Eqs (5.4) to (5.10).

The development of saturation concentrations of the tar constituents which result for the considered tar oils with the assumptions listed above is presented in Fig. 5.4.

From Fig. 5.4, it results that tar oil samples from different locations have different dissolution behaviour, depending on their composition. As it was expected, dissolution would complete faster for samples for which the process is already relatively advanced (B23, B55) and in which the analysed compounds have a lower concentration (higher percentage of compounds assumed to be insoluble in water). But by the time the water soluble fraction of these tars would be completely dissolved, other samples located up-gradient (B15, B50) would still cause some groundwater contamination, as those would not yet be completely depleted. The tars located down-gradient are thus permanently exposed to already contaminated groundwater, which could lead to enrichment effects as observed in B55 and discussed above for *Ace*.

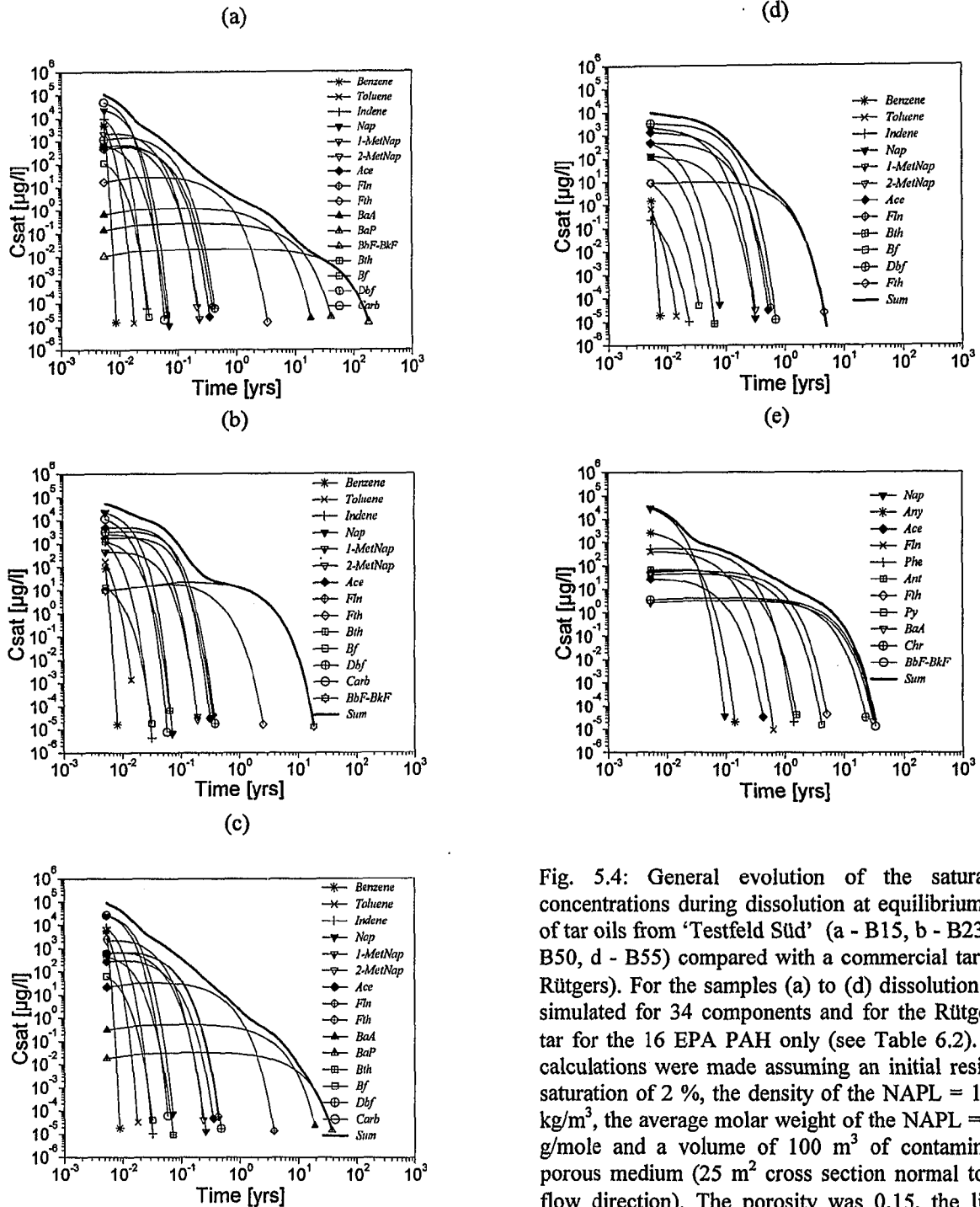


Fig. 5.4: General evolution of the saturation concentrations during dissolution at equilibrium out of tar oils from 'Testfeld Süd' (a - B15, b - B23, c - B50, d - B55) compared with a commercial tar (e - Rütgers). For the samples (a) to (d) dissolution was simulated for 34 components and for the Rütgers-tar for the 16 EPA PAH only (see Table 6.2). The calculations were made assuming an initial residual saturation of 2 %, the density of the NAPL = 1,200 kg/m³, the average molar weight of the NAPL = 250 g/mole and a volume of 100 m³ of contaminated porous medium (25 m² cross section normal to the flow direction). The porosity was 0.15, the linear flow velocity 2 m/d and the contact time 2 d.

The duration in years for complete dissolution resulting from these calculations applies for the most optimistic scenario, as a maximum concentration gradient is considered throughout the dissolution process (the concentration in water at the interface tar/water assumed to be zero at any time for all components) and there is no limitation to mass transfer due to reduced tar/water interfacial area or other effects. Real duration for dissolution under field conditions may be expected to be significantly greater due

to the heterogeneous spatial distribution of tar oil, higher residual saturation leading in the extreme (but not less frequent) cases to formation of pools and to much greater amounts of organic phase than the one considered here for these calculations (100 m³). A very simplified dissolution scenario was assumed here only in order to permit a relative comparison of different tar samples when a more complete chemical analysis of the tar oil was available. For additional factors

influencing the concentration profiles at the end of the contaminated domain see theory in Chapter 5.1.

There is also a small increase in saturation concentrations of low soluble compounds, especially 3ring and 4ring PAH. In order to compare this effect for the investigated samples, the relative increase in concentration was calculated as:

$$\Delta c_i = \frac{c_{\max,i} - c_{i(t=0)}}{c_{i(t=0)}} \cdot 100 \quad (5.31)$$

where Δc_i is the relative increase in concentration of the component i [%], $c_{\max,i}$ the maximum saturation concentration of the component i during dissolution [$M L^{-3}$] and $c_{i(t=0)}$ the saturation concentration of component i at the beginning of dissolution (Table 5.2) [$M L^{-3}$].

The value of Δc in % indicates to what degree the saturation concentration would increase at some later time t during dissolution in comparison to the saturation concentration resulting from the tar analysis at $t=0$ (at the time when dissolution is starting). The values of Δc have been calculated for all compounds which showed an increase of saturation concentrations with time in the considered samples from Fig. 5.4. The results are listed in Table 5.4 and indicate that the effect of increasing saturation concentrations with time is the more significant, the greater the initial amount of substances with higher water solubility. In such tars (e.g. B15) there is an increasing of c_{sat} for all 16 EPA PAH, whereas for samples which have already undergone advanced dissolution (B55), Δc is less than 10 % (which is in fact comparable with the error of the analytic measurement). In the cases considered here, the absolute value of c_{sat} for low solubility compounds increased by maximum a factor of 2 when the more soluble ones were depleted.

The other conclusion is that the value of Δc is the higher, the lower the water solubility of the substance. For *BghiP* in B15, the maximum concentration during dissolution gets twice as high as the saturation concentration at the beginning (at $t=0$), but there is no increase of c_{sat} of *BghiP* in B50, although e.g. the

monoaromatics content of that sample is even higher than in B15. That is because the variation of the saturation concentration of a substance during dissolution depends on the variation in its concentration (molar ratio) in the tar and the latter connects the variations for all analysed components (sum of molar ratios is always 1).

Table 5.4: Relative increase in saturation concentration for less soluble compounds, caused by the well soluble ones being depleted from the mixture as the dissolution process advances

Tar Sample	B15	B50	B23	B55	Rüttgers- tar
Substance	$\Delta c(\%)$				
1-MetNap	8.5	4.4	< 5	< 5	< 5
2-MetNap	6.5	3.3	< 5	< 5	< 5
Dbf	21.2	15.6	5.9	< 5	< 5
Ace	17.5	11.5	3.2	< 5	< 5
Fln	21.2	14.8	6.2	< 5	0.25
Phe	38.6	29.8	22.7	< 5	14.5
Ant	43.5	33.7	31	< 5	6.5
Fth	62.5	51.3	83.2	9.7	13.3
Py	59.3	47.9	71.8	6.9	12.1
BaA	86.6	72.7	< 5	< 5	20.7
Chr	84.3	70.2	< 5	< 5	19.3
BbF-BkF	88	72.8	138	< 5	21
BaP	93.6	77.9	< 5	< 5	< 5
Indeno	71.2	< 5	< 5	< 5	< 5
BghiP	100	< 5	< 5	< 5	< 5

There is still the question whether an extensive and costly tar analysis is really necessary for predicting its change in composition during dissolution. To answer this, for the samples B15 and B50 the dissolution behaviour was also simulated accounting only for the 16 EPA PAHs and keeping the rest constant (as if it was insoluble) and was compared to the behaviour which results if all 34 analysed components (Table 5.2) are considered (Fig. 5.4 a and c). The obtained relative increase in saturation concentration for the two situations are shown in Fig. 5.5 (a) - B15 and (b) - B50).

From Fig. 5.5 (a) and (b) it results that the maximum saturation concentration is seriously underestimated when ignoring the compounds more soluble than the 16 EPA PAH. The value of Δc may be underestimated by up to 80 % (*BghiP* in B15) when only the 16 EPA PAHs-content of the examined coal tar is available. The error is the highest for the less soluble compounds. Due to their low solubility and high sorption capacity, this error may however be attenuated to some extent in a real aquifer by sorption and dilution, but might still play a role

for large amounts of residual phase spilled in the subsurface.

In conclusion, the depletion of more soluble substances during dissolution may determine an increase of the maximum concentrations of the less soluble ones. The available data do not permit to determine at this point whether there are also significant amounts of other well soluble coal tar constituents not analysed here, that possibly lead to even higher maximum

saturation concentrations. At least for 'fresh' coal tars, it could be expected for instance that higher phenols are also important from this point of view. So it appears that the quantification of the more soluble fraction in coal tar is important not only because of the mobility and toxicity of these compounds, but also because ignoring them might cause a too optimistic expectation of the maximum concentrations of the less soluble ones (PAH).

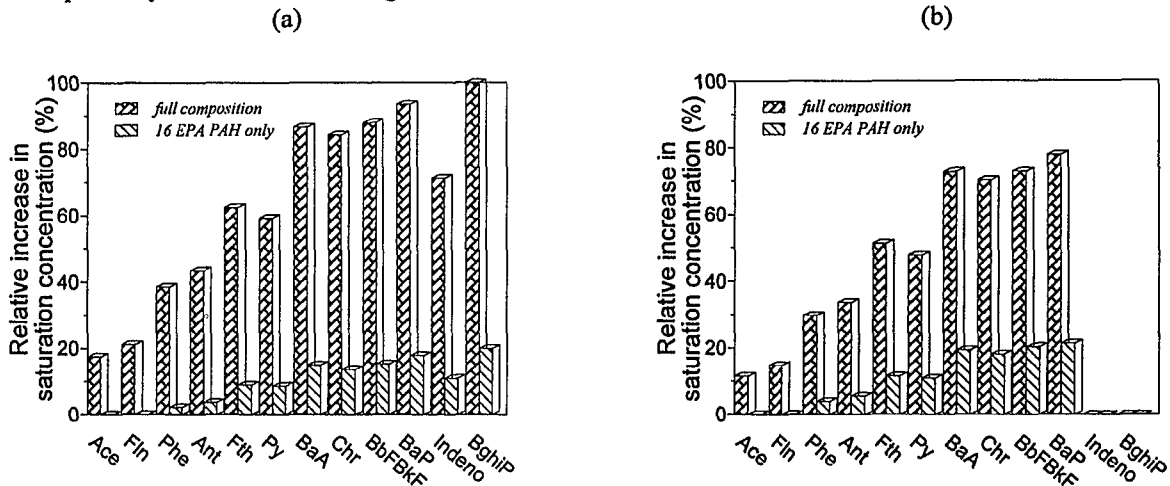


Fig. 5.5: Comparison between Δc in % (Eq. 5.31) resulting when the full (analysed) tar composition, respectively only the 16 EPA PAH are considered for simulation of dissolution at equilibrium, for two tar oil samples from 'Testfeld Süd' (a - B15, b - B50).

It does also not necessarily result that such an increase in c_{sat} during dissolution would be observed during a short term column experiment, or in the field in 'real time' monitoring. After what time this effect would appear and how long it would last depends on the spatial distribution, the amount and the composition of the residual phase. Especially in the field, a significant limitation to mass transfer (e.g. due to reduced specific interfacial area tar/water at high residual saturation) is to be expected and it is not possible to exactly forecast these effects if the required parameters (location, amount, distribution and composition of coal tar) are not known.

5.3.3 Column Experiments with Disturbed Samples

Experimental Results. In the following, two column leaching experiments with disturbed samples of contaminated aquifer material from the source at 'Testfeld Süd' will be discussed. Both samples were taken in summer 1996 during drilling of the well B55 (see location in Fig. 2.1). The sample here called B55C1 is

from 4.5 m-5 m, B55C2 from 5 m - 5.5 m depth. For both columns, 560 g of homogenized contaminated aquifer material were used (value relates to the dry sample).

Both samples contained residual tar oil. From the well B55 tar oil has also been extracted from the bottom of the aquifer (ca 8 m depth) (composition in Table 5.3). Tar oil films coating the coarse gravels could be observed, but most of the residual NAPL (see estimated initial residual saturation in Chapter 5.3.3.2) was probably distributed as blobs entrapped in the finer fractions.

Both columns were leached with distilled water for more than two months at high linear velocity (14.8 m/d). During that time, the concentrations of the 16 EPA PAHs were monitored at the columns outlet.

There was no measurable turbidity increase in the column leachate from neither samples, which allows the conclusion that the tar constituents were released only in dissolved form (no separate NAPL phase, no emulsions, no particle enhanced transport detectable in the

column leachate). The evolution of concentrations at the columns outlet during

time is shown in Fig. 5.6 for *Ace*, *Fln* and *Phe* and in Appendix III for the other relevant PAH.

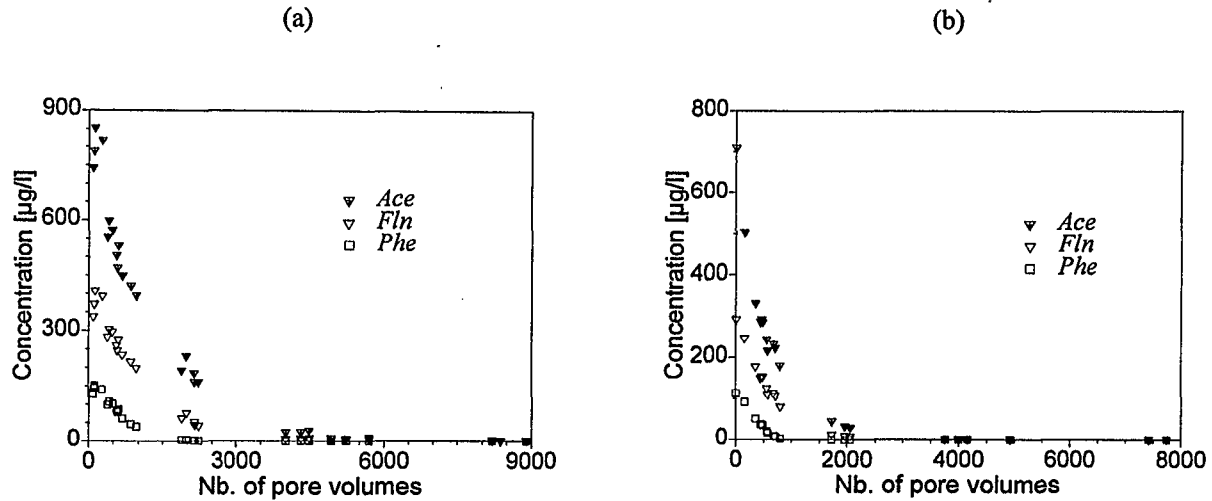


Fig. 5.6: Measured concentrations of *Ace*, *Fln* and *Phe* in the leachate from the columns B55C1 (a) and B55C2 (b) during 80, respectively 63 days; $v_a=14.8$ m/d.

For dissolution at equilibrium, the concentration in the water leaving the columns would normally equal the saturation concentration for all PAH. As there was still some residual phase left in the columns at the end of the experiment, the dissolution of the residual NAPL was not complete.

Since both samples used contained residual organic phase, the contaminant desorption out of intraparticle pores has to be excluded (or at least plays a secondary role for the overall contaminant fluxes) and dissolution out of residual phase is considered to be the main release mechanism of contaminants into water.

Mass Balance and Estimation of the Initial Residual Saturation. At the end of the leaching experiment, the remaining PAHs content in the aquifer material from these two columns was determined by extraction with cyclohexane. However, as it turned out later, this method is not fully effective (cyclohexane is not miscible with water and therefore the PAH molecules in narrower pores maybe have to diffuse through stagnant water to reach the solvent).

There was no pure organic phase available from the same depth as the contaminated aquifer material used in the leaching experi-

ments, its composition is therefore unknown. For this reason, for the following estimations it is assumed that the composition of the tar oil from the two samples should have been similar to the composition of the organic phase pumped out from the bottom of the aquifer from the same well (B55). The composition is shown in Table 5.3.

According to this, the 16 EPA PAHs represent about 9 % from the total tar mass. To account for the error in mass balance due to incomplete cyclohexane extraction of the 16 EPA PAH and because the aged organic phase is probably enriched also in other high molecular PAH-like compounds not accounted for in the analysis, it was though assumed that the initial PAH content in the tar (eluted plus extracted) was only 5 % from the total tar mass.

The total mass of PAHs in B55C1 was 142.4 mg, in B55C2 74 mg (Tab 5.5).

Assuming for the tar oil a density of 1.2 g/cm^3 and an average molar weight of 250 g/mole , it results that B55C1 contained about 2.38 cm^3 and B55C2 1.24 cm^3 residual phase. For an average porosity of 0.15 for both samples, the initial NAPL saturation in B55C1 and B55C2 was respectively $S_1^0 = 0.08$ and $S_2^0 = 0.04$.

Table 5.5: Mass balance for the samples B55C1 and B55C2. The dissolved fraction was calculated assuming complete cyclohexane extraction.

Subst.	B55C1 (4.5 m-5 m)		B55C2 (5 m - 5.5 m)	
	Total [μg]	Dissolved [%]	Total [μg]	Dissolved [%]
Nap	928	42	723	55
Any	1,413	58	2,031	40
Ace	66,406	81	31,964	71
Flu	35,449	67	18,672	55
Phe	31,690	18	16,561	13
Ant	3,637	17	1,933	13
Fth	1,726	16	1,016	8
Py	840	16	590	9
BaA	89.2	20	113	8
Chr	97.9	20	122	4
Bb/kF	48.1	21	100	6
BaP	15.9	1.2	45.4	0.02
Indeno	25.7	69	29.3	3
DahA	10.9	79	9.3	28
BghiP	12.1	39	26.8	0.89
Sum	142,390	-	73,937	-
	[μg]			

With these values, assuming for the aquifer material an average particle diameter $d_{50} = 5$ mm (HERFORD, 1999) and the average blob diameter half as great, the specific interfacial area of the tar blobs, A_0 [$\text{L}^2 \text{M}^{-3}$], can be calculated from:

$$A_0 = \frac{3 \cdot n \cdot S^0}{r_b} \quad (5.32)$$

where r_b is the average blob radius [L] and S^0 the initial NAPL residual saturation [-].

The total (absolute) area of the blobs in the sample A [L^2] is then:

$$A = \frac{m_{\text{sample}}}{d_s} \cdot A_0 \quad (5.33)$$

with m_{sample} - the dry mass of the aquifer material [M] and d_s the density of the dry solids [M L^{-3}] ($\approx 2.7 \text{ g/cm}^3$).

With these considerations, the roughly estimated initial blob areas in the two columns

is $A_1 = 58 \text{ cm}^2$ and $A_2 = 29 \text{ cm}^2$ respectively.

Saturation Concentrations and Estimation of the Initial NAPL Composition. From the known total PAH mass (leached plus extracted) and with the above mentioned assumptions for the PAH content in the tar (5 wt %), average molar weight (250 g/mole) and density (1.2 g/cm^3) of the tar oil, the saturation concentrations for each component that would result for dissolution at equilibrium out of the original ideal organic mixture ($\gamma_i = 1$) can be easily calculated as:

$$c_{\text{sat},i} = S_{w,i} \cdot \chi_i \cdot \gamma_i \quad (5.34)$$

with:

$$\chi_i = \frac{m_{i,(el+ex)}}{n} \cdot \frac{\overline{M_{\text{tar}}}}{M_i} \cdot \frac{\text{g}}{100} \quad (5.35)$$

where $m_{i,(el+ex)}$ is the total mass of the component i (leached plus extracted) [M],

$\sum_{i=1}^n m_{i,(el+ex)}$ the total mass of all PAHs (leached plus extracted) [M], n the total number of components in the mixture, and g the total concentration of the n components in the mixture [wt %].

Since in these column experiments only the concentrations of the 16 EPA PAHs have been monitored, for the interpretation of the results it is assumed that only these are dissolved out of residual phase ($n=16$).

The resulting saturation concentrations are shown in Table 5.6 and compared with the maximum concentrations from the two columns and the saturation concentrations determined for the residual phase from the bottom of the aquifer in B55 (Fig. 5.7).

Table 5.6: Saturation concentrations (calculated from the mass balance) and observed maximum concentrations from the columns B55C1 and B55C2 compared with the saturation concentrations of the residual phase found at 'Testfeld Süd' in the well B55 at the bottom of the aquifer. n.d. - not detected; S^0 - initial NAPL pore saturation.

Substance	B55C1 (4.5 m-5 m) ($S^0 \approx 0.08$)		B55C2 (5 m - 5.5 m) ($S^0 \approx 0.04$)		B55 (bottom of the aquifer)
	Saturation concentration	Maximum concentration	Saturation concentration	Maximum concentration	Saturation concentration
	$c_{sat,1}$ [$\mu\text{g/l}$]	$c_{max,1}$ [$\mu\text{g/l}$]	$c_{sat,2}$ [$\mu\text{g/l}$]	$c_{max,2}$ [$\mu\text{g/l}$]	c_{sat} [$\mu\text{g/l}$]
Nap	76.0	22.8	114	70	466
Any	69.0	12.0	191	24.9	18.7
Ace	756	852	700	709	1,359
Fln	338	408	343	292	482
Phe	130	151	131	113	286
Ant	11.4	10.2	11.7	7.41	3.08
Fth	1.6	2.34	1.8	1.24	8.79
Py	0.993	1.01	1.34	0.46	8.27
BaA	0.011	0.12	0.028	0.06	n.d.
Chr	0.017	0.22	0.04	0.06	n.d.
BbF-BkF	0.001	0.12	0.005	0.03	n.d.
BaP	0.001	0.03	0.004	0.003	n.d.
Indeno	0.001	0.16	0.002	0.02	n.d.
DahA	0.006	0.15	0.009	0.06	n.d.
BghiP	<0.001	0.09	<0.001	0.01	n.d.

Except for *Nap* and *Any*, the saturation concentrations resulting from the mass balance do not differ much in the two columns, the NAPL composition seems to be quite similar. There is however a great difference between the NAPL from 4 m - 5 m and the one from the bottom of the aquifer. The latter is strongly enriched in *Ace* and the saturation concentrations of *Fth* and *Py* are also greater in comparison with the samples used for the column experiments. If the residual phase found in the field at this location was spilled somewhere at or near the surface, it results an increasing 'ageing' of the NAPL with increa-

sing depth.

In an attempt to re-establish and to compare the initial NAPL composition in the two columns, four things will be addressed:

- ratios between calculated saturation concentrations and maximum concentrations for each column;
- ratios between calculated saturation concentration for the two columns;
- comparison of maximum concentrations in the leachate from the two columns;
- maximum PAH concentrations relative to each other in each column.

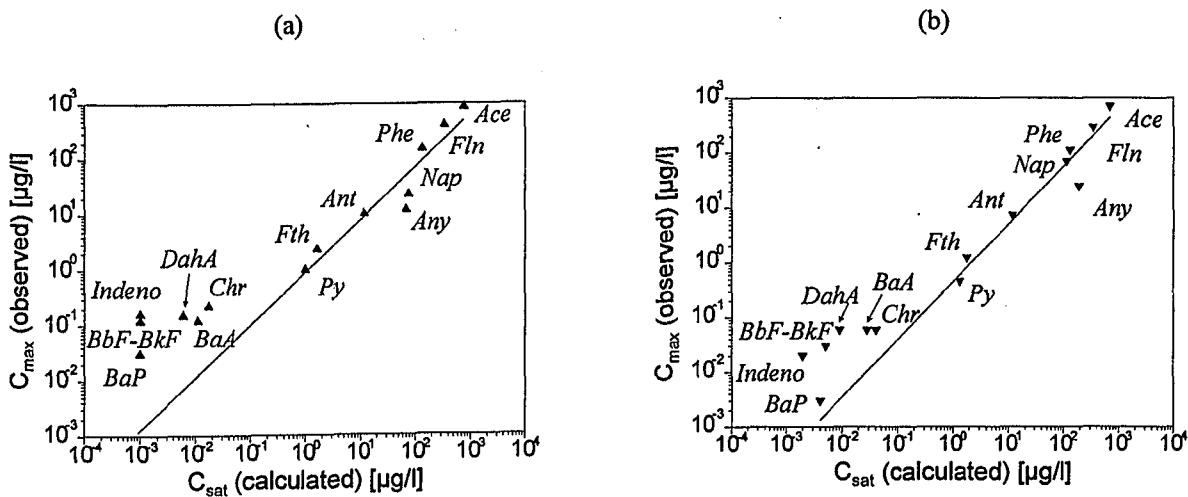


Fig. 5.7: Measured (maximum) concentrations, c_{max} , compared to the saturation concentrations c_{sat} calculated from the mass balance in the columns B55C1 (a) and B55C2 (b).

Ratios Between Calculated Saturation Concentrations and Maximum Concentrations for Each Column. Since it may be assumed that at the beginning of the column experiment the pore water was in equilibrium with the NAPL, it would be expected that for a homogeneous NAPL distribution in the cross section of the column and no lateral dilution, the maximum concentrations in the column leachate should be equal to the (calculated) saturation concentrations. The maximum concentrations are in good accordance with the calculated saturation concentrations for the first eight of the 16 EPA PAHs (up to *Py*), but this does not apply for higher molecular PAH. This is probably due to mass balance errors.

In Table 5.7 (column 1 and 2) the ratios between saturation and maximum concentrations are shown for the two samples. This ratio decreases with increasing K_{ow} and for the higher PAH (starting with *Py* or *BaA*) it becomes smaller than 1. This could be explained by the fact that the extraction efficiency was the poorer, the higher the octanol-water partition coefficient, which makes sense as the higher molecular PAHs exhibit higher sorption than the lower molecular ones. The mass balance was thus underestimated most for the PAHs with high K_{ow} , which resulted in an underestimation of their saturation concentrations (in the mass balance, the same correction was made for all PAH to account for incomplete extraction, irrespective of the value of K_{ow}). This is also suggested by the high percentage of eluted mass for high molecular PAHs (Table 5.5) which does not reflect advanced dissolution, but the poor efficiency of cyclohexane extraction.

Ratios Between Calculated Saturation Concentrations for the Two Columns. In column 3 of Table 5.5, the ratio between the saturation concentrations from the two samples is shown. From *Ace* to *Py*, this ratio is nearly 1,

which would indicate that the NAPL composition in the two samples was the same. *Nap* and *Any* are again an exception probably due to biodegradation, which seems to be more effective in the sample B55C1 (lower c_{sat} and c_{max} than B55C2). This effect might be correlated with the NAPL residual saturation - more degradation (smaller concentrations in the column outlet) for greater residual saturation, eventually due to better availability to microorganisms at greater interfacial area tar/water (lower hindrance due to non-uniform NAPL distribution and/or preferential flow paths in the column).

Comparison Between Maximum Concentrations in the Leachate From the Two Columns. As the calculated saturation concentrations are not exact due to errors in the mass balance, the maximum concentrations measured in the column leachate should give some more accurate information on the initial composition of the NAPL in the two samples .

The direct comparison of the values of c_{max} from the two columns shows that, with a few exceptions (e.g. *Nap*, *Any*), maximum concentrations from the column with higher initial residual saturation are greater than in the other column. This may be due to the heterogeneous NAPL distribution in the cross section of the column with less residual phase and/or because of some preferential flow, leading to dilution effects. Another indication for the heterogeneous NAPL distribution in the column is the fact that for some PAHs there is initially an apparent retardation in the column (concentration increase at very early times) (see Appendix III); this may occur e.g. if the residual saturation near the outlet was smaller than towards the middle of the column, and the dissolution front (carrying c_{max}) needs some time to reach the column outlet. This is not surprising, as the heterogeneity of the investigated aquifer material allows in fact but heterogeneous NAPL distribution.

Table 5.7 : Saturation versus maximum concentrations in B55C1 (index '1') and B55C2 (index '2'). $c_{max,i}$ is the maximum concentration of the component i and $c_{max,Ace}$ the maximum concentration of *Ace*.

Substance	$c_{sat,1}/c_{max,1}$ (1)	$c_{sat,2}/c_{max,2}$ (2)	$c_{sat,1}/c_{sat,2}$ (3)	B55C1 (4.5 m-5 m)	B55C1 (5 m-5.5 m)
				$c_{max,i}/c_{max,Ace}$ (4)	$c_{max,i}/c_{max,Ace}$ (5)
Nap	3.34	1.63	0.67	0.027	0.099
Any	5.75	7.67	0.36	0.014	0.035
Ace	0.887	0.987	1.08	-	-
Flu	0.828	1.17	0.99	0.49	0.41
Phe	0.861	1.16	0.99	0.18	0.16
Ant	1.12	1.58	0.98	0.01	0.01
Fth	0.684	1.45	0.88	0.003	0.002
Py	0.983	2.91	0.74	0.001	0.001
BaA	0.092	0.467	0.41	0.0001	0.0001
Chr	0.077	0.667	0.42	0.0003	0.0001
BbF-BkF	0.008	0.167	0.25	0.0001	0.00005
BaP	0.034	1.34	0.18	0.00004	0.00005
Indeno	0.006	0.1	0.46	0.0002	0.00003
DahA	0.04	0.15	0.61	0.0002	0.0001

Ratios Between Maximum PAH Concentrations in Each Column. Irrespective of the residual distribution and eventual dilution effects, if the initial NAPL was the same in the two columns, then the ratio of c_{max} for individual PAHs relative to each other should be the same in both samples. To verify this, all maximum concentrations were divided by the one of *Ace* (this PAH is known to be poorly biodegradable and *Ace* concentrations were the highest, hence the less sensitive to various measurement errors) (Table 5.7, columns 4 and 5). Again, with the exception of *Nap* and *Any*, these ratios are equal in the two columns for almost all PAH.

This leads to the final conclusion that the NAPL composition in the two samples was very similar. Assuming a point source that was spilled vertically, there is no significant change in the NAPL composition at the scale of 1 m vertical distance. However, given the extent of NAPL contamination at the site, the point-source assumption probably applies only for larger scales (the 'point' may mean some cubic meters), so that the samples B55C1 and B55C2 came rather from the same source. At that scale

(about 1 m) cross-contamination by some residual phase eventually being pushed downward during drilling may also have led to the similar NAPL composition in B55C1 and B55C2.

The amount of information now available does not permit to determine whether the aged NAPL from the bottom of the aquifer in B55 originates from the same source as the one in the samples investigated in the column experiments and its composition changed as it infiltrated in vertical direction, or if it is a separate source.

Theoretical Change of Saturation Concentrations During Dissolution. From the estimated initial composition of the dissolving NAPL and assuming that the aqueous concentration of any PAH is homogeneous throughout the contaminated domain and equal to its saturation concentration at any time (batch reactor), the change in saturation concentrations with time can be simulated as described in Chapter 5.1.1. The results of this simulation for both columns are shown in Fig. 5.8.

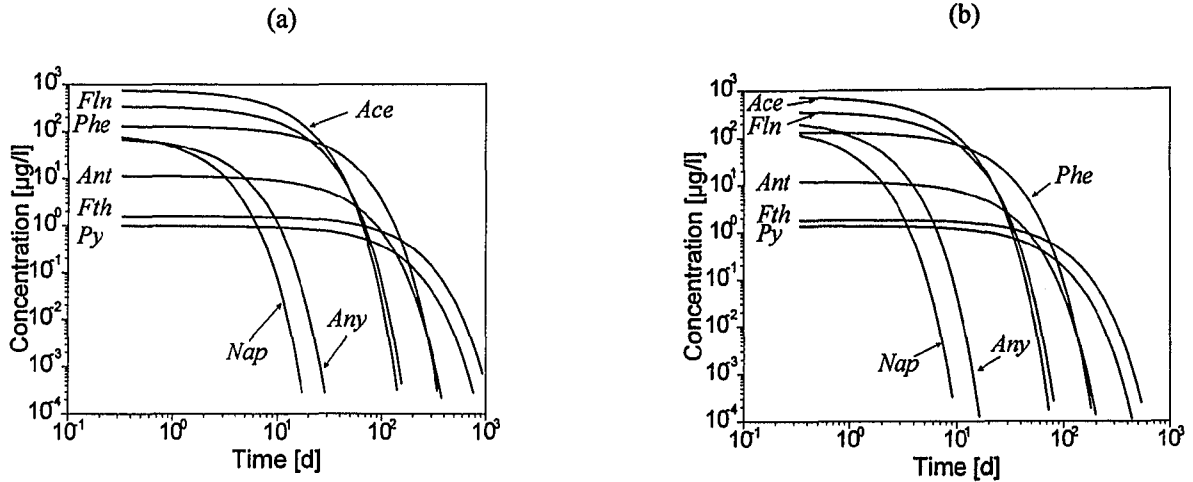


Fig. 5.8 Change of the saturation concentrations in sample B55C1 (a) and B55C2 (b) during dissolution under batch-reactor-assumptions (see chapter 5.1.1)

From Fig. 5.8 it results a similar dissolution behaviour for the two samples, based on the similar estimated initial NAPL composition. First the easier soluble components in the NAPL are depleted and it takes much longer to completely dissolve the less soluble PAH (the curves in the diagrams show the time needed to achieve for each PAH a saturation concentration less than $10^{-3} \mu\text{g/l}$). By the time the column experiments have been started, the dissolution process was already advanced (aged contamination), and the well soluble compounds washed out. Therefore it is not expected that the saturation concentrations of the considered PAH would increase significantly due to further change in NAPL composition during dissolution.

In reality, the domain contaminated with residual NAPL cannot be approximated by a batch-reactor, but there is a dissolution front advancing through it in the direction of the water flow. The dissolution front of each dissolving species is theoretically retarded with respect to the velocity of the advecting water, by a factor as defined in Eq. 5.28.

Retardation of the Dissolution Front in the Two Columns. The retardation factors for the considered PAH in the two columns have been calculated using Eq. 5.28 and are listed in Table 5.8.

Table 5.8: Retardation factors of the dissolution front and the time needed for constant concentration in the column leachate to be achieved.

Subst.	B55C1 (4.5 m - 5 m)		B55C2 (5 m - 5.5 m)	
	$R [-]$	$t_c \cdot R^*$ [days]	$R [-]$	$t_c \cdot R^*$ [days]
Nap	448	3.6	215	1.8
Any	752	6.1	361	3.1
Ace	3,221	26	1,544	13
Fln	3,840	31	1,840	16
Phe	8,931	73	4,280	36
Ant	11,646	95	5,581	47
Fth	39,960	325	19,148	162
Py	30,998	252	14,854	126

* For a column length of 12 cm and a linear flow velocity of 14.8 m/d i.e. ca 1 cm/min), the contact time in the column was about 12 min.

Because the dissolution front advances through the column while the sample is leached, for some time the concentration in the leachate equals the saturation concentration. This will not change, as long as in the flow direction in the column there are still enough blobs with virtually unchanged composition, yielding maximum c_{sat} .

The time during which the concentration in the leachate remains constant (initial c_{sat}) is equal to the retardation factor times the contact time of the advecting water in the column. Since the contact time t_c is a function of the linear flow velocity (inverse proportionality), it results that,

the slower the linear flow velocity through the column, the longer one would measure a constant concentration in the leachate. E.g. from Table 5.8 it results that for *Nap* in the sample B55C1, the concentration would remain constant for 3.6 days, whereas for *Fth* it would be so for 325 days. After ($t_c \cdot R$) days there will

be an exponential decrease in saturation concentrations according to Raoult's law.

For this scenario, the evolution of the saturation concentrations for the two samples is shown in Fig. 5.9.

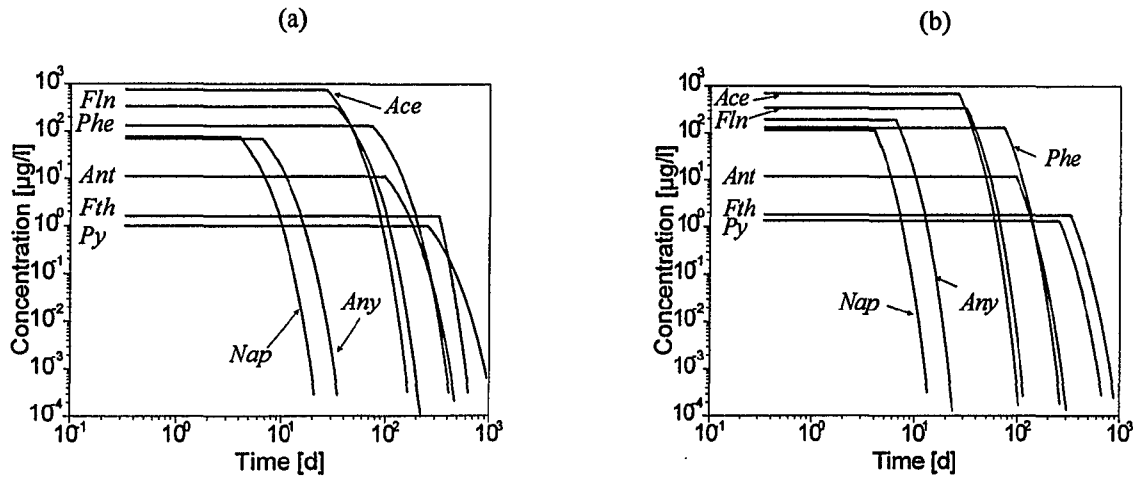


Fig. 5.9: Effect of the retardation of the dissolution front on saturation concentrations at the column outlet for the samples B55C1 (a) and B55C2 (b).

Length of the Mass Transfer Zone for Dissolution (Saturation Length). Since the flowing water does not instantaneously get saturated due to dissolution, the evolution of the concentrations measured in the column leachate is also significantly determined by the length of the mass transfer zone (saturation length) defined in Chapter 5.1.4. The concentration profiles in Fig. 5.9 apply for saturation lengths shorter than the length of the domain containing residual blobs (in this case equal with the length of the column). The length of the mass transfer zone can be only estimated using empirical correlations obtained for other systems (experiment designs), as shown in Chapter 5.1. This involves the following steps:

- estimation of the modified Sherwood number Sh' from empirical correlations;
- with the estimated Sh' , calculation of $(k_{diss} \cdot A_0)$ from Eq. 5.15 as:

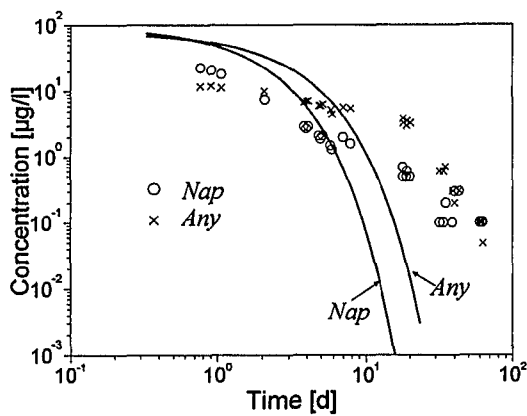
$$(k_{diss} \cdot A_0) = \frac{Sh' \cdot D_{aq}}{d^2} \quad (5.36)$$

- estimation of X_s using Eq. (5.25).

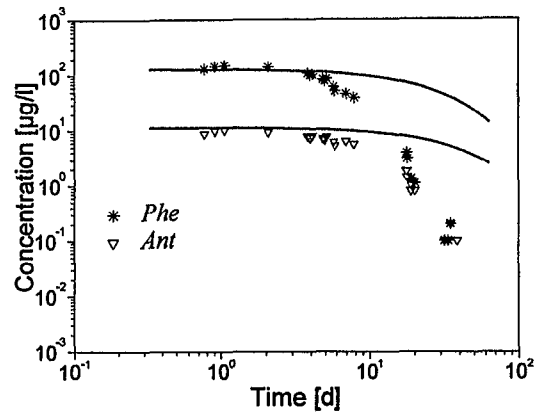
Fig. 5.1 shows the variation of the saturation length with the grain diameter for the investigated samples, as it results from different correlations for the modified Sherwood number Sh' for dissolution out of residual blobs. From Fig. 5.1 it follows that for the column experiments discussed here, the minimum saturation length was presumably about as long as the column. In this case, the contact time in the mass transfer zone is at least as long as the total contact time in the column and the concentrations in the leachate should decrease exponentially already at early times, as shown above in Fig 5.8.

Measured versus Calculated PAH Concentrations. In the following, the measured concentrations are compared to those resulting from the forward calculations presented above. For the column B55C1 the results are shown in Fig. 5.10 and for the column B55C2 in Appendix IV.

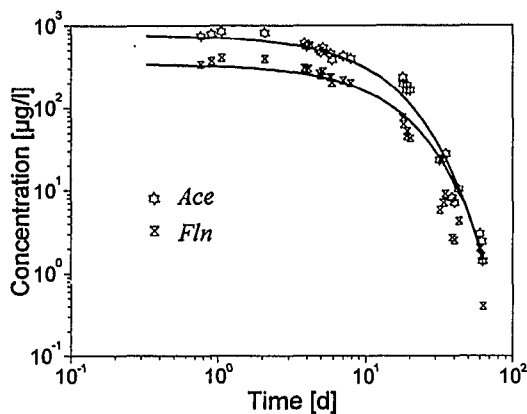
(a)



(b)



(d)



(c)

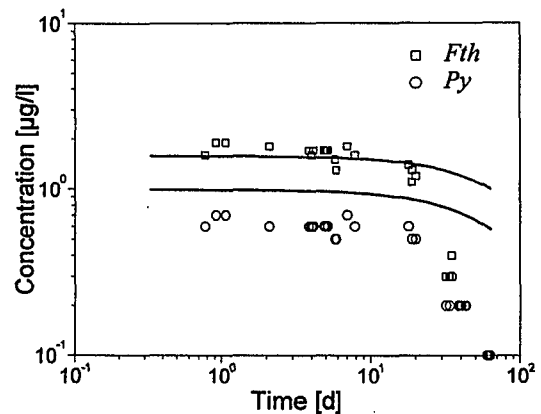


Fig. 5.10: Measured (symbols) versus calculated concentrations (curves) during dissolution for the column B55C1. The calculated curves are those shown for all PAH in Fig. 5.8 (a).

From Fig. 5.10 it follows that solely for *Ace* the calculated curves fit the measured data for the entire time domain, whereas the measured *Nap* and *Any* concentrations seem to follow some other rule than the exponential decrease in concentration as predicted by Raoult's law. For these two PAH, the saturation concentrations as estimated from the mass balance are not reached even at very early times. There is also a relatively good fit for *Fln* and *Fth*. Measured *Phe* and *Ant* concentrations match well the calculated ones only for some time, then they decrease faster than it would result from the change in NAPL composition alone. *Py* concentrations systematically deviate from the model curve.

The fact that measured *Ace* and to some extent *Fln* concentrations are very well predicted by the model, indicates that the approach used is correct (length of the mass transfer zone about as long as the column, concentrations decreasing exponentially due to the temporal change in NAPL composition). If it applies for

two PAHs, the same dissolution mechanism must apply at the same time for any other component dissolving out of the same mixture. When data for other components deviate from the model, the measured concentrations are always lower than the predicted ones (Fig. 5.10). Since in the system sorption can be excluded (all materials the sample and the contaminated water came in contact with were made out of glass or steel), it is believed that the mass loss for several PAHs is due to biotic processes in the columns, the more as these experiments were conducted with water containing oxygen. There is no mass loss for *Ace*, which is known to be not at all or poorly biodegradable. The deviation of the measured concentrations from the calculated ones (curves) turns at different times for different PAHs, in the order $Phe < Ant < Fth < Py < Fln$. This lag time (t_{lag}) is probably due to different adaptation of the microorganisms to different PAHs (*Phe* is used as a substrate earlier than *Fln*, *Ace* is not degraded at all). There was virtually no lag time for the biodegradation of

Nap and *Any*, known to be the easiest biodegradable among the 16 EPA PAHs. The maximum concentrations measured in the column leachate for these two PAHs were from the beginning lower than the saturation concentration predicted by Raoult, i.e. probably some biodegradation occurred in the column already within the first pore volumes of water exchanged. However, *Nap* as well as *Any* persisted at late times at higher concentrations than predicted by Raoult's law. This behaviour could not be explained (fitted) by simple forward calculations. *Py* (the less soluble among the PAHs considered here) shows for long time a concentration plateau, but the measured concentration is less than the saturation concentration; this difference is probably due to errors in the mass balance (e.g. incomplete solvent extraction).

Estimation of the Mass Loss Due to Biodegradation. The theoretical decrease in concentration (rate) during time according to Raoult's law is an exponential function. The domain of measured fluxes deviating from Raoult's law could also be fitted by an exponential function, but the decrease was steeper. This suggests some that dissolved PAHs undergo some (at least apparent) first order decay process.

The decrease of PAH release rates with time follows an exponential law of the form $F = F_0 \exp(-kt)$, F in $\mu\text{g/l}$ and t in days. For the measured data, k [d^{-1}] is an apparent first order decay rate.

Fig. 5.11 shows the measured versus calculated release rates [$\mu\text{g/d}$] for *Flu*, *Phe*, *Ant* and *Fth* in the sample B55C1.

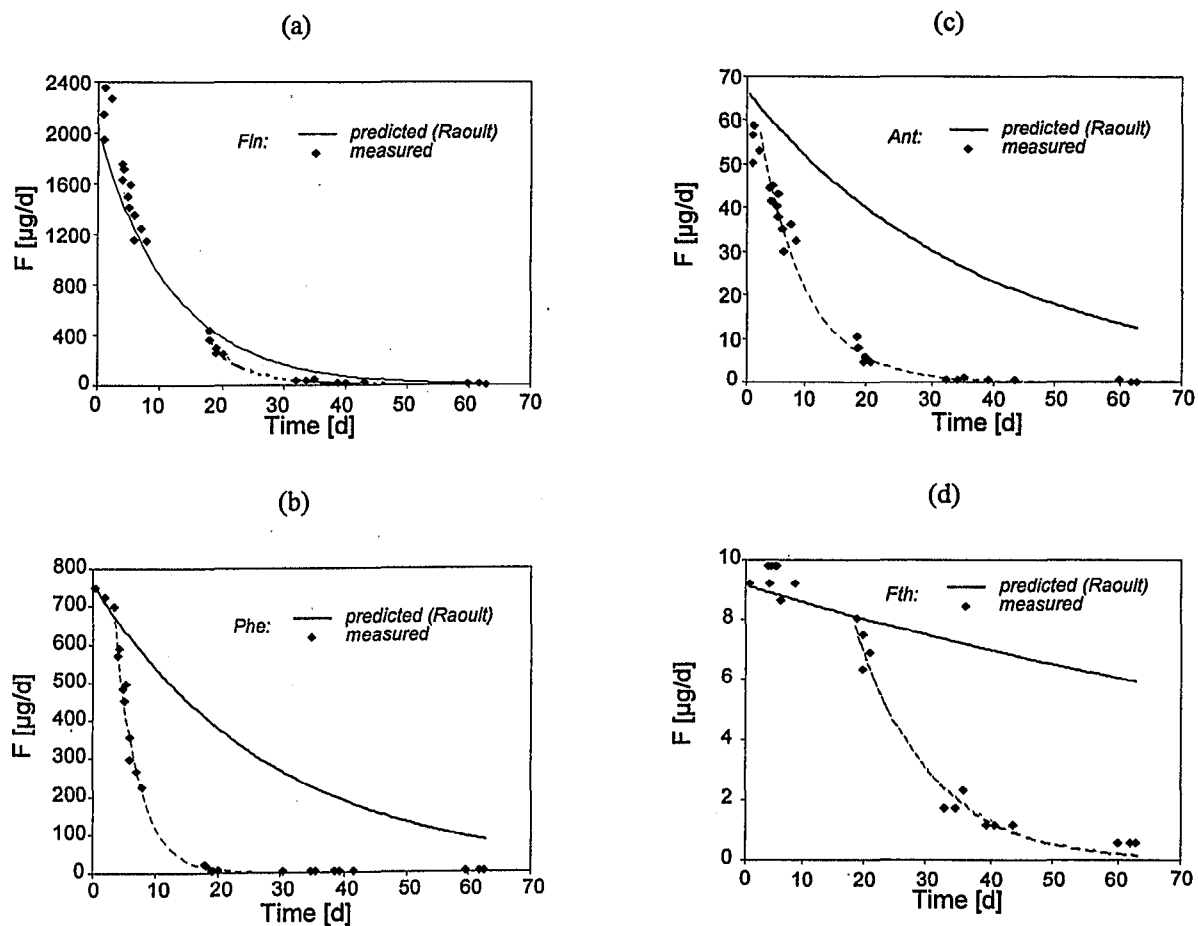


Fig. 5.11: Measured (symbols) versus theoretical PAH rates [$\mu\text{g/d}$] calculated according to Raoult's (exponential) law (solid curves). The deviation of the measured rates from Raoult's law also follows an exponential function (dotted curves). The difference between the areas below the two curves (solid and dotted) represents the total mass loss [μg] in the system believed to be due to biodegradation.

Table 5.9 shows the parameters (F_0 , k , r^2) of the exponential regressions.

Table 5.9: Exponential fit of the expected dissolution rates [$\mu\text{g/d}$] (calculated for dissolution out of the mixture according to Raoult's law) and of the measured rates (in the domain where there is a deviation from the values predicted by Raoult's law). For *Ace*, the measured data are practically coincident with the calculated curve (no mass loss due to biodegradation).

PAH	Raoult*			Measured**		
	F_0 [$\mu\text{g/d}$]	k [d^{-1}]	r^2	F_0 [$\mu\text{g/d}$]	k [d^{-1}]	r^2
Ace	4530	0.1	0.999	4536	0.099	0.979
Fln	2016	0.084	0.999	3380	0.129	0.938
Phe	760.9	0.035	0.999	1710	0.271	0.986
Ant	66.71	0.027	0.999	76.87	0.134	0.976
Fth	9.159	0.007	0.999	34.12	0.084	0.959

For each PAH, the area under the solid curve (Fig. 5.11) is the total mass [μg] expected to be released during the experiment (i.e. 62.8 days) by dissolution out of residual phase. The area under the dotted curve (which at early times overlaps the one for Raoult's law) is the total mass [μg] of PAH actually leached during 62.8 days (i.e. effectively measured in the column leachate).

For each PAH, the difference between the area under the solid curve (Raoult) and the area under the dotted one (Raoult until t_{lag} , then steeper exponential decrease) approximates the total mass loss during the experiment. This mass loss is thought to be due to biological decay.

The area I under a curve described by the function $F(t)$ is given by its integral over the time interval t_0 to t_n .

$$I = \int_{t_0}^{t_n} F(t) dt \quad (5.37)$$

In this case the curve describes the variation of the calculated, respectively measured PAH rates [$\mu\text{g/d}$] during time.

Each curve has been integrated numerically using the method of Simpson. For n equal time intervals, the area under the curve is:

$$I = \frac{t_n - t_0}{6 \cdot n} \{ F(t_0) + F(t_n) + 2 \cdot [F(t_1) + F(t_2) + \dots + F(t_{n-1})] + 4 \cdot [F(t_{1/2}) + F(t_{3/2}) + \dots + F(t_{(n-1)/2})] \} \quad (5.38)$$

with n - the even number of equal time intervals for the integration (here $n=70$), $t_0=0$ and $t_n=62.8$ days.

Table 5.10 shows for the PAH considered the total mass [μg] dissolved, respectively leached during 62.8 days (calculated with Eq. 5.38), as well as the lag time t_{lag} [d] until begin of biodegradation and the weight percentage biodegraded with respect to the amount dissolved.

Table 5.10: Theoretical (calculated according to Raoult's law) versus measured amount of PAHs leached from the sample B55C1 during 62.8 days.

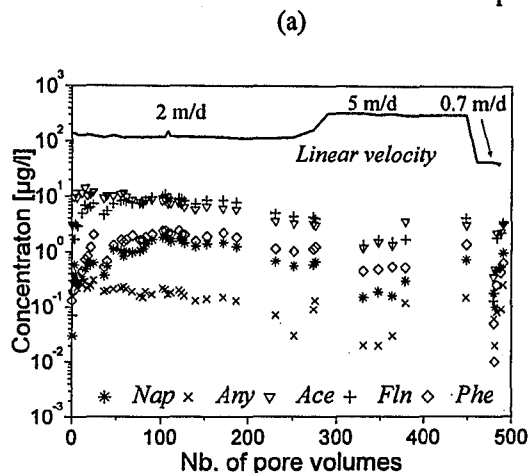
PAH	Total mass [μg] in 62.8 days		t_{lag} [d]	% loss
	Raoult	Measured		
Ace	43567	44125	-	< 1.5
Fln	23305	20510	17.8	12
Phe	19050	4666	2	75.5
Ant	2015	545	2	73
Fth	463	240	17.8	48.2

From Table 5.10 it follows that in the leaching experiments presented, the only PAH not affected by biodegradation was *Ace*. The difference between the amount of *Ace* theoretically dissolved (after Raoult) and the amount leached was only 1.3 %, which is within the analytical error. The loss of *Fln* was also relatively low, whereas only about 75 % of the total *Phe* dissolved was measurable in the leachate, the rest probably being biodegraded.

It follows that a considerable error in mass balance may be made in column experiments for dissolution out of residual phase (tar) performed with O_2 -saturated (tap), because biodegradation cannot be excluded. For biodegradable compounds, the dissolution mechanism out of residual phase only apparently does not follow Raoult's law. The error in mass balance can be estimated by forward calculations if the initial amount and composition of the residual phase are known.

5.3.4 Column Experiments with Undisturbed Samples

Experimental Results. Apart from being all just point measurements, the disadvantage of laboratory experiments with disturbed aquifer material is the fact that the natural porous



matrix and the original distribution of the residual phase within are perturbed and the natural flow conditions through the contaminated zone (as they were in the field) can not be preserved.

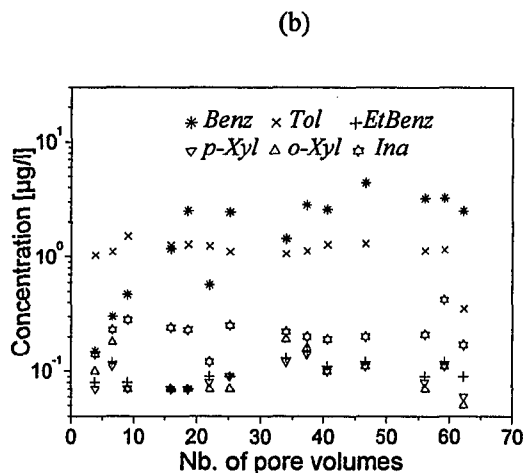


Fig 5.12: Concentrations in the leachate from an undisturbed sample (B49 7 m - 7.7 m) for PAH (a) and volatile aromatics (b).

Here the suitability of undisturbed samples (drilling liners) from 'Testfeld Süd' for determining release rates at equilibrium was investigated. The experimental set-up is described in Chapter 5.2. A contaminated sample from B49 (see location in Fig 2.1) was used, with the PVC liner as the column. The sample was from 7 m - 7.7 m depth and taking into account the high concentrations of poly- and monocyclic aromatic hydrocarbons found in groundwater at that location, it must have contained some residual phase. The amount, distribution and composition of the residual NAPL were unknown when the experiment was started.

The undisturbed sample in the liner was leached with degassed water for 124 days. The concentrations in the column leachate are shown in Fig. 5.12 (a) (PAHs) and (b) (MAHs and *Ina*).

All measured PAHs concentrations were corrected by the background value due to desorption out of the liner material (PVC). The background concentrations have been determined after completion of the leaching experiment by leaching the empty liner in the same way as when it contained the contamina-

ted sample. The background concentration was assumed to be the maximum value in the liner-leachate and was equal to 0.1 µg/l for *Any* and *Flt*, 0.4 µg/l for *Nap*, 0.7 µg/l for *Ace* and 0.9 µg/l for *Flt*, *Phe* and *Ant*. There was a high background concentration for *Tol* (around 1 µg/l); the stable *Tol* concentration measured in the column leachate is most probably due to laboratory artefacts.

Influence of the Heterogeneity on Measured Concentrations From Undisturbed Samples.

From Fig. 5.12 following facts can be observed: The maximum concentrations of both PAHs and BTEX in the columns leachate are much smaller compared to any of the saturation concentrations listed in Tab. 5.2. The maximum concentrations of PAH are by 2-4 orders of magnitude lower compared to the saturation concentrations from the fresh tars from B15, B16 and B50 and by 1-3 orders of magnitude lower compared to B56 (this well is located in the field in the same area as B49). For monocyclic aromatics the difference was even greater. The maximum BTEX concentrations did not exceed a few µg/l (highest for *Benzene*) and after about 60 exchanged pore volumes they were no longer detectable. Other EPA PAHs and BTEX not shown in Fig. 5.12 were

not detectable or were present in concentrations lower than 0.1 µg/l.

The low concentrations of all substances in the column leachate can be explained by the heterogeneity of the sample and of the distribution of the residual phase in it. Since the amount of residual phase in the column was quite low, there was probably a small (thin) plume in the column. If the residual phase was not uniformly distributed in the cross section available to water flow, there was some dilution at the sides, so that the concentrations measured in the leachate were all lower than saturation. In the ideal case, the dilution ratio must equal the ratio of the areas of contaminated (containing residual phase) and total flow effective cross section of the column.

The difference between maximum concentrations in the column leachate (Fig. 5.12) and saturation concentrations (Table 5.2) is greatest for monocyclic aromatics and *Nap* and generally decreases with increasing K_{ow} .

With the exception of *Ace*, there is some lag time until the maximum concentration in the leachate is reached, equivalent to some apparent retardation in the column. The lag time is the longest for *Nap*, the less sorbing and easiest soluble EPA PAH. *Ace* and *Fln* come out with maximum concentration practically from the beginning of the leaching. Among the monocyclic aromatics, *Benzene*, which is the most soluble, again shows the longest lag time (47 pore volumes).

Since the lag time is not directly, but inversely proportional to the K_{ow} , the apparent retardation in the column cannot be attributed to sorption. The apparent retardation is on the contrary the highest for the easiest biodegradable of the monitored substances. This allows the supposition that the lag time until maximum concentration is attained may have something to do with microbial biodegradation in the column.

It looks like at the beginning of the column experiments biodegradation was more effective (highest for *Benzene* and *Naphthalene*). There was almost no biodegradation of *Ace*, since this PAH showed maximum concentration in the leachate from the beginning of the experiment.

The formation of a black precipitate in the column indicated that, at least at early times, a certain amount of the dissolved substances were consumed by anaerobic microbial activity (as outlined in Chapter 5.2). Sulfate reduction has been most effective for the easiest biodegradable compounds such as *Nap* and *Benz* especially at early times during leaching, until there was some limitation of the biodegradation process (e.g. most of the sulfate already consumed or some inhibition of the sulfate reducers). The biodegradation of a certain amount of the dissolved compounds led to a delay of maximum concentration in the leachate, equivalent to an apparent retardation in the column. There was almost no retardation of *Ace* and *Fln*, known to be poorly biodegradable under anaerobic conditions.

After a certain time, there probably was no more significant biodegradation, the concentrations in the leachate remained more or less constant - the slight decrease is attributed to the depletion of individual substances in the residual phase as the dissolution process advanced.

The variation of concentrations with varying linear flow velocity indicates some non-uniform flow conditions in the column. If the main release mechanism is dissolution out of residual phase at equilibrium, at 2 m/d linear flow velocity in the column, the concentrations in the leachate should be constant, i.e. saturation concentration with or without dilution (a slight decrease in saturation concentration is possible due to decreasing molar fractions in the organic phase). The saturation concentration is usually reached after few centimeters, at high linear flow velocities (10 m/d) the length of the mass transfer zone should not exceed 1 m (GRATHWOHL, 1998). If the column is longer than the length of the mass transfer zone, the concentration in the column leachate is constant for a certain time (as discussed above).

The effect of the variation in linear flow velocity was a drop in concentration, followed by an increase back to the value attained before flow velocity changed (Fig. 5.12 (a)). This behaviour was similar for the increase and for the decrease of the linear flow velocity as well.

This indicates that there was some perturbation of the flow in the column due to the variation of the linear velocity. When the velocity increased, the flow was probably preferential through the zones of lowest hydraulic resistance where there was no residual phase (e.g. along the liner wall), first inducing some additional dilution in the column leachate. The drop in flow velocity had a similar effect, but the recovery period was shorter. Such instabilities are an disadvantage of greater scale columns (liners) versus smaller glass columns.

Comparison with a Disturbed Sample from the Same Depth. The material removed from the top and the bottom of the liner was leached at the same time with the undisturbed sample using degassed water at a linear flow velocity of 2 m/d. The concentrations of PAHs and BTEX were monitored in the column leachate. The PAHs concentrations are shown in Fig. 5.13; the concentrations of the volatile compounds were lower than 0.1 µg/l.

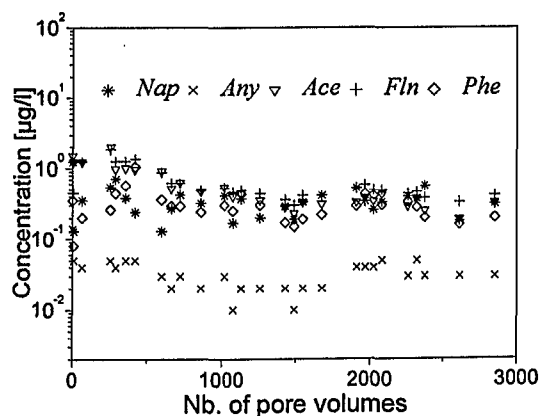


Fig: 5.13: PAH concentrations in a disturbed, homogenized sample (B49 7 m - 7.7 m)

The concentrations in the leachate were about 10 times lower than in the undisturbed sample. Although homogenized, the overall contamination of the disturbed sample was lower than that of the undisturbed one. There must have been still some residual phase in the disturbed column too, as the concentrations for individual substances did not drop significantly even after about 3000 pore volumes had been exchanged.

Similarly to the undisturbed sample, some precipitate (sulfide) was formed during leaching, indicating some anaerobic microbial activity. There was some apparent retardation

for the lower PAH (*Nap*) and almost no retardation for *Fln* and *Ace*, probably connected to the relative biodegradability of these compounds.

5.3.5 Conclusions

Since the experiments presented in this chapter were conducted using non-ideal samples, there is a lot of uncertainty in the calculations above, mainly because many parameters had to be roughly approximated. But since the exact characterisation of natural systems is not possible and approximations are allowed, the effort to estimate unknown parameters is still worth. The initial NAPL composition in the field samples from B55 (4.5 m - 5 m) and B55 (5 m - 5.5 m) was probably very similar.

The results of the column experiments with disturbed samples confirm the model for dissolution out of residual NAPL blobs outlined in Chapter 5.1. In disturbed, homogeneous samples, the release by dissolution of any compound out of residual phase proceeds with maximum (saturation) concentration (maximum contaminant fluxes), unless the contaminated domain is shorter than the saturation length. When the source composition at the site is not known (most cases), column experiments with disturbed samples are a good tool for the determination of saturation concentrations out of residual phase.

Differences between measured maximum concentrations in the leachate from the columns B55C1 and B55 C2 (disturbed) are believed to be due to biodegradation and/or non-uniform distribution of the NAPL. From the difference between measured PAH fluxes and the predicted ones assuming only dissolution out of residual phase, the mass loss due to biodegradation can be estimated (provided there was no dilution in the system). Biodegradation does not influence maximum contaminant fluxes (used for risk assessment) as long as the equilibrium assumption between tar and pore water holds at the time point when the column experiment was started. Failure to account for biodegradation in column experiments with oxygen containing water may lead to underestimation of the total time needed for complete contaminant removal by dissolution only.

The dissolution behaviour out of the undisturbed sample was basically the same as for the disturbed one; the difference in measured concentration in the leachate is given by the degree of contamination with residual phase (residual saturation) and its distribution in the flow-effective cross section of the column. The dissolution out of residual phase at equilibrium yields locally saturation concentrations for all compounds. At low residual saturation (the case of the investigated samples from B 49) there is an important dilution effect in the column, leading to concentrations in the leachate much lower than the saturation concentration. The saturation

concentrations would be observed in the leachate only in the case of high residual saturation and homogeneous distribution of the residual phase in the flow-effective cross section of the column, when no dilution would occur (Fig. 5.14). The heterogeneous distribution of the residual phase also explains why in groundwater samples taken in the field from conventional wells by pumping, concentrations are generally lower than saturation, even immediately near the source. Only multilevel samples can distinguish between individual plumes in different horizons (see also Chapter 7).

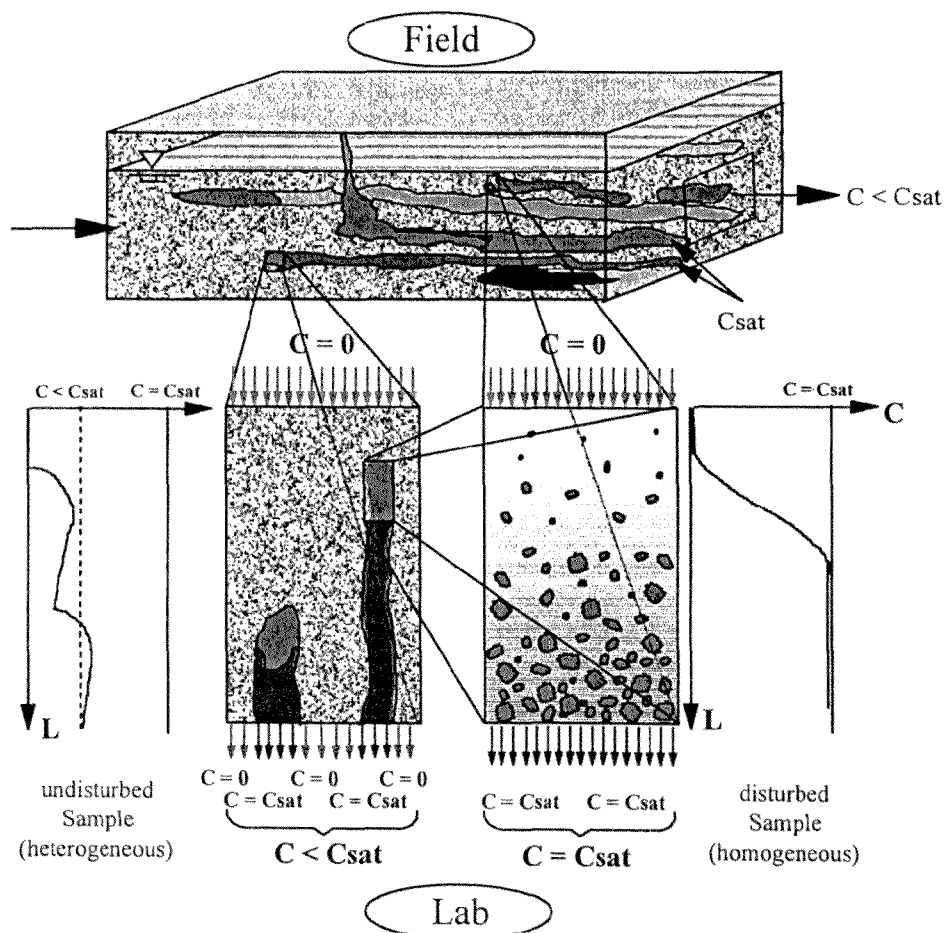


Fig. 5.14: Influence of the observation scale on measured concentrations, when the residual phase is distributed homogeneously (disturbed samples, local scale in the field), and heterogeneously (undisturbed samples in the laboratory, multiple sources in the field).

6. Diffusion Limited Desorption

6.1 Theory

6.1.1 Desorption out of Spherical Grains and Aggregates

Solute diffusion in porous aquifer materials in the sorptive uptake and desorption mode may be described with Fick's 2nd law in spherical coordinates:

$$\frac{\partial c}{\partial t} = D_a \left[\frac{\partial^2 c}{\partial r^2} + \frac{2}{r} \frac{\partial c}{\partial r} \right] \quad (6.1)$$

where c is the concentration [$M L^{-3}$], t the time [T], r the radial distance to the centre of the sphere [L] and D_a the apparent diffusion coefficient [$L^2 T^{-1}$].

In the field and in columns experiments as well, contaminant transport often occurs at large concentration gradients between the mobile and the immobile phase (non-equilibrium). During desorption out of a sample in which at the beginning the dissolved substance is in equilibrium with the one sorbed into the solid grains and aggregates, for a step change in concentration from a constant value (in the solid particles) to almost zero (in the bypassing water), the initial and boundary conditions for Eq. 6.1 are (infinite bath):

$$\begin{array}{lll} 0 < r < a & t = 0 & c = c_{eq} \\ r = a & t > 0 & c \cong 0 \\ r = 0 & t < 0 & \partial c / \partial r = 0 \end{array}$$

c_{eq} denotes the equilibrium concentration which is uniform throughout the aquifer material (particles and/or aggregates) at $t = 0$.

The cumulative mass desorbed after a certain time t , respectively the contaminant flux can be calculated using the following equations (CRANK, 1975):

$$M = M_{eq} \left(1 - \frac{6}{\pi^2} \sum_{n=1}^{\infty} \frac{1}{n^2} \exp \left[-n^2 \pi^2 \frac{D_a}{a^2} t \right] \right) \quad (6.2)$$

$$F = 6 M_{eq} \frac{D_a}{a^2} \sum_{n=1}^{\infty} \exp \left[-n^2 \pi^2 \frac{D_a}{a^2} t \right] \quad (6.3)$$

The ratio $(D_a t)/a^2$ (Fourier number) denotes the dimensionless time.

Depending on the value of the Fourier number, the series expansions in Eqs (6.2) and (6.3) may be approximated by a short time (Fourier number < 0.15), respectively a long time solution (Fourier number > 0.15) (GRATHWOHL, 1998).

For short times:

$$M = 6 M_{eq} \sqrt{\frac{D_a t}{\pi a^2}} - 3 \frac{D_a t}{a^2} \quad (6.4)$$

$$F = 3 M_{eq} \sqrt{\frac{D_a}{\pi a^2}} \frac{1}{\sqrt{t}} - 3 \frac{D_a}{a^2} \quad (6.5)$$

The long-time approximations are:

$$M = M_{eq} \left(1 - \frac{6}{\pi^2} \exp \left[-\pi^2 \frac{D_a}{a^2} t \right] \right) \quad (6.6)$$

$$F = 6 M_{eq} \frac{D_a}{a^2} \exp \left[-\pi^2 \frac{D_a}{a^2} t \right] \quad (6.7)$$

According to the last two equations, for late times the diffusion process is analogous to first order reaction kinetics resulting in a slope of $(-\pi D_a/a^2)$ in a semi-logarithmic plot.

The diffusion rate constants D_a/a^2 for diffusion limited desorption can be obtained as fitting parameters by applying the analytical solutions mentioned above to measured data.

M_{eq} [$M M^{-1}$] (mass of contaminant per mass of dry solids) is a function of the aqueous concentration at equilibrium c_{eq} [$M L^{-3}$]:

$$M_{eq} = c_{eq} \frac{\alpha}{\rho} \quad (6.8)$$

where $\alpha = \varepsilon + K_d \rho$ is the capacity factor of the porous medium [-], $\rho = (1 - \varepsilon) \cdot d_s$ the bulk density [$M L^{-3}$], K_d the distribution coefficient between solids and water at equilibrium [$L^3 M^{-1}$] and d_s the density of the solids [$M L^{-3}$].

From the long term approximation for the desorbed mass (Eq. 6.6) the time t [T] can be calculated until a certain fraction of the mass initially sorbed is recovered by diffusion limited desorption:

$$t = \left(-0.233 \log \left[1 - \frac{M}{M_{eq}} \right] - 0.05 \right) \frac{a^2}{D_a} \quad (6.9)$$

6.1.2 Desorption out of Layers of Low Permeability

Dissolved contaminants can diffuse over long time periods into low permeability layers such as silt, limestone, thick confining layers at the bottom of the aquifer (e.g. 'Gipskeuper' at 'Testfeld Süd'). If the aqueous concentrations decrease after a certain contact time (e.g. during remediation actions such as pump and treat), these substances may diffuse back into the aquifer.

Assuming that the low conductivity zone (initially free of contamination) is exposed to a constant concentration c_0 for a given contact time t_e , the concentration profile in the confining layer at a given time t is (GRATHWOHL, 1994, 1998):

$$\frac{c}{c_0} = \operatorname{erfc} \left[\frac{x}{2\sqrt{D_a t}} \right] \quad (6.10)$$

where $D_a = D_e / \alpha$ is the apparent diffusion coefficient and x the depth [L].

Eq. (6.10) can be used to calculate the expected profile of a solute in the confining layer, if the contact time t_e and the constant concentration c_0 are known.

If after the contact time t_e the concentration at the surface becomes zero, one fraction of the solute will diffuse further into the confining layer, while another fraction will diffuse back in the aquifer. The diffusive flux out of the low conductivity zone is:

$$F = c_0 \alpha \sqrt{\frac{D_a}{\pi t}} \left(1 - \frac{1}{\sqrt{1 + \frac{t_e}{t}}} \right) \quad (6.11)$$

and the mass of solute that has left the confining layer after a given time t is:

$$M = 2c_0 \alpha \sqrt{\frac{D_a t}{\pi}} \left(1 - \sqrt{1 + \frac{t_e}{t}} + \sqrt{\frac{t_e}{t}} \right) \quad (6.12)$$

In a double logarithmic plot versus time, the fluxes decrease with a slope of -1/2 at early times and for $t \gg t_e$ they decrease with a slope of -3/2 (GRATHWOHL, 1998).

6.2 Materials and Methods

6.2.1 Experimental Setup

The contaminant release (emission) out of disturbed and undisturbed aquifer material, as well as out of an undisturbed sample from the confining layer at the bottom of the aquifer (Keuper), was quantified in the laboratory using long-term column experiments.

For desorption out of permeable aquifer material (grains and aggregates), the experimental setup was the same as for the dissolution experiments (Chapter 5.2). The disturbed samples were leached in glass columns, the undisturbed ones in the PVC liners. The column leachate was analysed for PAHs and MAHs as described for water samples in Chapter 4.

For the quantification of the diffusion limited desorption out of the confining layer at the bottom of the aquifer, a small undisturbed sample (12 cm long, ca 2.5 cm Ø) was incorporated in a stainless steel cylinder (Fig. 6.1). The cylinder, tightly closed at one end, was inserted into a glass column (same as for leaching experiments). At the upper end the cylinder was open. There was a constant water flow through the column; the diffusion limited desorption took place only through the defined area at the upper end of the stainless steel cylinder, where the sample was permanently in contact with water.

The column effluent was extracted for cyclohexane and analysed for 16 EPA PAHs (the BTEX concentrations were lower than 0.1 µg/l and dropped fastly below the detection limit).

In order to determine the boundary conditions for desorption, the initial PAHs profile with depth was measured in an identical sample from the same depth, by solvent extraction of thin slices (ca 0.5 cm) of the low conductivity material.

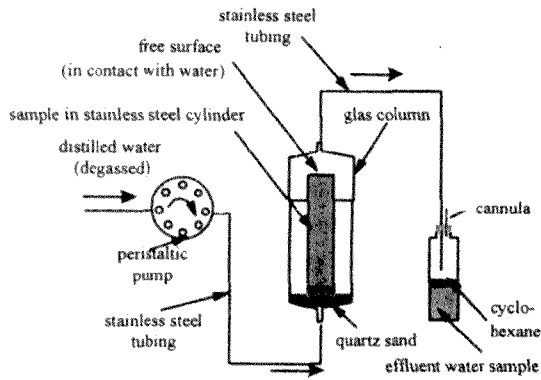


Fig. 6.1: Experimental setup for the quantification of diffusion limited desorption out of low conductivity layers.

6.2.2 Samples Used in Column Experiments for Desorption

The samples used in the laboratory for the quantification of diffusion limited desorption and discussed in this Chapter are listed in Table 6.1.

Table 6.1: Samples used in column tests for the quantification of contaminant release by diffusion limited desorption

Sample (well)	Depth [m]	Type
B56	8.05 - 8.4	undisturbed / aquifer material
B56	8.05 - 8.4	disturbed / aquifer material
B55	8.6 - 9	undisturbed / confining layer

The sample for the quantification of diffusion limited desorption out of confining layers was from the bottom of the aquifer in B55. At this location, at the contact between aquifer and Keuper was some residual NAPL (see saturation concentrations, respectively composition in Tables 5.2 and 5.3). Initially it

was intended to conduct experiments with more than one Keuper sample; because on the free surface (at the contact with water) of the other samples some fungi were growing during the experiment, only the results from one column will be discussed.

6.2.3 Analysis of PAHs from Contaminated Aquifer Material

In both types of desorption experiments (with permeable aquifer material and as with material from low permeability layers as well), it was necessary to measure the PAH content in the solid matrix.

As outlined in Chapter 5, the extraction method with acetone and cyclohexane proved to be not very effective, especially for compounds with higher molecular weight, leading to considerable error in the mass balance. The effectiveness of PAHs extraction using hot methanol was found by other authors to be up to 100 % (BALL et al., 1997; KLEINEIDAM, 1998). Methanol extraction is much more effective as this polar solvent is miscible with water which wets mineral surfaces, allowing also the extraction of molecules sorbed into the solid grains/aggregates. For this reason, in the desorption experiments all solid samples have been extracted using methanol as a solvent at 60 °C for about one week. The methanol extracts have been re-extracted with cyclohexane, adding distilled water to separate the cyclohexane when an emulsion was formed with methanol; the cyclohexane extracts were then analysed by GC-MS as previously mentioned.

6.3. Results and Discussion

6.3.1 Desorption out of Spherical Grains and Aggregates

6.3.1.1 Column Experiments with Undisturbed Samples

Experimental Results. Fig. 6.3 shows the concentrations of PAH (a) and volatile aromatic hydrocarbons (b) measured in the column leachate of an undisturbed sample from 'Testfeld Süd' (B56 8.05 - 8.4 m). After about 50 exchanged pore volumes, the maximum

concentration was reached for all compounds, then the concentrations drop, typically almost with the same slope. The concentrations of most PAH dropped after about 400 pore volumes below the detection limit (all concentrations shown here are corrected by the background value for desorption out of the liner inner walls, see also Chapter 5.3.4). The concentrations of the volatile compounds are much lower (generally less than 1 µg/l) and the values strongly scatter, possibly also due to some background in the same concentration range.

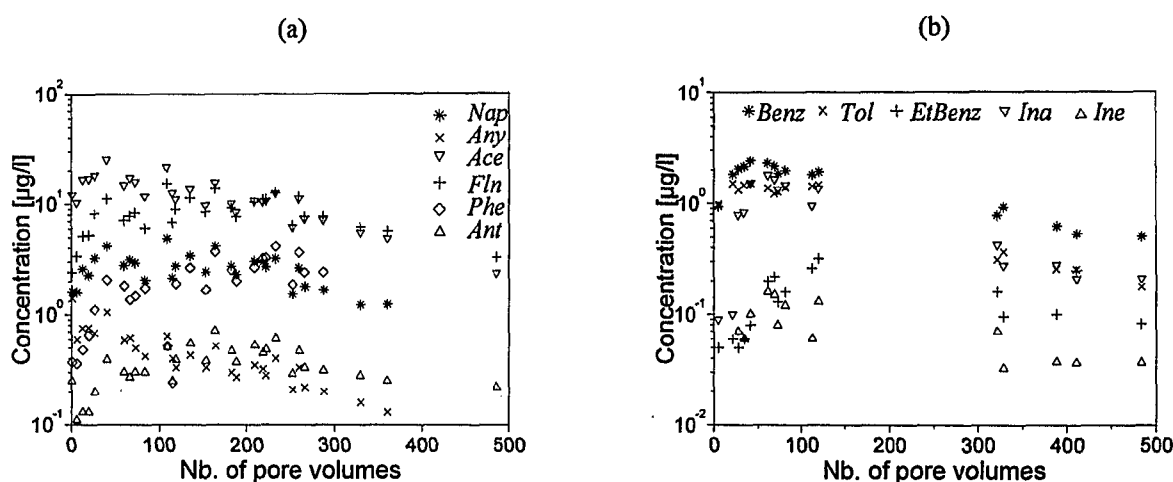


Fig. 6.3: Concentrations of PAH (a) and BTEX, *Ina* and *Ine* (b) measured in the column leachate of an undisturbed sample over 72 days (about 500 pore volumes exchanged); column length: 30 cm; linear velocity: 2 m/d.

The delayed reaching of the maximum concentrations in the leachate cannot be explained by a classic retardation process in the column, as it is almost the same for all compounds. The most probable reason would be enhanced biodegradation during storage, starting at the ends of the liner (where atmospheric oxygen came in contact with the aquifer material) and advancing towards the middle. The undisturbed sample discussed in Chapter 5.3.4 showed the highest PAHs load in the middle of the liner and lower concentrations in the solids towards the ends. The same effect has been observed by HAJJAJI (1998) in liners containing contaminated brown coal samples from an industrial site. It could also be that the contaminated material in the liner was not entirely wet when the leaching experiment was started (the liners were closed with tight plastic caps at both ends immediately after drilling in the field, but have been stored at 4°C for about 10 months until leaching). During this time, the

sample in the liner probably dried to some extent, especially at the ends. When leaching was started, it took some time until the mineral surfaces become wet again and the maximum area was exposed to the flowing water. The initially smaller interfacial area between contaminated grains and water lead at early times to an apparent retardation in the column. The maximum concentration was reached only when the whole grain area was water-wetted. Only from this point monitored concentrations can be described using the diffusion limited desorption approach.

The concentrations in the leachate may eventually also been reduced by biodegradation in the filter sand.

Diffusion Rate Constants and Long Time Desorption. The input parameters for the diffusion limited desorption model are the initial concentration in the sample M_{eq} (mass

substance per mass of dry solids) and the mass of the contaminated aquifer material investigated. M_{eq} is the sum between the mass desorbed during the leaching experiment and the mass which remained sorbed at the end of the experiment. The latter is determined by solvent extraction of the solids and its value is highly dependent on the extraction efficiency. If the extraction is not complete, modeling of the experimental data becomes more difficult because M_{eq} and D_d/a^2 have to be fitted simultaneously. Table 6.2 shows the mass balance for the undisturbed sample from B56 (8.05 - 8.4 m). Only PAHs up to *Py* are discussed here. For the higher ones the concentrations in the column leachate were too low and dropped after short time below the detection limit. The values for M_{eq} in the first column of Table 6.2 resulted by summation of amounts desorbed and extracted with hot methanol.

The values $M_{eq,fit}$ needed to fit the measured data (Table 6.2) were greater than the measured ones (M_{eq}), indicating that the extraction was not complete even with hot methanol. It appears that the results of the extraction efficiency tests of BALL (1997) and KLEINEIDAM (1998) may not apply for aged samples as the ones investigated in this study, in which the sorbed PAHs seem to be more strongly bounded to the solids (organic matter) and harder to recover by extraction than such which shorter and known sorption history. In the sample considered here, there was e.g. no *Py* detectable in the methanol extract at the end of the desorption experiment. This is most probably because *Py* was resistant even to methanol extraction, and not because it was entirely desorbed (for *Py* $M_{eq,fit}$ was 0.703 mg/kg). Because of difficulties with the mass balance for higher molecular PAHs, probably only the results for *Nap* to *Fth* are realistic.

The desorption rates measured in the column experiments were modeled using analytical solutions of Fick's 2nd law in spherical

coordinates, as described in Chapter 4.1.2. Some authors (GRATHWOHL et al., 1994; MERKEL, 1996, WEIB, 1998) observed during desorption experiments initially high fluxes, modeled by first order kinetics. But in those experiments only heterogeneous disturbed samples have been used. The measured values and the fitted curves are shown in Fig. 6.4 and the obtained diffusion rate constants in Table 6.3. In the experiment discussed here, the amount of the so called 'fast fraction' was very low or zero. This is equivalent to a, to some extent, homogeneous sample with respect to desorption. Probably it is due to the fact that in the liner PAHs are desorbed out of bigger aggregates, with no domination of desorption near their surface ($X_i \approx 0$). This situation is probably closer to field conditions than the one usually created when desorption is monitored out of disturbed samples.

Table 6.2: Mass balance for desorption out of an undisturbed sample from 'Testfeld Süd' (B56 8.05 - 8.4 m).

Substance	M_{eq} [mg/kg]	$M_{eq,fit}$ [mg/kg]	% of $M_{eq,fit}$ desorbed
Nap	0.203	0.280	37
Any	0.033	0.050	31
Ace	0.510	1.20	35
Fln	0.480	1.60	22
Phe	0.248	0.500	22
Ant	0.101	0.140	35
Fth	0.034	0.070	14

Table 6.3: Diffusion rate constants and t^{90} (the time until 90 % of the sorbed mass is removed) for an undisturbed sample from 'Testfeld Süd' (B56 8.05 m - 8.4 m)

Substance	D_d/a^2 [s ⁻¹]	t^{90} [years]
Nap	$2.2 \cdot 10^{-9}$	2.6
Any	$1.5 \cdot 10^{-9}$	3.9
Ace	$1.7 \cdot 10^{-9}$	3.4
Fln	$8 \cdot 10^{-10}$	7.3
Phe	$4.3 \cdot 10^{-10}$	13.5
Ant	$2 \cdot 10^{-10}$	29
Fth	$9.4 \cdot 10^{-11}$	61.7

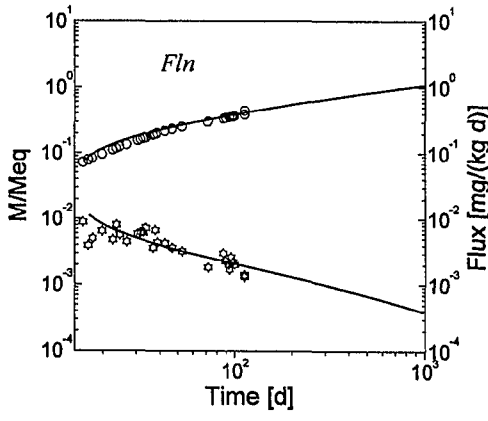
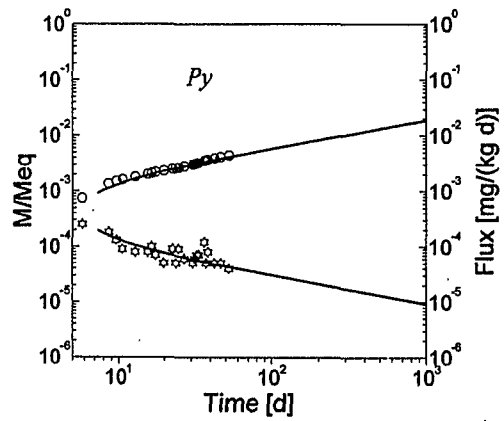
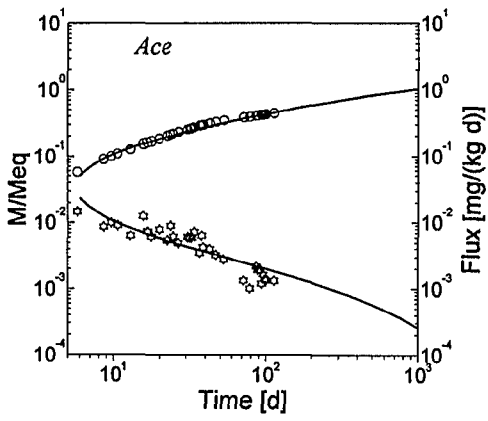
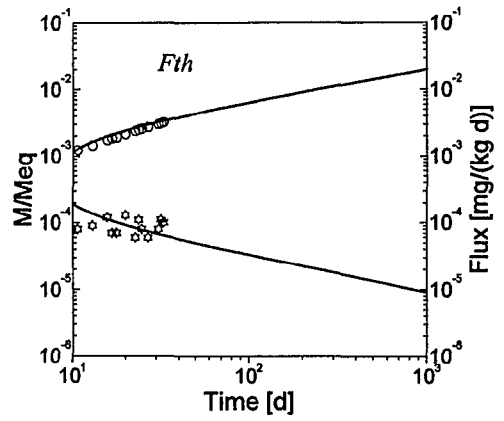
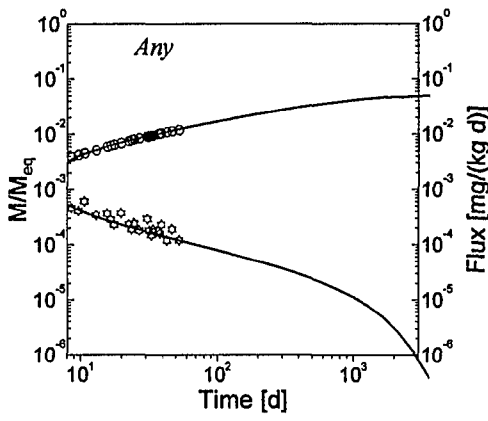
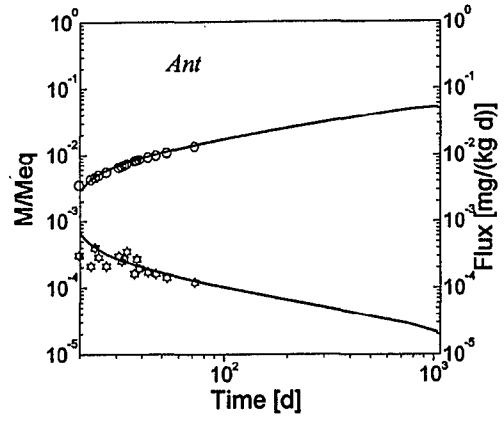
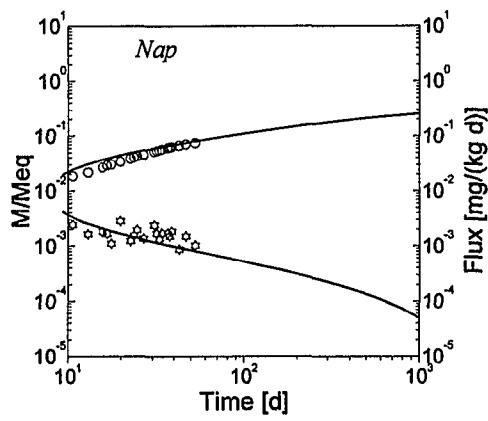


Fig. 6.4: Desorption kinetics modeling for undisturbed aquifer material from 'Testfeld Süd' (B56 8.05 - 8.4 m)

For lower molecular PAH (*Nap* to *Fln*) there is an almost linear dependence of the diffusion rate constants on the octanol/water partition coefficients, respectively the subcooled liquid water solubility (Fig. 6.5). The deviation from linearity increases with increasing K_{ow} . *Py* (not shown in the diagram) strongly deviates from linearity: compared to *Fth*, which has the same K_{ow} , *Py* shows a diffusion rate constant lower almost by a factor of 100 (Table 6.3).

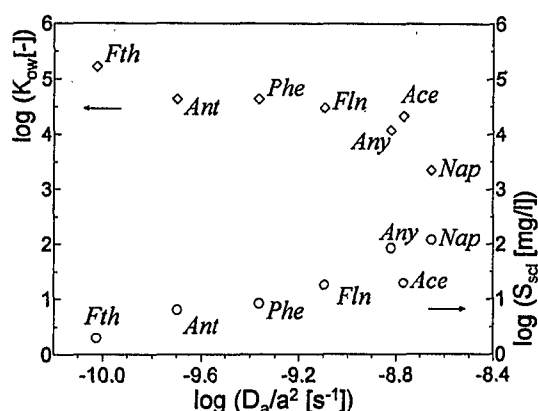


Fig. 6.5: Dependence of the diffusion rate constants on the octanol/water partition coefficient (open diamonds), respectively the aqueous solubility of the subcooled liquid (open circles) for an undisturbed sample from 'Testfeld Süd'

The time needed to remove 90 % of the mass initially sorbed depends on the diffusion rate constants and was calculated with Eq. 6.9 (values in Table 6.3). Except for the 2-ring PAH, which desorb faster, t^{90} is of the order of decades.

Estimation of Equilibrium K_{ds} from Desorption Data. If at $t = 0$ the sample was in equilibrium, the maximum (equilibrium) concentration is observed at the beginning of the experiment and this yields the maximum flux of the desorbing substance. For very early times ($(D_a t)/a^2 < 0.1$), the maximum flux due to desorption F_{max} can be expressed as in Eq. 6.5 by neglecting the second term on the right hand and depends on the inverse of the square root of time:

$$F_{max} = \frac{3\alpha c_{eq} \sqrt{\frac{1}{\pi t} \frac{D_a}{a^2}}}{\rho} \quad (6.13)$$

Since the fraction of natural organic carbon cannot be measured for already contaminated

samples from the field, the following calculations are made assuming that $f_{oc} = 0.1$.

The ratio between the total initial concentration of the substance before desorption (M_{eq} [M M⁻¹]) and the aqueous equilibrium concentration c_{eq} corresponds then to the distribution coefficient K_d [L⁻³ M] of the substance at equilibrium. The values of c_{eq} and K_d calculated for the investigated PAH are shown in Table 6.4. The K_d values are compared with those resulting after SONTHEIMER (1983). As it can be noticed, the values calculated here from diffusion limited desorption data and those of SONTHEIMER are within the same order of magnitude.

The slightly non-linear dependence of calculated K_{ds} (this work) on those predicted after SONTHEIMER as a function of K_{ow} , indicates that for this type of samples, the traditional K_{oc} approach (linear sorption isotherms) possibly does not apply (Fig. 6.6). The deviation from linearity increases with increasing K_{ow} and implies smaller aqueous equilibrium concentrations, respectively a greater concentration in the solids (sorbed mass) than the linear model would predict, leading to longer clean-up times.

Table 6.4: Calculated aqueous equilibrium concentrations in an undisturbed sample containing sorbed PAH and resulting K_{ds} ; solid-water distribution coefficients calculated from desorption data are within the same order of magnitude with those calculated after SONTHEIMER (1983). All values calculated for $f_{oc} = 0.1$.

Subst.	c_{eq} [mg/m ³]	$K_{d, desorption}$ (= M_{eq}/C_{eq}) [l/kg]	K_d (SONTHEIMER) [l/kg]
Nap	4.11	68	59
Any	0.423	118	177
Ace	10.2	118	170
Fln	2.31	693	473
Phe	0.432	1158	637
Ant	0.116	1206	637
Fth	0.041	1701	1908
Py	0.623	1128	1908

This is believed to be due to a relatively great amount of soot, cinder and coal particles found in the samples from 'Testfeld Süd'. Such particles are commonly present in the bulk mass at former gas-work sites; these are formed during the carbonisation process and generally exhibit high PAH concentrations and very high organic carbon contents associated with higher internal surfaces and intraparticle porosities

(MERKEL, 1996). It is probably the fraction sorbed into such materials which is resistant even to extraction methods using high energy input.

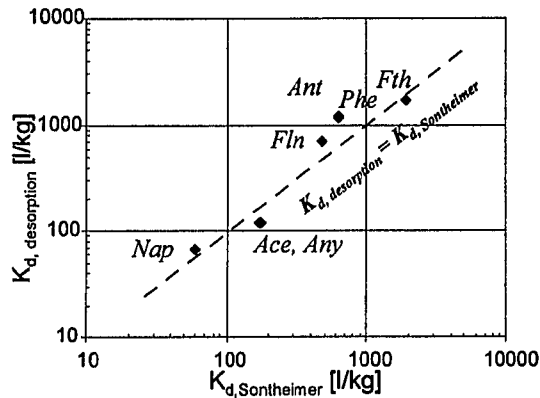
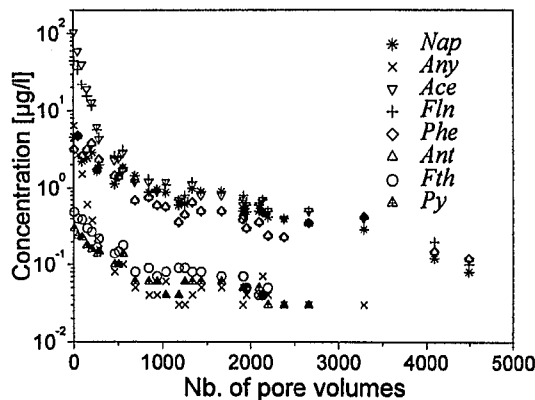


Fig. 6.6: $K_{d,s}$ calculated from desorption data (undisturbed sample from 'Testfeld Süd') versus $K_{d,s}$ calculated after SONTHEIMER et al. (as a function of $\log K_{ov}$).

6.3.1.2 Column Experiments with Disturbed Samples

Experimental Results. The disturbed column was leached at the same time with the undisturbed sample in the liner. Fig. 6.7 shows the concentrations measured in the leachate from this disturbed sample. The concentrations of *Tol* (constant during more than 2 months) correspond to the background concentration in the laboratory (the same as in the leaching experiments for dissolution out of residual phase discussed in Chapter 5). For this reason,

(a)



(b)

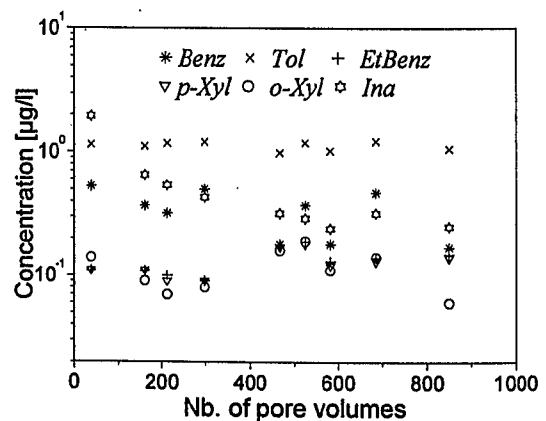


Fig. 6.7: Concentrations of some PAHs (a) and BTEX and *Ina* (b) measured in the column leachate of a disturbed sample over 79 days (about 4500 pore volumes exchanged); column length: 12 cm; linear velocity: 2 m/d.

Interestingly, the concentrations of *Ace* and *Fln* first decrease much faster and then remain on

the desorption behaviour of *Tol* could not be investigated.

The initial PAH concentrations are by about one order of magnitude higher than those from the undisturbed sample. This is probably because the contaminants have been uniformly distributed in the sample trough homogenisation, leading to the absence of dilution in the column (virtually the same concentration in the pore water at any point in one flow-available cross section of the column). Additionally, as the concentration in the solids before leaching is unknown, it also cannot be excluded that the overall PAH and BTEX concentration in the disturbed column was initially higher than in the liner. This appears to be correct, if the values of M_{eq} in the disturbed (Table 6.5) and undisturbed sample (Table 6.2) are compared (higher in the disturbed one).

The concentrations measured at early times in the leachate are also the maximum ones, sustaining the highly homogeneous distribution of sorbed PAH throughout the sample. In the beginning (few hundreds of exchanged pore volumes) they drop drastically, then the concentration curves decline with the same slope, indicating a diffusion-controlled release mechanism.

the same concentration level with other PAHs which started with about 10 times lower con-

centrations (e.g. *Nap*, *Phe* and *Ant*). This could be an indication that in the sample taken from the field, the initial *Ace* and *Fln* concentration in the pore water was higher than the one corresponding to the sorption equilibrium (K_d). The difference might be e.g. due to a plume of constantly high concentration of poorly biodegradable *Ace* and *Fln* which overlaps the one due to sorbed PAHs (in equilibrium to those dissolved in the pore water). The same applies for *Any*. Such a scenario would also imply that in the field different contamination events occurred at different points during time. In this hypothesis, the maximum concentrations of *Any*, *Ace* and *Fln* due to desorption are

Table 6.5: Summary of the initial concentrations in the solids (input parameter), the obtained diffusion rate constants, the fast fractions and corresponding first order rate constants (fitting parameters) and the time until 90% of the sorbed mass is removed

Substance	M_{eq} [mg/kg]	X_i [-]	k_i [s ⁻¹]	D_d/a^2 [s ⁻¹]	t^{90} [years]
Benz	0.030	0.7	1.05E ⁻⁷	6E ⁻⁸	0.1
Ina	0.150	0.02	2E ⁻⁸	7E ⁻⁹	0.8
Nap	0.650	0.08	1E ⁻⁶	5E ⁻⁹	1.2
Any	0.100	0.25	4E ⁻⁶	8E ⁻¹⁰	7.3
Fln	2.15	0.22	3.8E ⁻⁶	7.5E ⁻¹⁰	0.6
Phe	1.150	0.09	2E ⁻⁶	6E ⁻¹⁰	9.7
Ant	1.150	0.09	2E ⁻⁶	6E ⁻¹⁰	9.7
Fth	0.160	0.08	5E ⁻⁷	4.5E ⁻¹⁰	12.9
Py	0.150	0.035	3E ⁻⁷	3.5E ⁻¹⁰	16.6
BaA	0.104	0.0001	1E ⁻⁷	2.8E ⁻¹⁰	19.3
Chr	0.090	0.015	3E ⁻⁶	2.4E ⁻¹⁰	19.3
BbF-BkF	0.040	0.3	1.28E ⁻⁶	8E ⁻¹¹	72.5

In contrast to the undisturbed sample (previous chapter), the data from the disturbed one could be fitted only using a two-site model. The high initial fluxes of a fast desorbing fraction (X_i) are governed by first-order kinetics (k_i - rate constant of the fast fraction), while at later times the intraparticle diffusion model applies (D_d/a^2 - diffusion rate constant of the slow fraction). Generally, the model underestimates the short-term fluxes.

The need of some fast fraction to fit the measured data from the disturbed sample indicates that the sample became more heterogeneous because of mixing; by breaking aggregates initially present in the liner, the sample was split in faster and slower fractions relative to desorption. At the same time, no coal

probably overestimated in this experiment.

Diffusion Rate Constants and Long Time Desorption. The diffusion rate constants were determined by fitting the measured data. The time needed for 90 % of the initial mass to be desorbed was calculated as presented in chap. 6.3.3.1. The input and fitting parameters for the model as well as the values of t^{90} are shown in Table 6.5, the diagrams for the desorption kinetics are shown in Fig. 6.8.

particles were detected in the disturbed sample, which could explain the faster desorption and higher aqueous concentrations monitored out of it.

For the disturbed sample, *Ace* and to some extent *Fln* clearly deviate from the diffusion-limited desorption model. For *Ace*, the model doesn't hold, 99 % of the mass initially present in the column was already released within about 30 days. The supposition that, at least locally, this compound did not reach sorption equilibrium seems to be correct. *Fln* shows a similar behaviour, still it leaches slower than *Ace* (about 81 % removed after 79 days), but much faster than all other PAHs (see Appendix V).

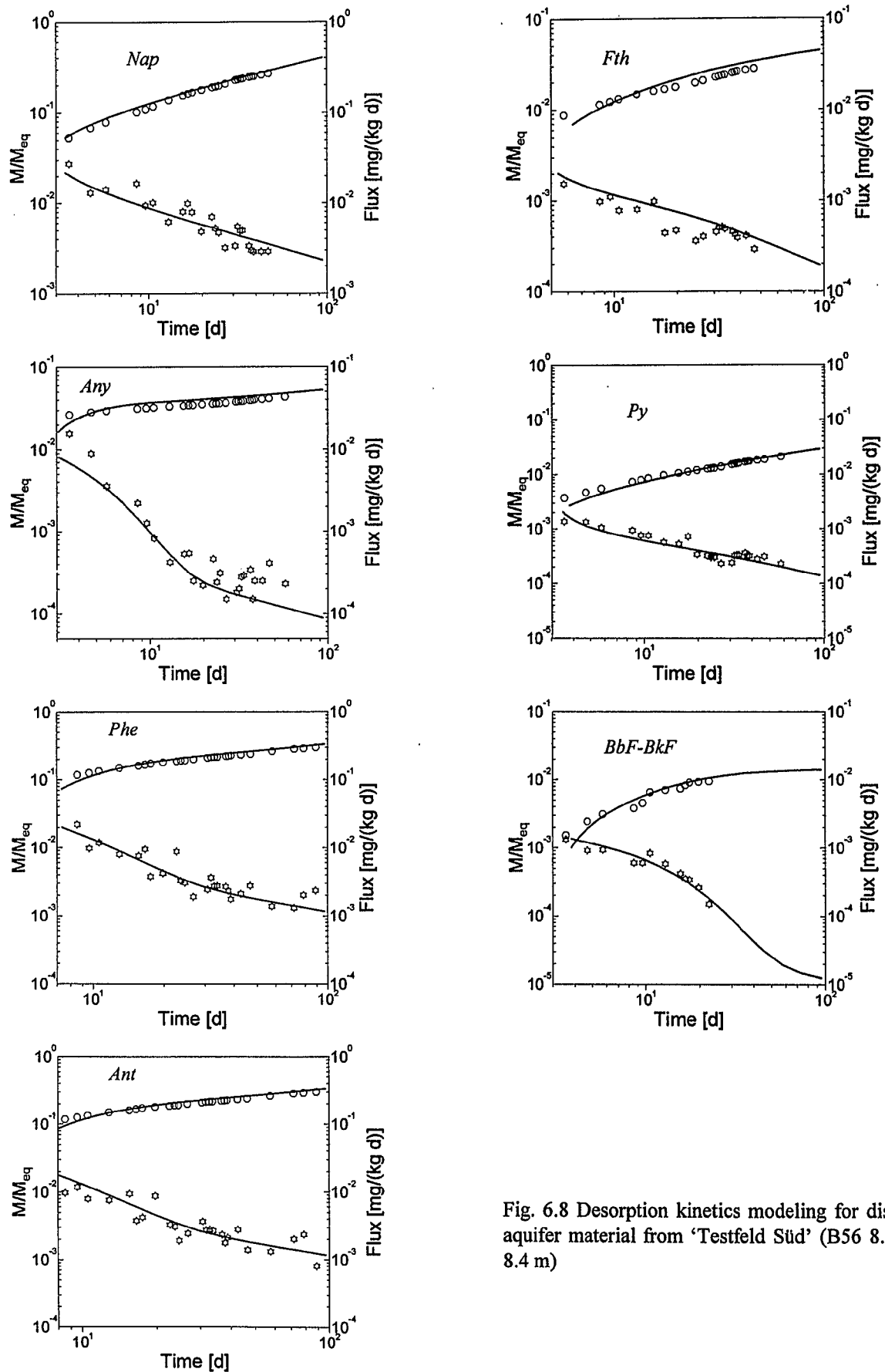


Fig. 6.8 Desorption kinetics modeling for disturbed aquifer material from 'Testfeld Süd' (B56 8.05 m - 8.4 m)

For most of the measured PAHs there is an almost linear dependence of the diffusion rate constants on the octanol/water partition coefficients, respectively the subcooled liquid water solubility (Fig. 6.9). *Ace* and *Flu* are an exception.

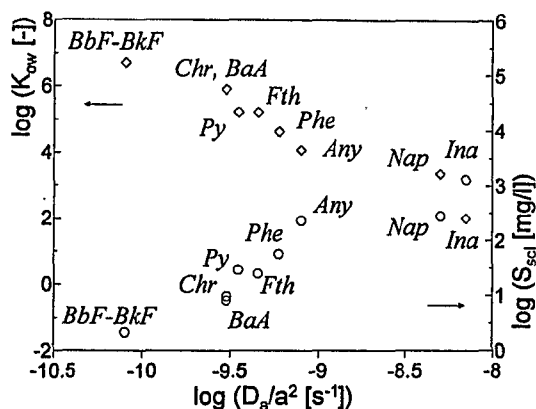


Fig. 6.9: Dependence of the diffusion rate constants on the octanol/water partition coefficient (open diamonds), respectively the aqueous solubility of the subcooled liquid (open circles) for a disturbed sample from 'Testfeld Süd'

Estimation of Equilibrium K_{ds} from Desorption Data. The equilibrium concentrations for desorption calculated with Eq. 6.13 were used to estimate solid-water distribution coefficients (Table 6.6).

Table 6.6: Calculated aqueous equilibrium concentrations in an undisturbed sample containing sorbed PAHs and the resulting K_{ds} ; solid-water distribution coefficients calculated from desorption data are within the same order of magnitude with those calculated after SONTHEIMER et al. (1983). All values calculated for $f_{oc} = 0.1$.

Subst.	C_{eq} [mg/m ³]	$K_{d, desorption}$ (= M_{eq}/C_{eq}) [l/kg]	K_d (SONTHEIMER) [l/kg]
Ina	3.45	44	43
Nap	11.9	55	59
Any	5.89	17	177
Phe	3.19	361	637
Fth	1.05	153	1908
Py	0.071	2121	1908
BaA	0.014	5510	6877
Chr	0.013	5263	6877
BbF-BkF	0.01	4474	23442

For all PAHs they are by one to two orders of magnitude greater than the equilibrium concentrations in the undisturbed sample (Table 6.4). This effect is due to an increase of availability of the contaminants to desorption (greater contact area and shorter diffusion

distances due to breaking up of aggregates by mixing), and probably also to the absence of soot particles. Equilibrium concentrations are still a lot smaller than saturation concentrations corresponding to dissolution out of residual phase (Chapter 5.3.1). The distribution coefficients calculated from desorption data are in concordance with those predicted after SONTHEIMER only for the 2-ring PAHs. For higher molecular PAHs, K_{ds} from desorption data are smaller; the deviation from linearity increases with increasing K_{ow} (Fig. 6.10). This may be due to incomplete sorption equilibrium of these PAHs with the solids (that is in the field) before desorption started.

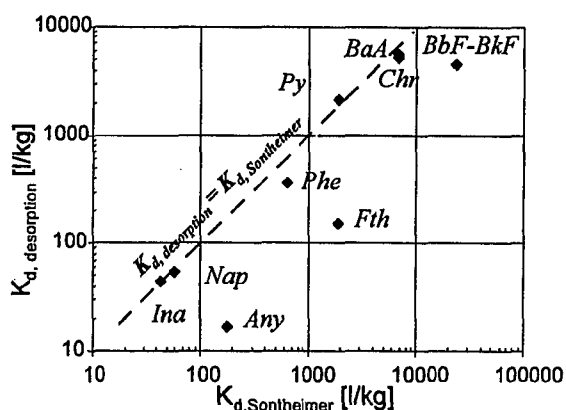


Fig. 6.10: K_{ds} calculated from desorption data (disturbed sample from 'Testfeld Süd') versus K_{ds} calculated after SONTHEIMER (function of $\log K_{ow}$)

6.3.1.3 Conclusions

From the experiments presented in this chapter it results that desorption out of undisturbed samples is slower than out of disturbed ones; in the latter maximal fluxes and equilibrium concentrations are higher. There are two in a sense opposite consequences resulting from this:

1. For the prediction of the release rates, the disturbed samples are more suited, as the results will represent the 'worst-case' scenario.
2. In terms of remediation times, the results from column experiments with disturbed samples underestimate the duration until a certain degree of desorption is achieved.

In the field, desorption probably occurs much slower than in the small-scale experiments, firstly due to diffusion distances longer than of the order of grain diameters. Additionally, at

former gas-works it must be counted with a relatively large amount of 'dark fractions' in the bulk mass of the aquifer, made up of soot, cinder and coal, which slow up the desorption process. This was also observed by MERKEL (1996). Fig. 6.11 shows a comparison between diffusion rate constants from this work and those obtained by MERKEL (1996) and WEIB (1998).

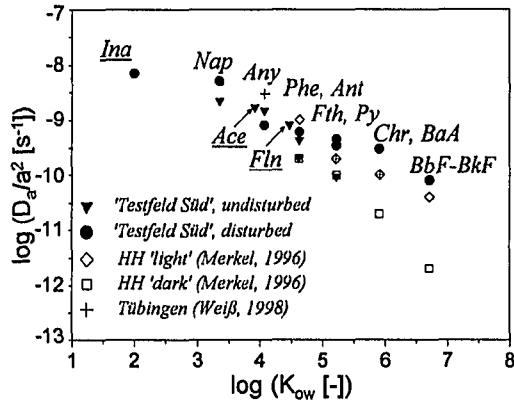


Fig. 6.11: Diffusion rate constants for desorption out of disturbed (filled circles) and undisturbed samples (filled triangles) from 'Testfeld Süd' (this work), compared to those obtained by WEIB (1998) for a sample from the former gasworks Tübingen (crosses) and by MERKEL (1996) for samples from Heidenheim. Prior to desorption, the sample from the gasworks Heidenheim had undergone wet mechanical treatment on-site. The desorption was consequently measured separately for the 'light fraction' 0.25-0.5 mm (open diamonds) and the 'dark fraction' 0.25-0.5 mm (open squares). For the underlined substances, data were available only from the present work.

It appears that the diffusion rate constants for the undisturbed sample (this work) are identical (for *Ant* and *Fth*) or very similar with those obtained by MERKEL for 'dark fractions' (0.5-2.5 mm) from the former gas-work Heidenheim (HH). As for the undisturbed sample from 'Testfeld Süd', the diffusion rate constants for the 'dark fraction' from HH do not depend linearly on the K_{ow} , the deviation from linearity

increases as K_{ow} increases. The very slow desorption out of the undisturbed sample is probably controlled by the same 'dark fraction', which probably is also the case in the field. The time scale involved in the removal of PAHs out of this fraction is well beyond the experimental time scale (up to thousands of years) (Fig. 6.12). It has been already observed by other authors that pyrogenically derived PAHs associated with soot particles deposited in sediments are less available to partition into water and may withstand desorption at temperatures up to 650 °C (MCGRODDY and FARRINGTON (1995) and STEINER and BURTSCHER (1994), cited by MERKEL, 1996).

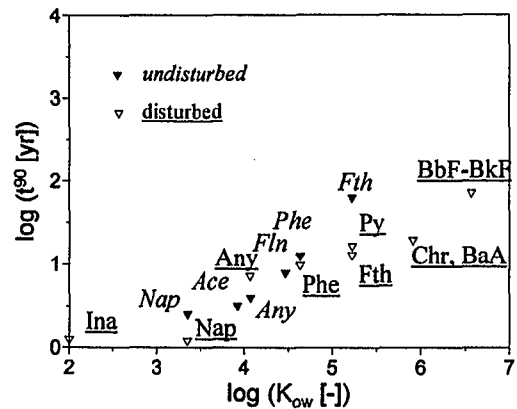


Fig. 6.12: Dependence of the time needed to desorb 90 % of the sorbed mass on the octanol/water partition coefficient. The time increases with increasing K_{ow} and is longer for undisturbed samples than for disturbed ones.

The comparison of K_d values calculated as a function of K_{ow} with those estimated from desorption data out of undisturbed contaminated aquifer material from 'Testfeld Süd' (Fig. 6.10) indicates that in the field at least higher molecular PAHs may not have yet reached sorption equilibrium. This implies that, although the contamination is already 50-100 years old, in terms of contaminant transport there is still a sink term due to sorption which has to be accounted for in reactive transport modeling.

6.3.2 Desorption out of Layers of Low Permeability

6.3.2.1 Experimental Results

Fig. 6.13 shows the PAH concentration profiles measured in the upper 12 cm of the low permeability layer (immediately at the contact with the aquifer).

The measured concentration profiles do not confirm the supposition that the Gipskeuper is contaminated only by diffusion of dissolved molecules from the groundwater into the low conductivity layer. During extraction of the Keuper, it could be noticed that, at the contact with the groundwater, this formation shows a distinct morphology (strongly eroded) and some residual NAPL from the aquifer is infiltrated in fissures. Some separate NAPL phase was present throughout the 12 cm long clay core.

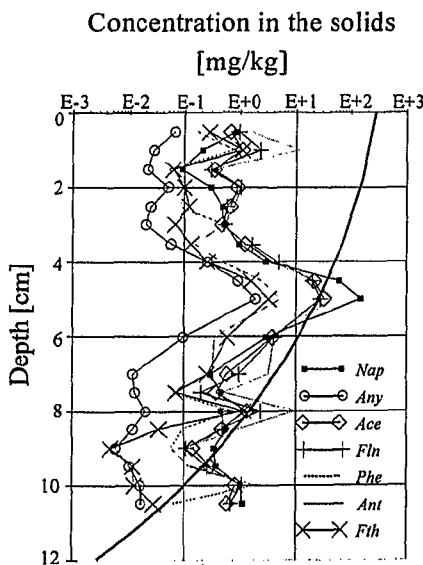


Fig. 6.13: Concentration profiles in the upper 12 cm of the confining layer in B55. At this location, there was some residual NAPL at the bottom of the aquifer (aqueous saturation concentrations in Table 5.2 and 5.3). The solid curve shows the expected concentration profile in the confining layer if it would be contaminated only by diffusion. E. g. for *Phe*, assuming an equilibrium concentration at the contact with the aquifer equal to the saturation concentration out of the NAPL from B55 (285.5 $\mu\text{g/l}$) and a contact time of 100 years, for a capacity factor $\alpha=34.88$, the concentration in the pore water of the confining layer in 40 cm depth should be ca 7 $\mu\text{g/l}$. The measured profiles cannot be explained by a pure diffusion mechanism.

The fluxes released through a defined area of the confining layer (measured in a column experiment as described in Chapter 6.2) are represented in Fig. 6.14. Given the contaminant distribution in the low conductivity layer, the release back into water is the effect of overlapping diffusion out of the matrix and dissolution out of NAPL present in fissures as a separate phase; the measured fluxes cannot be fitted if only diffusion limited desorption (Eq. 6.11) is assumed (solid curve).

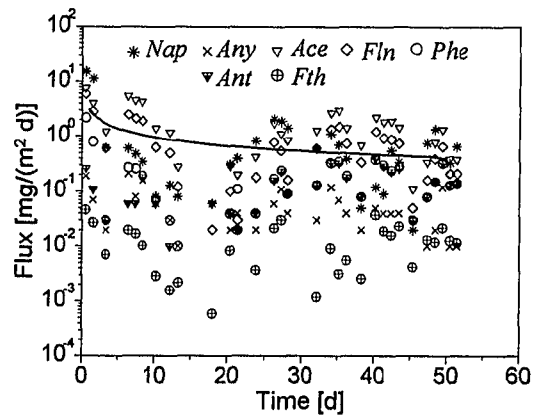


Fig. 6.14: PAH release out of the upper, eroded layers of the Gipskeuper at the bottom of the aquifer is not governed exclusively by diffusion limited desorption (solid curve), but also by dissolution out of residual NAPL phase infiltrated in fissures. The solid curve shows the expected shape of the variation of the desorbed flux during time (if only diffusion limited desorption would occur).

6.3.2.2 Conclusions

The residual NAPLs can infiltrate into fissures in the confining layer at the bottom of the aquifer. The contaminant release back into groundwater is the result of overlapping of diffusion limited desorption and dissolution out of residual phase. As long as some residual phase exists in fissures, the overall flux is dominated by dissolution.

The volume of the separate NAPL phase per unit volume of Gipskeuper (the NAPL residual saturation of the confining layer) and the specific contact area with the bypassing groundwater is however smaller than for the residual NAPL in the permeable porous medium (aquifer).

According to the results shown above, assuming that the flux out of the Gipskeuper

would have remained constant (worst case scenario), i.e. about $10 \text{ mg/m}^2/\text{day}$ for *Ace*, out of 100 m^2 of contaminated Gipskeuper the emission would be about 1 g/day . Assuming the same area in the cross section of the aquifer (normal to the flow direction) containing residual blobs and a maximum aqueous concentration of $300 \text{ }\mu\text{g/l}$ for dissolution, the flux of *Ace* is 9 g/d . It results that the overall

emission in the aquifer is always dominated by dissolution out of residual NAPLs (blobs or pools) and is governed by the composition and spatial distribution of the residual NAPL phase. The absolute release rate due to desorption is however not that low and would become relevant if the NAPL sources were removed the contaminants would be released into the groundwater by desorption alone.

7. The Plume at 'Testfeld Süd'

7.1 PAH and MAH

7.1.1 Multilevel Wells

Several groundwater sampling campaigns took place at 'Testfeld Süd' between 1996-1998. Because most of the existing wells were located in the domain where NAPL is present as a separate phase, during summer 1996 some new groundwater wells were drilled and set up. These wells have been sampled by conventional pumping in July (when the drilling campaign took place), in August and September 1996.

In 1997, eight selected wells initially thought to be located immediately downstream from the area with residual NAPL (Fig. 2.1) were equipped with multilevel sampling devices. The concentrations in the groundwater were monitored in different depths in June, July and November (detailed results by SCHETTLER, 1998). The multilevel wells and the depths of the sampling horizons are listed in Appendix VI. In the wells B55 and B56 some residual phase was unexpectedly found at the bottom of the aquifer. There was also some residual NAPL in B49, in the area of the former benzene distillery.

Extremely high PAH and BTEX concentrations were found in the groundwater, by orders of magnitude higher than the concentrations admitted in groundwater by German regulations (e.g. 1 µg/l for *Benz*, 2 µg/l for *Nap*). There were also MAHs not quantified in routine groundwater analyses found in very high concentrations, mainly *trimethylbenzenes*, as well as *Ina*, *Ine* and *Bf*. The maximum concentrations of these substances and of the 16 EPA PAHs found in the multilevel wells are listed in Table 7.1. For many compounds they are in the order of magnitude of the saturation concentrations for dissolution out of residual phase (compare to Table 5.2).

In the multilevel wells, for some compounds there are considerable differences between concentrations in different horizons (e.g. in B54, Fig. 7.1), confirming the highly heterogeneous distribution of the residual NAPL as well as the aquifer heterogeneity.

Table 7.1: Maximum concentrations in the multilevel wells at 'Testfeld Süd'. The multilevel wells are located approximately at the downstream border of the source area (Fig. 2.1).

MAH and Bf	Maximum concentration [µg/l]	PAH	Maximum concentration [µg/l]
Benz	1893	Ina	1002
Tol	213	Ine	2129
EtBenz	887	Nap	3378
o-Xyl	612	Any	589
p-Xyl	820	Ace	956
Pb	140	Fln	298
IsoPb	94	Phe	486
1,2,3-Tmb	180	Ant	140
1,2,4-Tmb	407	Fth	206
1,3,5-Tmb	199	Py	122
Bf	987	BaA	31
		Chr	26
		BbF-BkF	19
		BaP	4
		DahA	1
		Indeno	4
		BghiP	3

Locally there are relatively well separated, smaller plumes. E.g. in B54, there are probably different PAHs and BTEX plumes overlapping (note that, similarly to B49, where peak BTEX-concentrations are found, B54 is also located in the area of the former benzene distillery). Within the class of MAHs, there can be distinguished three overlapping plumes in B54: *Tol*, *o-Xyl* and *trimethylbenzenes* which show increasing concentration with depth, *Pb* and *IsoPb* which show no differentiation with depth and *Benz*, *EtBenz*, *p-Xyl*, with almost vertical concentration profiles, but showing a slight increase at the bottom of the aquifer. Individual PAHs also show different concentration distributions - *Nap* and *Phe* with high concentrations at the top and bottom of the aquifer, *Any* and *Ant* (*Fln* similar to these two, but flatter concentration gradient towards bottom) and *Ace* with relatively constant concentrations throughout the entire depth (only slight decrease at the bottom of the aquifer).

Though some different concentration profiles are evident, it is difficult to say whether the differences in concentration profiles within the same compound class (PAHs, MAHs) are solely due to sources of different composition, or also to different degree and/or succession of biodegradation of individual compounds in the aquifer. It is believed that both effects overlap.

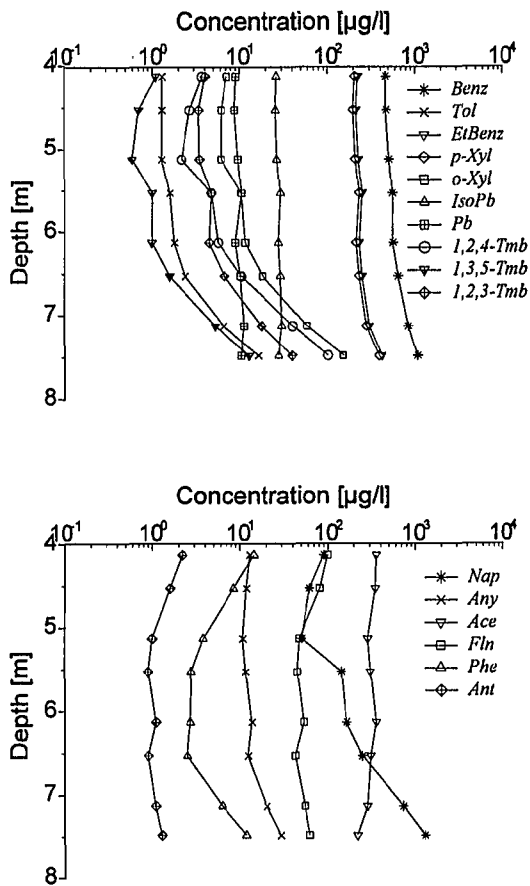


Fig. 7.1: BTEX (up) and PAHs (down) concentrations in different horizons in B54 (data from SCHETTLER, 1998).

If the multilevel concentrations are observed within the length of the mass transfer zone for dissolution, their vertical distribution also has to be seen in relation with the vertical distribution of the hydraulic conductivity. BÖSEL (1999) performed tracer tests at 'Testfeld Süd' and showed that in B54 the conductivity is highest at the top of the aquifer and decreases to the bottom. If the concentrations in the groundwater are caused by a source placed immediately in the vicinity of the well and smeared throughout the entire aquifer depth, then their vertical differentiation may be caused by different contact times at the source - lower in well permeable, higher in less permeable horizons (in Fig. 7.1: *Tol*, *o-Xyl*, *trimethylbenzenes*, *Nap*, *Phe* and to some extent *Any* and *Ant*). BÖSEL (1999) showed that the vertical differences between the tracer breakthrough curves within different horizons of the same well due to different values of k_f decrease with increasing distance from the tracer input well. At 'Testfeld Süd' these differences vanish after a distance of about

30 m, this distance approximating the scale of heterogeneity of the k_f distribution. Similarly, plumes with no vertical differentiation in concentrations (in B54 *Pb*, *IsoPb*, *Ace*, *Fln* - Fig. 7.1) probably originate from sources located at a greater distance upstream - presumably mainly tar pits around B15, B16 for PAHs and the area around B50 (the old benzene distillery) for MAH, all located at a distance of about 50 m (B50) to at least 100 m (B15, B16) from the source.

Most of the PAH sources are located upstream, but there is also some residual tar in the multilevel wells (e.g. B55 and B56). In B49 and B56 there are additionally very high *Nap* concentrations (around 3000 µg/l in B56). These peak concentrations match the saturation concentration of *Nap* estimated for the tar in B56 (Table 6.1); so here is probably the most downstream located *Nap* source at the site. On the contrary, the concentration of *Ace* in the groundwater in B56 (about 300 µg/l) is almost 10 times greater than the saturation concentration of this PAH out of the tar at the bottom of the aquifer in B56 (see Table 6.1). This indicates that *Ace* comes from up-stream and arrives in the area of the multilevel wells in relatively constant concentrations of 200-300 µg/l, which remain so over at least 200 m distance in the main groundwater flow direction (about 200 µg/l in NT01, see further).

The concentrations measured in the field in multilevel wells are in good accordance with the maximum concentrations from column leaching experiments with disturbed samples of aquifer material from the same location. Table 7.2 shows an example for B55.

Table 7.2: Concentrations in the groundwater from 5.09 m depth in B55 versus maximum concentrations in column experiments with aquifer material from the same location (Chapter 5.3). All values in µg/l.

PAH	Groundwater * (5.09 m)	Column (5- 5.5 m)
Ace	745	709
Fln	275	292
Phe	100	113
Ant	6.30	7.41
Fth	1.40	1.24
Py	0.50	0.46

* average between values from June, July and November 1997

7.1.2 The Plume Downgradient: B28 - B42 - NT01

The main flow direction in the plume away from the area of the multilevel wells was determined by BÖSEL (1999) using tracer tests and follows the line B28 - B42 - NT01. The distance between B28 and B42 is about 50 m, and ca 80 m between B42 and NT01 .

The concentrations of the 16 EAP PAHs, BTEX, *Ina*, *Ine*, and *Bf*, as well as of some cations, anions and O₂ along this line were monitored and discussed in detail by RIES (1998). The plume showed to be entirely anaerobic. A detailed delineation of redox zones in the plume was not possible so far, mainly due to the influence of mineral water ascending into the aquifer. With the exception of *Ace*, the concentrations of the other PAH and BTEX, as well as of *Bf* decreased down to less than 1 µg/l in NT01, the concentration of *Any* in NT01 was 3.7 g/l. The *Ace* concentration in NT01 however, was 183 µg/l, i.e. higher than in B42 (158 µg/l). This increase in concentration may be due to the fact that the monitoring wells are not located exactly along the centre line of the *Ace* plume. In contrast to *Ace*, the *Nap* concentration throughout the 'further plume' (B28 - B42 - NT01) was less than 1 µg/l.

These findings can possibly be explained by the results of SELIFONOV et al. (1998) who showed that *Ace* can not be degraded as the sole carbon source, but only to a limited extent via cometabolism initiated by *Nap*-dioxygenase or *Phe*-dioxygenase. The drop in concentration of the easier biodegradable *Nap* (and *Phe*) below a certain threshold causes the *Ace* degradation to

come to a standstill; probably for this reason, *Ace* is generally recalcitrant at former gas works sites, even after hundreds of meters from the source.

7.2 Substituted PAH and Heteroaromatic Compounds in B28 - B42 - NT01

7.2.1 Point Measurements

Since the analyses of NAPL from the site showed that also other compounds except MAHs and the 16 EPA PAHs are present in the mixture (Chapter 5.3.1), these substances were also analysed in the groundwater. Given the complexity of the site on one hand, and on the other hand the fact that really relevant for groundwater contamination are only the recalcitrant compounds, some have been quantified only in the 'further plume' (i.e. downgradient where, among the routinely monitored substances, only *Ace* is persistent).

Initially, 9 compounds formerly identified in the tars from the site were analysed in dichloromethane-extracts of groundwater from the three wells (see analytical method in Chapter 4): *Bf*, *Ina*, *Ine*, *Bth*, *1-MetNap*, *2-MetNap*, *Bph*, *Dbf* and *Carb*. None of these could be identified in B28, B42 or NT01 with the method used here. But there were other compounds - higher molecular alkyl-PAHs, heterocycles and oxidation products not investigated so far, present in great concentrations in the plume. The results for the three wells along the plume are summarised in Tab. 7.3.

Table 7.3: Concentrations of Alkyl-PAH, heterocycles and oxidation products in the plume at 'Testfeld Süd'.

Substance (Nb of Isomeres)	Target Ion m/z ⁺	Concentration [µg/l]*		
		B28	B42	NT01
<u>Alkyl-PAH</u>				
Methyl-Indane	117	12.8	0.40	0.23
Methyl-Indene (2)	130	7.84	0.68	0.55
		15.6	6.87	2.04
Dimethyl-Indene (6)	129	1.52	1.04	0.67
		1.18	1.11	1.05
		0.42	n.n.	0.24
		3.10	2.61	1.16
		1.43	1.20	1.19
		2.65	2.40	1.88
Dimethyl-Naphthalene (3)	156	1	0.66	n.n.
		8.93	6.72	6.15
		0.51	0.41	0.32
Ethyl-Naphthalene	141	3.52	3.31	3.43
Trimethyl-Naphthalene (5)	155	4.02	2.21	1.50
		1.09	0.52	0.33
		4.95	3.37	2.13
		3.42	2.46	1.58
		1.72	1.22	0.89
<u>Heterocycles</u>				
Methyl-Benzofuran (3)	131	26.9	13.1	0.75
		9.41	0.15	0.24
		17.9	17.5	14.6
Dimethyl-Benzofuran (2)	145	13.1	12.6	12.7
		18.3	17.8	17.9
Dibenzofuran	168	5.1	4.01	3.19
Methyl-Dibenzofuran (2)	182	17.6	11.5	6.32
		18.3	12	6.27
Acridine	179	2.33	1.82	0.56
Xanthene	182	4.81	2.83	2.32
Thioxanthene	197	2.96	2.16	1.30
<u>Oxidation products</u>				
Methyl-Indanol / - Indanone	133	n.n.	1.14	0.87
Tetramethyl-Indanone	173	2.07	2.12	1.33
Methyl-Naphthol (2)	158	1.58	n.n.	n.n.
		0.53	n.n.	n.n.
Acridinone	195	4.77	2.99	2.30
Methylquinolinol/-quinolinone	159	13.23	8.55	1.84
		3.15	2.40	1.64
		2.91	2.30	1.73
Sum [µg/l]		243.6	154.2	101.5

* no standard (reference) substance; average between values calculated using reference substances with similar retention time and similar K_{ow} (see Chapter 4.3).

From Table 7.3 it results that even though in the plume downstream, except for *Ace*, routinely there can hardly be identified any contaminants in high concentrations, the overall groundwater contamination is seriously underestimated. The sum of the concentrations only of the compounds listed in Table 7.3 is about 240 µg/l in B28 and decreases after 180 m in NT01 only down to about 100 µg/l. At 'Testfeld Süd', no toxicity tests have been conducted so far with groundwater samples from the wells downstream. At other sites how-

ever, some apparently surprising lack of correlation between the concentrations obtained by GC analysis and measured toxicity (almost no peaks detected but high toxicity; MÜLLER et al., 1991) enforces the finding that many toxic and recalcitrant compounds in groundwater are simply overseen when using conventional analyses for water samples.

A general observation from Table 7.3 is that, although the parent-compounds are not anymore detectable, there are still high

concentrations of their alkyl-derivatives. This applies for PAHs and heterocycles as well. Because such molecules as *Ina*, *Ine* or *Bf* are not symmetric, the substitution of just one H atom by an alkyl-chain already leads to more than one possible isomers of position (e.g. three *Methyl-Benzofurans* identified). The number of possible isomers increases with increasing number of alkyl chains, which makes the analytical separation and quantification even more complicate.

Here, the most recalcitrant are the alkyl-aryl-ethers (O-heterocycles, derivatives of *Bf*). The ether bounds seem to be very stable and difficult to be destroyed in enzymatic reactions, at least under anaerobic conditions - e.g. MTBE, an alkyl-ether used as a gasoline additive, is also of high concern for human health but poorly biodegradable under field conditions (KELLER et al., 1998). There are almost no studies about O-heterocycles other than *Bf* and *Dbf* in groundwater, although some of them (e.g. *Methyl-Benzofurans*) have been detected in relatively high concentrations at former gas works (e.g. in the eighties, maximum concentrations of 100 µg/l *Alkyl-Benzofurans* have been found at Trige in Denmark and 140 µg/l in Pensacola, USA - JOHANSEN, 1996).

Also, at least as N-heterocycles are concerned (e.g. *Quinolines*), there is for sure a limitation of the analytical method used here (extraction with dichloromethane, concentration by solvent evaporation and GC-MS analysis). Due to their polarity which also accounts for a very high aqueous solubility (6300 mg/l for *Quinoline*), they are only poorly recovered by conventional solvent extraction on one hand, and they partially decompose in the GC column on the

other hand. Probably for these two reasons *Quinoline* itself or its alkyl-derivatives were not detected here, but there are high concentrations of the metabolite *Methylquinolinol* which is obviously easier to detect due to its lower polarity/water solubility compared to *Quinoline*, its parent compound. For derivatives of *Quinoline* and for polar metabolites, other methods for concentration and analysis have to be used, e.g. solid phase micro-extraction (SPME), eventually coupled to LC-MS, as recommended by JOHANSEN, 1996. Note that the parent compound *Quinoline*, a tar constituent, is known as carcinogenic to humans (Table 3.3).

7.2.2 Plumes Differentiation and Estimation of Mass Fluxes Using Pumping Tests

In order to overcome the uncertainty related to point measurements, a new method has been developed for the quantification of the total mass flux of contaminants from time-concentration curves obtained during pumping tests (SCHWARZ et al. 1998; TEUTSCH et al. 1998, HOLDER et al. 1998). This method, also allowing the reconstruction of the spatial (non-unique) concentration distribution, was first demonstrated at the Eppelheim site in the Rhine Valley (SCHWARZ et al., 1997) and applied in the Neckar Valley in an extended old industrial area (HOLDER et al., 1998).

At 'Testfeld Süd', pumping tests have been conducted for this purpose during 1998 in a first cross section normal to the main groundwater flow direction, which includes the well B42.

Some time-concentration curves measured during pumping in B42 are shown in Fig. 7.2.

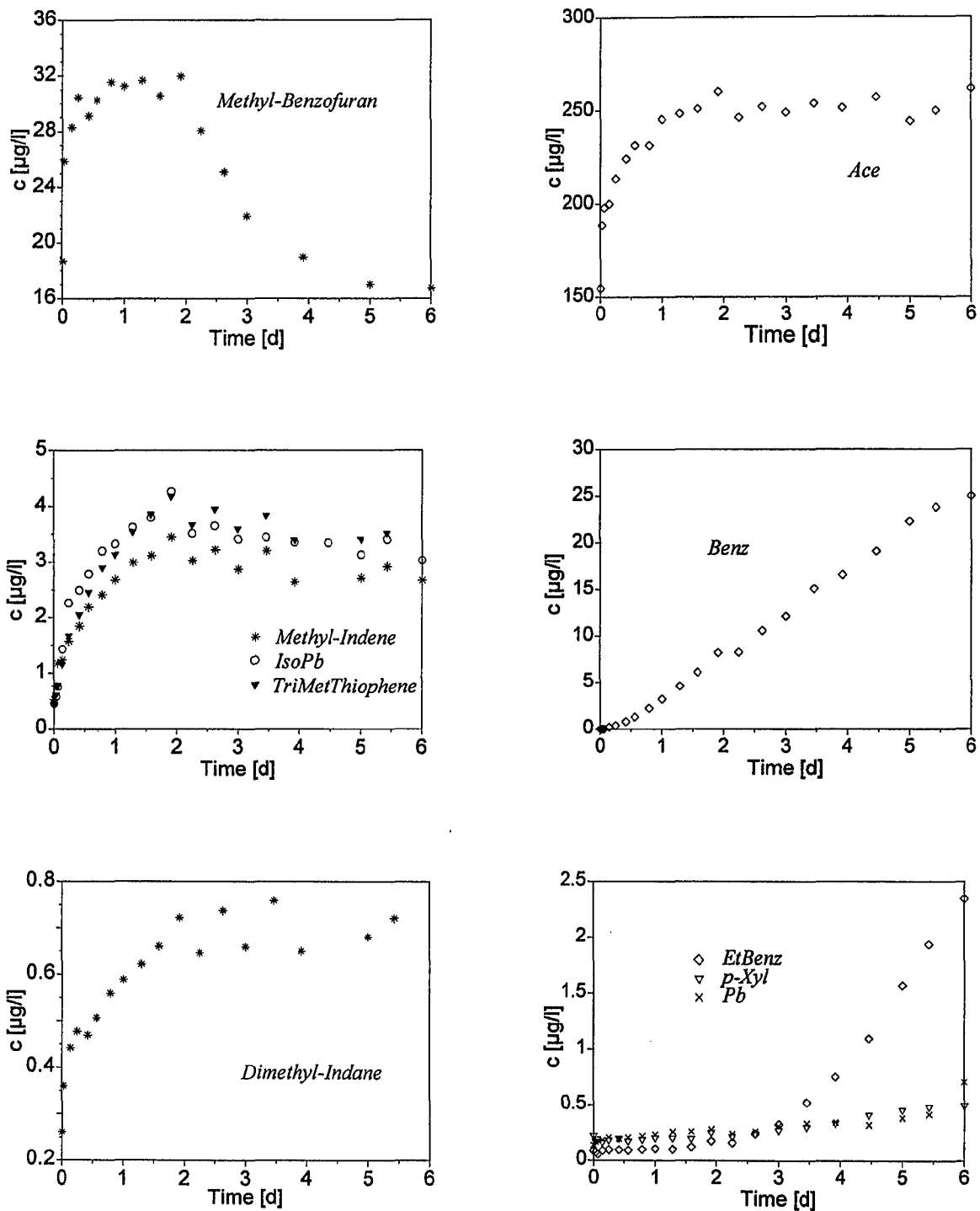


Fig. 7.2: Examples of time-concentration curves for a pumping test in B42. Different shapes of the curves are theoretically an indication for different plumes captured during pumping. (Pumping rate: 0.004 m³/s; hydraulic gradient: 0.0024; hydraulic conductivity: 0.0195 m/s; effective porosity: 0.15).

The curves seem to confirm the supposition derived from the concentration profiles with depth in the area of the multilevel wells that there are some different overlapping plumes captured during pumping in B42 as well. E.g. the concentrations of *Benz*, *EtBenz* and *p-Xyl*,

varied with time in a similar way (similar shape of concentration-time curves), as they had similar concentration profiles e.g. in B54 (Fig. 7.1).

Another plume contains e.g. *Ace*, *Alkyl-Indenes*, *IsoPb* and *Trimethyl-Benzothiophene*

and passes closer to B42 (maximum concentration is attained relatively fast). The start concentrations of *Methyl-Indene*, *IsoPb* and *Trimethyl-Benzothiophene* are practically the same. The ascending branch of the *Trimethyl-Benzothiophene*-curve is steeper, possibly indicating that this compound is less retarded than the others. *Methyl-Benzofurans* form a third plume with its centre almost passing through B42.

However, at least for easily biodegradable MAH, caution is needed with the interpretation of the results of imission pumping tests. Table 7.4 shows a comparison between concentrations determined in bailer groundwater samples from B42 (RIES, 1998) and concentrations at start and at the end of the pumping test. Under the assumption of a stationary plume, the concentration measured in the pumped sample at the beginning of pumping should be close or equal to the concentration in the conventional sample, irrespective of the extent and location of the plume relative to the pumping well.

For some aromatic compounds, mainly *Benz*, *EtBenz*, *p-Xyl* and *Pb*, this was not the case. The concentration at the beginning of pumping was very low, for *Benz* even zero, then increased slowly and reached the value found in the bailer sample only after 6 days. A similar behaviour has been observed again at the same site during later imission pumping tests at a different location (BOCKELMANN, 2000, personal communication).

This may indicate some sink, which could be mainly due to practically instantaneous biodecay in the pumped water, probably due to oxidizing conditions induced by mixing the contaminated water from the plume e.g. with oxygen (or other electron acceptors) containing water during pumping. As long as some electron acceptors are supplied, a fraction of the dissolved BTEX is biodegraded, so that the concentration measured in the pumped water is lower than the concentration in the bailer sample. This would hold if the biodegradation reaction would be fast enough compared to the contact time of different type waters (e.g. BTEX containing and electron acceptors containing water) mixed when they are pumped into the well. Biodegradation reactions are often considered instantaneous (e.g. STURMAN, 1995; NEWELL et al., 1996), but this is in most

cases rather a simplifying assumption for modeling purposes, than an experimentally funded reaction rate.

Another reason for initial continuous increase of BTEX concentrations during pumping could be the heterogeneity of the k_f distribution around the pumping well. It could be imagined that contaminated water only slowly flows into the pumping well because it has to pass through some low permeable horizons. However, if this was true, all dissolved compounds should show a similar behaviour (slow increase in concentration) if they came from the same plume. But since in B42 this is not the case, the existence of more than one plume has to be assumed (in this case the PAH plume meets no hydraulic 'obstacle', whereas the BTEX plume comes from somewhere else and follows a different flowpath towards the well during pumping).

Table 7.4: Concentrations of MAHs and PAHs in B42 without pumping (RIES, 1998) compared to those at the start (after about 10 minutes) and at the end (after 6 days) of an imission pumping test in the same well. At the beginning of pumping MAH concentrations were lower than the expected ones (in bailer samples), then increased constantly (compare to Fig. 7.2). The two values were in very good accordance for higher molecular, less biodegradable PAH (*Ant*, *Fth*). C_{bailer} - concentration in bailer samples (RIES, 1998), $C_{10\ min}$ - concentration in the first pumped sample, (after 5 minutes); $C_{6\ days}$ - concentration in the pumped water after 6 days; pumping rate: 0.004 m³/s.

Comp.	Pumping test			
	C_{bailer} [µg/l]	$C_{10\ min}$ [µg/l]	$C_{6\ days}$ [µg/l]	Time [d] to reach C_{bailer}
Benz	26.7	n.n.	25	≥ 6
EtBenz	3.77	0.07	2.34	>6
p-Xyl	0.63	0.17	0.5	>6
IsoPb	3.86	0.57	3	>6
Pb	0.72	0.17	0.71	6
Nap	0.72	0.46	0.16	-
Any	5.34	3.9	5.19	0.25
Ace	210	156	262	0.25
Ant	0.35	0.33	0.4	0
Fth	0.13	0.11	0.07	0

For PAH and BTEX the mass fluxes have been evaluated by HOLDER (1998) using measured time-concentration curves. Here, the mass fluxes mainly for *Alkyl-Indanes*, *Alkyl-Indenes* and *Alkyl-Benzofurans* have been evaluated using the same approach. The results for the well B42 are summarised in Table 7.5 and compared with the results for PAHs and BTEX obtained by HOLDER for the same wells.

The data show the greatest mass fluxes for *Ace* and *Alkyl-Benzofurans*; in the sum, the mass flux of all *Alkyl-Benzofurans* is about 5 times as great as for *Ace*. The results of the pumping tests in this cross section will have to be put in relation with those of pumping tests now running at the site in the frame of an ongoing project.

Table 7.5: Total mass flux (E) and mean and maximum concentrations (c_{av} , c_{max}) obtained from time-concentration curves during the unsteady-state period of a pumping test in B42 for some Alkyl-PAH and heterocycles, compared to 16 EPA PAH and 10 MAH (HOLDER, 1998). Pumping rate: 0.004 m³/s; hydraulic gradient: 0.0024; hydraulic conductivity: 0.0195 m/s; effective porosity: 0.15.

Substance	Isom. Nb	E [g/d]	c_{av} [µg/l]	c_{max} [µg/l]
Methyl-Indane (m/z = 117)	1	3.51	3.44	12.1
Dimethyl-Indane (m/z = 131)	1	0.009	0.94	2.12
	2	0.01	1.01	2.29
	3	0.009	0.89	1.99
	4	0.015	1.45	3.51
	5	0.018	1.34	3.22
Methyl-Indene (m/z = 130)	1	2.97	2.77	9.93
	2	6.67	6.22	20
Dimethyl-Indene (m/z = 129)	1	0.854	0.84	2.95
	2	1.18	1.16	3.31
	3	0.866	0.85	2.23
	4	1.43	1.4	3.63
Benzofuran *		n.n.	n.n.	n.n.
Methyl-Benzofuran (m/z = 131)	1	22.5	21	70.3
	2	24.8	23.1	67.2
Dimethyl-Benzofuran (m/z = 145)	1	14.9	14.6	5.8
	2	27.7	27.1	92.3
	3	10.4	10.2	26.7
Trimethyl-Thiophene (m/z = 111)	1	3.49	3.42	10.5
Methyl-Bezothiophene (m/z = 147)	1	0.059	5.38	14.9
Benz *		1.5	17	92.2
Tol *		0.034	0.38	1.42
Σ 10 MAH *		2.07	22.9	115
Ina *		n.n.	n.n.	n.n.
Ine *		0.031	0.35	0.56
Nap *		0.013	0.15	0.46
Ace *		22.7	251	627
Σ 16 EPA PAH *		23.2	257	633

* data from HOLDER, 1998

However, if there is really some significant instantaneous biodegradation in the pumped water for an approximative linear increase of concentration with time from zero to the real value without pumping - e.g. the case of *Benz* in Fig. 7.2 - about half of the pumped *Benz*

mass is lost during 6 days; the steady increase in concentration during this time probably reflects rather the increasing limitation of electron acceptors for *Benz* degradation (e.g. due to variation of mixing ratio between oxidising and reducing water during instationary pumping), than the interception of a *Benz* plume by the increasing well capture zone. Since the extent of biodecay during pumping cannot be easily predicted (depends on aquifer properties, redox conditions, contaminant cocktail, existing bacteria and pumping conditions), the suitability of pumping tests for the estimation of mass fluxes and plume localisation for easy biodegradable compounds needs some further clarification.

7.3 Relative Distribution of Various Compound Classes In the Plume

The variation in concentration of many of the investigated substances along the plume as well as the identification of other compounds (e.g. OH-derivatives) which are not tar constituents but oxidation products of those, together with the results of many studies at other contaminated sites, lead to the conclusion that at least some compounds are subject to biodegradation processes in the groundwater, so that even high aqueous concentrations at the source are relatively fast attenuated, mainly by natural biological processes. On the other hand, it became clear that beside *Ace*, there are also other tar constituents recalcitrant to natural biodegradation.

In the following, the question will be addressed, whether or not there are significant changes in the contribution of individual compound classes to the overall amount of dissolved substances in the plume and if there are any classes more persistent than others.

In an attempt to answer this, GC-MS full scans were performed with dichloromethane extracts from the three wells located along the centre of the plume (B28, B42 and NT01). Dichloromethane was chosen as a solvent in order to possibly identify also more polar molecules than PAHs and MAHs. Before extraction, the water samples were spiked with *Nap-d8* as an internal standard (equivalent to

about 50 µg/l). Only those peaks were considered for which the GC-MS library search yielded results with a search quality of at least 80 %. The peak with the smallest area considered was about 500 times smaller than the *Nap-d8* peak, i.e. it corresponded to about 0.1 µg/l (this was the case for about 100 to 150 peaks in every sample). Each peak was assigned to the corresponding compound class.

The contribution of the total peak area of each compound class to the overall peak area of the sample (sum of the areas of all classes) was then compared for the three wells considered. The results in % are summarised in Table 7.6. In these estimates, the routinely analysed compounds such as the 16 EPA PAHs, 10 MAHs, *Ina*, *Ine* and *Bf* were not considered.

Table 7.6: Relative contribution of individual compound classes to the total chromatographic peak area in three wells located along the centre of the plume at 'Testfeld Süd'

B28	B42		NT01		
	Area % (ca 50 m from B28)		Area % (ca 130 m from B42)		Area %
Nap-Derivatives	17.5	O-Heterocycles	19.7	O-Heterozykl.	20.7
O-Heterocycles	13.0	Aromatic hydrocarbons	12.0	N-Heterozykl.	15.0
Aldehydes / Ketones	12.6	Nap-Deriv.	11.5	Aromatic hydrocarbons	9.3
N-Heterocycles	10.8	Alcohols	10.1	Aromatic Amines	9.2
Aromatic hydrocarbons	5.6	Ketones	6.8	Nap-Deriv.	8.7
S-Hetrocycles	5.3	Phenols	6.7	S-Heterocycles	5.3
Carboxilic acids	5.0	N-Heterocycles	6.3	Aldehydes / Ketones	4.1
Cycloalcanes	5.0	Aromatic Amines	5.9	Cycloalcanes	3.3
Alcohols	4.8	S-Heterocycles	5.7	Ethers	3.3
Aromatic Amines	3.9	Quinoline-Deriv.	2.2	Phenols	3.0
Aryl-Cycloalcanes	3.4	Aryl-Cycloalcanes	2.1	PAH	1.8
Phenols	3.3	Ethers	1.4	Quinoline-Deriv.	1.6
Indene-Deriv.	2.3	Cycloalcanes	1.4	Hydroxi-PAH	1.3
Ethers	1.8	Hydroxi-PAH	1.3	Indene-Deriv	1.3
Hydroxi-Indanes	1.2	Carboxilic Acids	1.2	Carboxylic Acids	1.2
Indane-Deriv.	1.1	Indene-Deriv.	1.2	O-Heterozykl.OH	1.2
PAH	0.7	Indane-Deriv.	0.8	Aryl-Cycloalcanes	1.0
		Hydroxi - Indanes	0.4	Indane-Deriv	0.3
		PAH	0.4		
n.i.	2.6	n.i.	2.9	n.i.	8.4
Sum (%)	100	Sum (%)	100	Sum (%)	100

n.i.: not identified (peaks at least as great as about 1/500 from the *Nap-d8* peak, but for each the search quality of the spectrum was less than 80 %)

There are some important conclusions following from the data in Table 7.6. In B28 (nearest to the source area), the dissolved compounds are dominated by higher molecular Alkyl-Naphthalenes, O- and N-heterocycles. The relative amount Alkyl-Naphthalenes decreases by about 50 % to NT01. From B28 to NT01 there is also a drastic increase of compounds which could not be identified, in spite of their relatively great peak area, indicating an advanced fragmentation of higher molecular components to smaller, probably more polar molecules.

In B28 there were also high amounts of oxidation products such as aldehydes, ketones

and carboxylic acids. The contribution of all oxygen-containing intermediate oxidation products, including alcohols and phenols to the total peak area decreases from B28 to NT01. On the contrary, there is an important increase of the aromatic amines; these may result as intermediates during ring cleavage of N-heterocycles.

Aryl-cycloalcanes and aromatic hydrocarbons decrease from B28 to NT01, whereas cycloalcanes first decrease in B42 and then are relatively enriched in NT01. Both compound classes may eventually result as intermediates in ring-cleavage reactions, e.g.out of PAHs.

The relative amount of *Indane*- derivatives and *Indene*-derivatives also decreases from B28 to NT01. They are possibly degraded via some hydroxylated intermediates, since e.g. Hydroxi-*Indane* is depleted from B28 to B42 and is no more detectable in NT01.

Hydroxi-O-heterocycles were detected only in NT01, possibly indicating that at least some aryl-ethers are degraded only after other substrates are depleted. Similarly, *Quinoline*-derivatives and higher hydroxi-PAHs are not present in B28 but are detected in B42 (for

Quinoline-derivatives this may be also due to problems with the GC analysis).

Generally it can be noticed that with increasing distance there is a relative enrichment in heterocyclic compounds (mainly O- and N-containing), confirming their persistence in groundwater. Alkyl-ethers are also enriched from B28 to NT01, possibly supporting the supposed difficulty to biologically cleave as well alkyl- as aryl-O-C bounds. An eventual underestimation of the N-heterocycles content due to analytical limitations is possible.

8. Quantitative Evaluation of Intrinsic Bioremediation at 'Testfeld Süd'

8.1 Theory

BUSCHEK and ALCANTAR (1995) proposed a method to calculate biodecay rates from field data, by coupling the regression of concentration versus distance for stable (stationary) plumes to an analytical solution for one-dimensional, steady state contaminant transport and assuming that biodegradation is a 1st order reaction (a minimum of three monitoring wells is required for the regression).

With these assumptions, given a constant source, the solution to the first order decay is (KEMBLOWSKI et al., 1987):

$$c(x) = c_0 \cdot \exp\left(-k \frac{x}{v_x}\right) \quad (8.1)$$

where $c(x)$ denotes the concentration as a function of distance [M L⁻³], c_0 - the concentration at the source [M L⁻³], k - the first order overall attenuation rate [T⁻¹], x - the distance travelled [L], v_x - the linear groundwater velocity [L T⁻¹], x/v_x - the residence time of pore water [T].

From the exponent of Eq. (8.1), the slope of the line $\ln(c)=f(x)$ is $m=k/v_x$.

The solution for the general one-dimensional transport equation with first-order decay of the contaminant, assuming that decay occurs only in the aqueous phase and that there is no sorption is given by (BEAR, 1979):

$$c(x) = c_0 \cdot \exp\left[\left(\frac{x}{2\alpha_x}\right)\left[1 - \left(1 + \frac{4\lambda\alpha_x}{v_x}\right)^{\frac{1}{2}}\right]\right] \quad (8.2)$$

with α_x - the longitudinal dispersivity [L] and λ - the first order decay rate [T⁻¹].

For $\alpha_x \rightarrow 0$, Eq. (8.2) becomes:

$$\ln \frac{c(x)}{c_0} = \lim_{\alpha_x \rightarrow 0} \left[\left(\frac{x}{2\alpha_x}\right) \left[1 - \left(1 + \frac{4\lambda\alpha_x}{v_x}\right)^{\frac{1}{2}}\right] \right] =$$

$$= \lim_{\alpha_x \rightarrow 0} \left[\left(\frac{x}{2\alpha_x}\right) \cdot \frac{1 - \left(1 + \frac{4\lambda\alpha_x}{v_x}\right)^{\frac{1}{2}}}{1 + \left(1 + \frac{4\lambda\alpha_x}{v_x}\right)^{\frac{1}{2}}} \right] \quad (8.3 a)$$

with the solution:

$$\ln \frac{c(x)}{c_0} = \lambda \frac{x}{v_x} \quad (8.3 b)$$

Eq. (8.1) is a particular case of (8.2) for $\alpha_x \rightarrow 0$. The ratio λ/k gives the contribution of biodegradation to the overall decay.

Equations (8.1) and (8.2) are of the same form:

$$c(x) = c_0 \cdot \exp(m \cdot x) \quad (8.4)$$

where m is the slope of the log-linear data.

It follows:

$$m = \left(\frac{1}{2\alpha_x}\right) \left[1 - \left(1 + \frac{4\lambda\alpha_x}{v_x}\right)^{\frac{1}{2}}\right] \quad (8.5)$$

Eq. (8.5) can be solved to calculate the decay rate λ , with the slope m , the longitudinal dispersivity α_x and the linear groundwater velocity v_x as input parameters:

$$\lambda = \left(\frac{v_x}{4\alpha_x}\right) \left[\left(1 + 2\alpha_x \cdot m\right)^2 - 1\right] \quad (8.6)$$

Assuming a constant decay rate, Eq. (8.2) also allows to calculate the distance x to be travelled

for $\left(1 - \frac{c(x)}{c_0}\right) \cdot 100$ (%) degradation to be achieved (i.e. after the distance x the concentration drops below a threshold c):

$$x = \frac{2\alpha_x \cdot \ln\left(1 - \frac{c(x)}{c_0}\right)}{1 - \sqrt{1 + \frac{4\lambda\alpha_x}{v_x}}} \quad (8.7)$$

For $\alpha_x \rightarrow 0$, Eq. (8.7) becomes:

$$x = \lim_{\alpha_x \rightarrow 0} \frac{2\alpha_x \cdot \ln\left(1 - \frac{c(x)}{c_0}\right)}{1 - \sqrt{1 + \frac{4\lambda\alpha_x}{v_x}}}$$

$$= \lim_{\alpha_x \rightarrow 0} \frac{2\alpha_x \cdot \ln\left(1 - \frac{c(x)}{c_0}\right) \left[1 + \left(1 + \frac{4\lambda\alpha_x}{v_x}\right)\right]}{1 - \left(1 + \frac{4\lambda\alpha_x}{v_x}\right)}$$

(8.8 a)

with the solution:

$$x = -\frac{v_x}{\lambda} \cdot \ln\left(1 - \frac{c(x)}{c_0}\right)$$

(8.8 b)

The same expression would result by solving Eq. (8.3 b) for x .

The distance $x_{0.5}$ corresponding to the half-life of individual chemicals (the distance to be travelled for the concentration to be reduced to the half, i.e. $c=0.5 c_0$) is:

$$x_{0.5} = \frac{2\alpha_x \cdot \ln 0.5}{1 - \sqrt{1 + \frac{4\lambda\alpha_x}{v_x}}}$$

(8.9)

The biodecay rate is a measure of intrinsic bioremediation and can be used in more sophisticated models.

8.2 Materials and Methods

Three wells along the plume are considered: B28, B42 and NT01. For these wells, it has been demonstrated by tracer tests that they are placed practically along the centre of the main contaminant plume, in the groundwater flow direction.

For PAHs and BTEX, the decay rates have been calculated using the concentrations measured by RIES (1998) in the three wells considered. All other compounds have been extracted from the groundwater samples using dichloromethane, concentrated and analysed by GC-MS as described in Chapter 4.

Assuming that the decrease in concentration with travelled distance is a first order reaction, the overall decay rate can be estimated from the

linear regression of the concentration data versus distance in a log-linear plot. The slope of the line $\ln c = f(x)$ is an input parameter for the calculation of the decay rate λ [T^{-1}] (Eq. 8.6). The decay rate also depends upon the longitudinal dispersivity and the linear flow velocity of the groundwater. If in reality the concentration decrease is also due to sorption, the calculated rate would be a function of the retarded velocity of the dissolved compounds. It incorporates all the effects (biotic and abiotic) leading to the attenuation of concentrations with distance.

8.3 Results and Discussion

8.3.1 Decay Rates in the Plume

Because numerous compounds showed to be relevant for the plume (Table 7.3), when more isomers were quantified, the decay rates have been calculated for the sum of isomers. It must be however taken into account that not always all isomers show the same behaviour with respect to biodegradation. For comparison, the decay rates have also been calculated for the EPA PAH and BTEX using the concentrations measured by RIES (1998).

Fig. 8.1 shows the log-linear concentration-distance plots. The slope m of the regression lines, the decay rates in % per day and the distance from B28 after which the concentration of each substance decreases to the half (half-life distance) are listed in Table 8.1.

From the diagrams in Fig. 8.1 it results that for many compounds there is a linear concentration decrease with distance in a log-linear plot (the decay follows an exponential function). At the same time, this does not apply for other compounds, mainly PAHs (*Nap*, *Any*, *Ace*, *Fln*, *EtNap*, *MethylIndane*). For those, the slope of the curves $\ln c = f(x)$ decreases with distance, which is equivalent to a drop in decay rates with distance. *Ine*, *MethylIne*, *Dimethyl-* and *TrimethylNap* also show a slight decrease of the decay rate with distance, but for these the curves can still be reasonably well approximated by straight lines. In some cases, the concentration remains almost constant between B42 and NT01, in spite of the long distance (80 m) between these two wells (e.g. *Nap*, *Any*, *Ace*, *EtNap*).

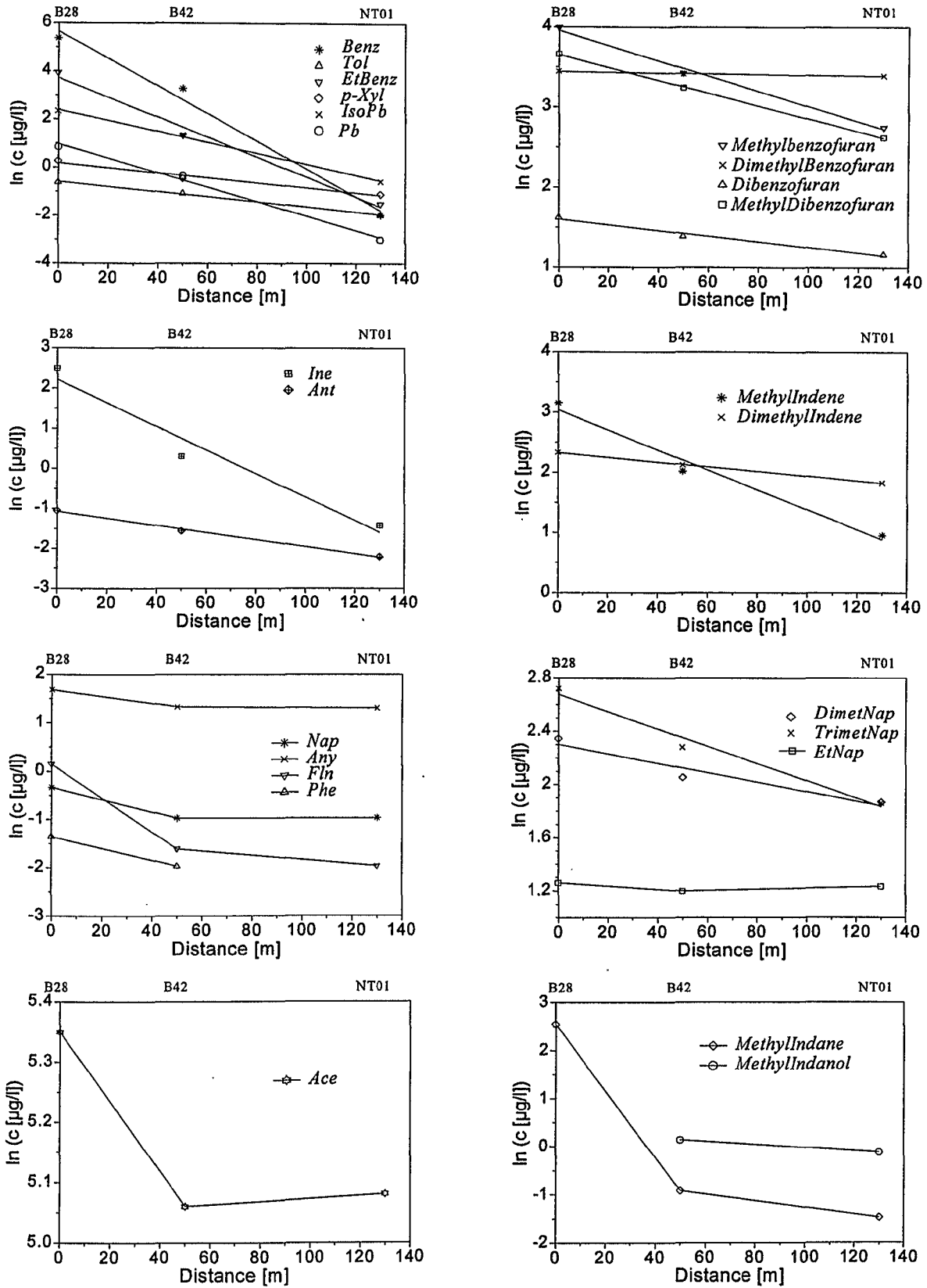


Fig. 8.1: Regression of concentration versus distance at 'Testfeld Süd' (B28-B42-NT01). For many compounds, there is a linear decrease of concentration with distance in a log-linear plot, suggesting a first order overall decay rate.

This suggests that, at least for some compounds, the decay rates are concentration-dependent, i.e. after the aqueous concentration has dropped under a certain threshold, the decay comes to a standstill. This threshold is less than 0.5 µg/l *Nap*, but much higher for other PAHs: 160 µg/l for *Ace*, 3.7 µg/l for *Any* and 1.2 µg/l for *EtNap*. High thresholds are

possibly an indication that those compounds are biodegraded only by cometabolic pathways (for *Ace* this was demonstrated by SELIFONOV et al.,1998) and cannot be consumed anymore if the concentration of the primer substrate becomes too low. Here, no such effect can be observed for MAHs.

Table 8.1: Regression data, overall decay rates k (Eq. 8.31) and first order decay rates for biodegradation λ (Eq. 8.36) calculated after BUSCHEK and ALCANTAR (1995). The ratio λ/k yields the percentage concentration reduction due to biodegradation. The half-life distances have been calculated according to Eq. 8.39. Longitudinal dispersivity: 10 m; linear flow velocity: 2.42 m/d (BÖSEL, 1999). The results are listed in the order of decreasing decay rates.

Substance (Nb of isomers)	Regression	overall decay	biodecay	contribution	half-life
	Slope $m / (r^2)$	rate k [% per day]	rate λ [% per day]	of biodegradation to overall decay [%]	distance $x_{0.5}$ [m]
Benz	-0.0573 / (0.989)	13.9	5.92	42.7	34
EtBenz	-0.0413/ (0.989)	10	5.86	58.7	34
PB	-0.03/ (0.993)	7.26	5.08	70	39
Ine	-0.0294/ (0.96)	7.11	5.02	70.6	39
IsoPB	-0.0226/ (0.997)	5.47	4.23	77.4	46
Methyl-Indene (2)	-0.0166/ (0.978)	4.02	3.35	83.4	56
Acridine	-0.0113/ (0.95)	2.73	2.42	88.7	76
Tol	-0.0104/ (0.998)	2.52	2.25	89.6	81
p-Xyl	-0.0104/ (0.972)	2.52	2.25	89.6	81
Methyl-Quinolinol / -one	-0.0102/ (0.988)	2.47	2.22	89.8	82
Methyl-Benzofuran (3)	-0.00948/ (0.993)	2.29	2.08	90.5	87
Ant	-0.0088/ (0.996)	2.13	1.94	91.2	93
Methyl-Dibenzofuran (3)	-0.00798/ (1)	1.93	1.78	92	101
Trimethyl-Naphthalene (5)	-0.00649/ (0.978)	1.57	1.47	93.5	121
Acridinone	-0.00538/ (0.915)	1.30	1.23	94.6	143
Xanthene	-0.00531/ (0.855)	1.29	1.22	94.7	144
S-Heterocycl	-0.00489/ (0.967)	1.18	1.12	95.1	156
Dimethyl-Indene (6)	-0.0039/ (0.999)	0.94	0.91	96.1	192
Dimethyl-Naphthalene (3)	-0.00355/ (0.933)	0.86	0.83	96.5	209
Dibenzofuran	-0.00349/ (0.98)	0.84	0.82	96.5	213
Dimethyl-Benzofuran (2)	-0.00042/ (0.968)	0.102	0.101	99.5	1653
Ethyl-Naphthalene	not linear	-	-	-	-
Methyl-Indane (2)	not linear	-	-	-	-
Methyl-Indanol (3)	not linear	-	-	-	-
Nap, Any, Ace, Fln	not linear	-	-	-	-

A groundwater velocity of 2.42 m/d and a longitudinal dispersivity of 10 m were used for the calculations (data from BÖSEL, 1999; between B49 and NT01, he determined for α_L a value of 30 m, but since the dispersivity increases with distance and B28 - here considered the source - is closer to NT01 than B49, $\alpha_L = 10$ m was considered more realistic).

From Table 8.1 it appears that MAHs are degraded with the highest rate. The degradation rates are generally smaller for alkyl-derivatives and decrease with increasing number of carbon

atoms in the alkyl-chains. The most recalcitrant are Alkyl-Benzofurans, especially the Dimethyl-derivatives. Dimethyl-Benzofurans practically behave as conservative tracers and could eventually be used for tracing plumes caused by residual coal tar, if the location and extent of the source are known.

The overall decay rates of the most volatile MAHs seem to be too high, respectively, the contribution of biodecay to the overall degradation rate too low. The biodegradation rate of Benzene, e.g., appears to be quite high

for field conditions. SALANITRO (1993) reviewed biodecay rates of BTEX obtained in the laboratory and at different field sites, actually under aerobic conditions (at 'Testfeld Süd' the plume is entirely anaerobic). For *Benzene* concentrations of 0.01-1.5 µg/l, the reported values for decay rates in the field were between 0.7 and 2.4 % per day, depending on site and on concentration range. The rates of biodegradation were 10 to 50 times higher in microcosm studies with material from the considered sites. In the plume at 'Testfeld Süd', the biodecay rates are eventually higher because of the higher concentration of *Benzene* compared to the mentioned study (the *Benzene* concentration in B28 was 214 µg/l and decreased to 0.14 µg/l in NT01, see also Fig. 8.1).

According to the results in Table 8.1, e.g. for *Benzene*, over 57 % of the total decay should be due to abiotic processes such as sorption and volatilisation. This is probably not realistic. *Benzene* has a relatively low K_{ow} ($\log K_{ow} = 2.13$) and the contribution of sorption to the loss of dissolved mass in the plume should be minimal. Possibly, a higher loss may be due to volatilisation, especially if the *Benzene* plume is located in the less deep horizons, immediately under the groundwater table. Even then, the diffusion into the air is strongly slowed down due to the water content in the capillary fringe (MAIER, 1998). For these reasons, the contribution of sorption and volatilisation to the overall mass loss of dissolved low molecular compounds is believed to be maximum 10 - 20 %.

These considerations lead to the hypothesis that the groundwater wells considered for the calculation of biodecay rates (B28, B42 and NT01), are eventually not located exactly along the centre of the BTEX plume. Since the anomaly in decay rates (high overall decay rates, high apparent biodecay rates but low contribution of biodegradation to the overall decay rate) does not apply for all compounds, but only for some volatile substances (*Benz*, *EtBenz*, *Pb*, *IsoPB*), and since separated BTEX sources are present at the site in the area of the former benzene distilleries, it cannot be excluded that the main BTEX plume (mainly containing MAHs) does not entirely coincide in space with the main plume originating from the tar pitches and other coal tar sources. The three

wells are eventually located on a line which deviates to some extent from the centre line of the BTEX plume, but is very probably coincident with the main PAHs plume (also containing other coal tar constituents). A direction to some extent deviating from the main flow direction in the plume would explain the too high attenuation rates calculated for MAHs.

Unfortunately, since only the three wells (B 28, B42 and NT01) were available in the plume, at this point this hypothesis cannot be further elucidated using the existing data.

8.3.2 Extrapolation of Concentrations Towards the Source Area

The groundwater flow at 'Testfeld Süd' is very complex (BÖSEL, 1998, HERFORT, 1999). This applies especially for the area where the multilevel groundwater wells are located. The aquifer heterogeneity combined with the spatial and compositional heterogeneity of the NAPL sources makes it practically impossible to generate a direct connection between plume(s) and source(s). The results presented so far rather suggest that there are several overlapping plumes, originating from sources which in most cases cannot be directly localised.

Tracer tests at the site showed that the well B28, considered here the source for the above biodecay calculations, is hydraulically connected to B49, a multilevel well situated in or very close to one of the main BTEX source areas (former benzene distillery). In B49, located about 40 m up-stream from B28, especially the BTEX concentrations are very high. The position of B49 relative to the plume(s) center line(s) is not known.

In the following, the regression lines obtained for the path B28-B42-NT01 (Table 8.1) are extrapolated towards the source area, for a distance of 40 m up-stream where B49 is located. Because of the multiple sources and the complicated, not entirely known groundwater flow in the source area, the extrapolation of decay rates cannot be performed further upstream. The resulting concentrations are compared to those obtained by SCHETTLER (1998) by direct sampling in B49 (where data available) and listed in Table 8.2. The concentrations in B49 are depth-

averaged between four individual horizons sampled in this well.

Table 8.2 Concentrations in B49 (source area) calculated by extrapolation of the overall decay rates in the plume versus depth average of concentrations measured in four horizons in B49 (data from SCHESSLER, 1998).

Substance (Nb of isomers)	Concentrations in B49 [µg/l]	
	Extrapolation of calculated decay rates	Measured (depth average)
Benz	2120	1823
EtBenz	264	878
PB	8	17
Ine	39	1795
IsoPB	26	50
Methyl-Indene (2)	45	#
Acridine	4	#
Tol	1	124
p-Xyl	2	816
Methyl-Quinolinol / -one	29	#
Methyl-Benzofuran (3)	79	#
Ant	0.5	3.6
Methyl-Dibenzofuran (3)	50	#
Trimethyl-Naphthalene (5)	20	#
Acridinone	6	#
Xanthene	6	#
Dimethyl-Indene (6)	12	#
Dimethyl-Naphthalene (3)	12	#
Dibenzofuran	6	#
Dimethyl-Benzofuran (2)	32	#

not analysed

From Table 8.2 it results that many compounds follow more or less the same rate of attenuation between B49 and B28 as further downstream. For compounds as *Benz*, *EtBenz*, *PB* and *IsoPB* and *Ant* the correlation is satisfactory. The best correlation between measured and calculated concentrations is obtained for benzene. This sustains the hypothesis that there is a major BTEX source in the area of B49 (former distillery). There is no accordance between measured and calculated concentrations of *Ine*, *Tol* and *p-Xyl* (Fig. 8.2). For these compounds,

either B49 cannot be considered a source for the plume following the path B28-B42-NT01, or the degradation rates between B49 and B28 are by orders of magnitude higher than in the plume downstream.

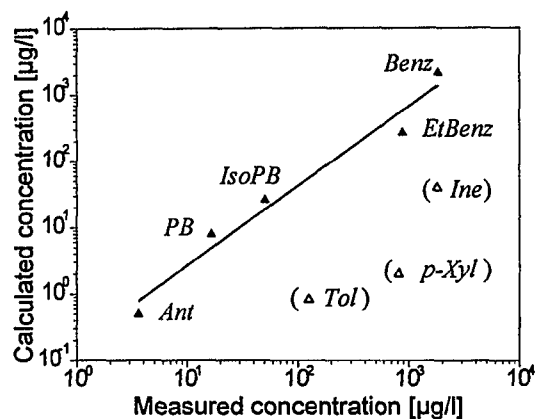


Fig. 8.2: Correlation between concentrations calculated from overall decay rates downstream by extrapolation and measured concentrations in B49.

A general observation from Table 8.2 is that the measured concentrations are always higher than those calculated using first order decay rates; this difference is dramatic for *Ine*, *Tol* and *p-Xyl* (2 to 3 orders of magnitude). If all assumptions made above hold, (position of the wells along the centre of the plume, first order decay) this implies that the attenuation rates are generally higher in the source area than further in the plume. Given the anaerobic conditions throughout the plume and certainly in the source area, it would mean that the anaerobic degradation potential is higher near the source but is considerably diminished within less than 50 m flow distance from the supposed downstream border of the source area, causing a rapid decrease of the attenuation rates. This is probably also associated with the succession of different redox zones along the anaerobic plume.

8.4 Conclusions

At 'Testfeld Süd' there are not enough groundwater wells as to permit to map out the plume only basing on point measurements. However, the combined information from conventional groundwater samples, multilevel samples (wells equipped with inline packers) and concentration variations during pumping allowed to gain some insight into the distribution and fate of some classes of organic compounds dissolved in the groundwater.

Based on vertical concentration distributions and also on concentration variations during pumping, it could be confirmed that there is more than one plume emerging in the source area. Depending on the location and composition of the sources, at a smaller scale and close to the source area there are different plumes with different compositions (dissolved compounds) which are not necessarily overlapping near to the source. Some additional pumping tests in a further cross section normal to the normal groundwater flow direction will be needed, in order to find out whether the spatial plume heterogeneity still holds after longer travel distances. Probably these differences vanish with distance, due to the fact that the aquifer narrows towards NT01.

The variation of the concentrations of many compounds with distance from B28 to B42 and further to NT01 supports the results of field-tracer tests, showing that the main groundwater flow direction and the centre of the main plume follow approximately the imaginary line connecting the three wells. The overall attenuation of concentrations along the plume can be generally described as a first order decay. Based on too high attenuation rates of BTEX along this line, it is believed however, that the main MAH plume (probably originating from the former benzene distilleries) deviates from this line to some extent. Because no other groundwater wells were available, a more exact localisation of the plume was not possible.

This 'further plume' contains more numerous compounds than usually quantified in groundwater; these are expected to be present at all former gas works. There are both original coal tar constituents and degradation products of those, many still present in high concentrations even after long distances from

the source. *Ace* and heterocyclic compounds are the most recalcitrant. It is not known how long the plume really is at 'Testfeld Süd'; in the most downstream located well at the site (NT01) there are still very high concentrations of dissolved organic compounds of concern. Some N-heterocycles of concern, mainly *Quinoline* and derivatives, could not be assessed with the analytical methods used in this study; because of their toxicity they will have to be studied in more detail in the future.

A further supposition which must be though verified by further research is that imission pumping tests possibly yield erroneously low fluxes for easily degradable compounds, such as monoaromatic hydrocarbons. This is believed to be mainly due to simultaneous capturing of the plume and of some water containing an excess of oxygen or other electron acceptors, which determines some biological transformation of the target compounds in the pumped water before analysis. At least for higher molecular PAHs and for compounds generally recalcitrant to biodegradation, this effect may be negligible. A possible indication of the extent of the mass loss due to biological processes during pumping and sample storage may be obtained by comparing the concentrations at the very start of pumping with those routinely measured before at the same location in conventional samples. Theoretically it can though not be excluded that some electron acceptors may be captured only at later times during long duration of instationary pumping.

9. Summary

The main NAPL sources causing the groundwater contamination at 'Testfeld Süd' are related to the location and nature of the former facilities for gas manufacturing out of coal, for on-site disposal and further processing of the by-products. Two main types of NAPLs have been spilled in the subsurface: coal tars/tar oils in the area of the former tar distilleries and lighter distillation fractions in the area of the former benzene distilleries further downstream. The gas manufacturing plant was operated between 1870 and 1970, but individual facilities have been built at different points in time. This determined contamination events to occur at different (unknown) points in time; some organic mixtures in the subsurface are therefore more aged than others. E.g. the MAH sources are probably not as old as some tar spills, since the first benzene distillery on site has started to operate 1910. Until then, tar was probably not further processed, but disposed on site in pits as a residuum. This is confirmed by different compositions of NAPLs sampled from different locations at the site. The sources are spread over a wide area (about 20,000 m²); their spatial distribution became even more complicated due to extensive war damage. The variety of the organic mixtures separated by distillation on-site, the spatial distribution of the spills and the aquifer heterogeneity are the main factors determining the spatial and compositional complexity of the underground contamination. The exact localisation of all NAPL sources is not possible and the amount present today in the subsurface is not known.

The composition of the sources has changed during decades, mainly due to the faster release of easy soluble compounds into the groundwater and enrichment of the less soluble ones. The fact that the groundwater passes successively through/by different NAPL sources, causes the release not to take place always at maximum gradients. It is believed that in the field there are even situations where the concentration gradient is inverse, (i.e. higher concentration of a dissolved compound in the groundwater than its saturation concentration out of a given NAPL). This is mainly the case of compounds recalcitrant to biodegradation, which persist in high concentrations in the

aqueous phase. This is why residual NAPLs located more downstream may become enriched with poorly biodegradable compounds (e.g. *Ace*).

Beside the 16 EPA PAHs and the BTEX, there are other coal tar constituents, mainly alkyl-PAHs and heterocyclic aromatic compounds, present in the groundwater in relatively high concentrations. Although many are more soluble and more mobile than the EPA PAHs and at least some are of known health concern, so far they are not routinely monitored at former gasworks. Very little is known about their fate in groundwater. There are indications that some products of biological transformations of coal tar constituents are often more toxic than the parent compounds; others accumulate in groundwater as dead-end metabolites. Several such original coal tar constituents and presumed metabolites have been identified and partially quantified at 'Testfeld Süd'.

The main release mechanisms of contaminants into groundwater - dissolution out of residual NAPL phase and diffusion limited desorption out of contaminated aquifer material or out of low conductivity zones - have been investigated in laboratory column leaching experiments with disturbed and undisturbed samples from the field. The maximum concentrations for dissolution out of residual phase are equal to the saturation concentrations and depend on the composition of the dissolving mixture. Maximum (equilibrium) concentrations are reached after short distances (some centimeters at laboratory scale or a few meters in the field). Within the domain where saturation is not yet attained and mass transfer occurs (mass transfer zone), the composition of the organic mixture changes as the more soluble compounds are depleted faster (their dissolution front advances faster) than the lower soluble ones, which are enriched in the mixture). Assuming that there is no dilution, whether or not the water leaving the zone with residual NAPL is saturated with a certain compound depends on the ratio between the length of the mass transfer zone and the length of the contaminated domain in the flow direction. If the domain with residual NAPL is longer than the mass transfer zone (most frequent case), saturation is reached fast and at the end of the contaminated domain maximum

concentration would be observed. This means however that in this case dissolution takes place only within a short domain relative to the entire contaminated volume, i.e. after a relatively short distance there is no more mass transfer due to lack of driving force. More advantageous for remediation purposes is the case where the mass transfer zone is longer than the contaminated zone, permitting higher mass fluxes (due to greater concentration gradients) for dissolution. The length of the mass transfer zone becomes longer for enhanced hydraulic gradients (greater linear flow velocities).

When saturation is reached, the measured concentration still depends on the observation scale: in small, homogeneous (disturbed) columns in the laboratory or locally in the field (e.g. individual sampling ports in multilevel wells) the measured concentration may be equal to the saturation concentration. Concentrations in multilevel groundwater samples were indeed in very good accordance with saturation concentrations calculated for the NAPL composition from the same location. In bigger (undisturbed) columns or in conventional groundwater samples, the observed concentration would be lower due to dilution, although the dissolution process takes place at equilibrium (saturation is locally attained).

The results of desorption experiments with disturbed samples from 'Testfeld Süd' are in good accordance with those obtained in other works (MERKEL, 1996; WEIB, 1998) for contaminated aquifer material from similar sites. The diffusion rate constants for desorption out of undisturbed aquifer material are lower due to longer distances for diffusion (contaminants must diffuse out of greater aggregates) and probably closer to the reality in the field. At least high molecular PAH have not yet reached sorption equilibrium in the field. The maximum concentrations for desorption are much lower than those resulting during dissolution out of residual phase.

For a given volume of contaminated aquifer material, the PAH flux due to desorption out of grains and aggregates is negligible in comparison to the flux due to dissolution. As long as residual NAPL is present, the diffusion limited desorption plays a secondary role.

At 'Testfeld Süd', some residual NAPL has infiltrated in fissures into the confining layer (Gipskeuper) at the bottom of the aquifer. This is at least the case for the first centimeters of the Keuper; it is not known how deep the separated organic phase penetrates this layer. The contaminant release out of the confining layer takes place simultaneously by dissolution out of the organic phase from the fissures and diffusion limited desorption out of the matrix. The overall flux through a defined surface depends on the contribution of the interfacial area tar (in fissures)/water to the total area (i.e. the contribution of each process - dissolution and desorption - to the overall flux). Although this ratio is unknown, it is believed that for this scenario the overall mass flux through a given surface would be lower than for pure dissolution out of residual blobs through the same area (higher tar/water interfacial area for blobs than for NAPL in fissures and larger distance).

The release rates measured in column experiments cannot be extrapolated to field conditions without knowing the amount, composition and spatial distribution of the contamination. Because in most cases it is impossible to map out the source, other methods are required in order to determine release fluxes in the field (e.g. pumping tests).

The results of field investigations (concentrations in multilevel wells, pumping tests) showed that at least close to the source area there are several different plumes. Sharp vertical concentration profiles probably attenuate with increasing distance. Mainly because they emerge from different sources, at a greater scale (ca 200 m downstream from the source area) there seem though to exist two different plumes for PAH and MAH. As indicated by the examination of the decay rates calculated from field data, the centre lines of these two main plumes are probably not perfectly coincident.

The plume at 'Testfeld Süd' is entirely anaerobic. Almost all compounds investigated (MAH, PAH, heterocycles and presumed metabolites) are attenuated with different rates. An exception are *Ace* as well as *Dimethyl-Benzofurans* which behave practically as conservative tracers. They could be eventually

used to trace plumes caused by known NAPL sources (tar).

Although the delineation of redox zones at 'Testfeld Süd' is unknown so far, the results of this study are suggesting that the potential for anaerobic biodegradation in the aquifer is relatively high close to the source and rapidly decreases (within ca 50 m from the source area). For many substances it seems that there are thresholds below which no more significant biodecay can occur. It is not known how far the plume extends downstream beyond NT01 (Fig. 2.1).

References

- ACTON, D. W., BARKER, J. F., (1992): In situ biodegradation potential of aromatic hydrocarbons in anaerobic groundwaters. - *J. Contam. Hydrol.* 9: 325-352.
- ALEXANDER, M. (1995): How toxic are chemicals in soil? - *Environ. Sci. Technol.* 29: 2713-2717.
- ARCANGELI, J.-P. (1994): Biological degradation of aromatic hydrocarbons in biofilm systems.- PhD Dissertation, Department of Environmental Science and Engineering, Technical University of Denmark, Lyngby. 171.
- BALL, W. P., XIA, G., DURFEE, D. P., WILSON, R. D., BROWN, M. J., MACKAY, D. M. (1997): Hot methanol extraction for the analysis of volatile organic chemicals on subsurface core samples from Dover Airforce Base, Delaware. - *Winter GWMR*: 104-121.
- BELLER, H. R., DING W.-H., REINHARD, M. (1995): Byproducts of anaerobic alkylbenzene metabolism useful as indicators of in situ bioremediation. - *Environ. Sci. Technol.* 29: 2864-2870.
- BÖSEL, D. (1998): Entwicklung eines Strömungs- und Transportmodells für das Testfeld Süd (Neckartal bei Stuttgart) - Felderkundung und Tiefenkartierung. - Diplomarbeit am Lehrstuhl für Angewandte Geologie, Geologisches Institut der Universität Tübingen.
- BUSCHEK, T. E., ALCANTAR, C. M. (1995): Regression techniques and analytical solutions to demonstrate intrinsic bioremediation. - in: Hinchee, R. E., Wilson, J. T., Downey, D. (Eds.) (1995): *Intrinsic bioremediation*. Battelle Press. 109-116.
- CANADIAN WORLD WILDLIFE FUND (WWF) (1999): Persistent organic pollutants: criteria and procedures for adding new substances to the global POPs treaty. 19.
- CHANG, S., HYMAN, M., WILLIAMSON, K. (1998): Nitrifying bacteria as 'priming' catalysts for the biodegradation of xenobiotics. - in: Wickramanayake, G. B., Hinchee, R. E. (Eds.) (1998): *Natural attenuation. Chlorinated and recalcitrant compounds*. Battelle Press, Columbus, Ohio. 51-55.
- CHERRY, J. A., BARKER, J. F., FEENSTRA, S., GILHAM, R. W., MACKAY, D. M., SMYTH, J. A. (1996): The Borden site for groundwater contamination. Experiments: 1978-1995. - in: Kobus, H., Barczewski, B., Koschitzky, H.-P. (Hrsg.) (1996): *Groundwater and subsurface remediation. Research strategies for in-situ technologies*. Springer Verlag, Berlin, Heidelberg: 102-127.
- CHRISTENSEN, TH. H., KJELDSSEN, P., ALBRECHTSEN, H.-J., HERON, G., NIELSEN, P. H., BJERG, P. L., HOLM, P. E. (1994): Attenuation of landfill leachate pollutants in aquifers. - *Critical Reviews in Environ. Sci. Technol.* 24: 119-202.
- COHEN, B. A., KRUMHOLZ, L. R., KIM, H., HEMOND, H. (1995): In-situ biodegradation of Toluene in a contaminated stream: 2. Laboratory studies. - *Environ. Sci. Technol.* 29: 117-125.
- DUTTA, T. K.; SELIFONOV, S. A.; GUNSALUS, I. C. (1998): Oxidation of methyl-substituted naphthalenes: pathways in a versatile *Sphingomonas paucimobilis* strain. - *Environ. Sci. Technol.* 64: 1184-1889.
- DYREBORG, S. (1996): Microbial degradation of water-soluble creosote compounds.- PhD Dissertation, Department of Environmental Science and Engineering, Technical University of Denmark, Lyngby. 179.
- EATON, R. W., NITTEAUER, J. D. (1994): Biotransformation of Benzothiophene by Isopropylbenzene-degrading bacteria. - *J. Bacteriol.* 176: 3992-4002.
- EISENBRAND, G., METZLER, M. (1994): *Toxikologie für Chemiker. Stoffe, Mechanismen, Prüfverfahren*. Georg Thieme Verlag Stuttgart, New York. 320.
- FITZER, E., FRITZ, W., EMIG, G. (1995): *Technische Chemie. Einführung in die chemische Reaktionstechnik*. 4. Aufl., Heidelberg, 541.
- FOWLER, M. G., BROOKS, P. W., NORTHOTT, M., KING, M. W. G., BARKER, J. F., SNOWDON, L. R. (1994): Preliminary results from a field experiment investigating the fate of some creosote components in a natural aquifer.- *Org. Geochem.* 22: 641-649.
- GIDDINGS, J. M., HERBES, S. E., GEHRS, C. W. (1985): Coal liquefaction products. - *Environ. Sci. Technol.* 19: 14-18.

- GIEG, L. M., OTTER, A., FEDORAK, P. M. (1996): Carbazole degradation by *Pseudomonas* sp. LD2: metabolic characteristics and the identification of some metabolites. - *Environ. Sci. Technol.* 30: 575-585.
- GEOLOGISCHES LANDESAMT BADEN-WÜRTTEMBERG (1989): Hydrogeologisches Gutachten zur Verunreinigung des Untergrundes und des Grundwassers im Bereich des Erdgasspeichers auf dem Gelände der Technischen Werke Stuttgart. 28 + Anlagen.
- GEOLOGISCHES LANDESAMT BADEN-WÜRTTEMBERG (1992): Hydrogeologisches Gutachten zur Grundwasser-Abstromüberwachung der kontaminierten Bereiche im ehemaligen Gaswerksgelände der Technischen Werke Stuttgart in der Neckar-Talau in Stuttgart-Gaisburg. 48 + Anlagen.
- GRATHWOHL, P. (1994): Diffusion limited sorption and desorption of organic contaminants in soils and sediments. - Habilitationsschrift an der Geowissenschaftlichen Fakultät der Universität Tübingen. 152.
- GRATHWOHL, P. (1997): Gefährdung des Grundwassers durch Freisetzung organischer Schadstoffe : Methoden zur Berechnung der in-situ-Schadstoffkonzentrationen. - *Grundwasser* 4/97: 157-166.
- GRATHWOHL, P. (1998): Diffusion in natural porous media. Contaminant transport, sorption/desorption and dissolution kinetics. Kluwer Academic Publishers, Boston / Dordrecht / London. 207.
- GRATHWOHL, P., PYKA, W., MERKEL, P. (1994): Desorption of organic pollutants (PAHs) from contaminated aquifer material. - in: Dracos, T. H., Stauffer, F. (Eds.): Proceedings of the IAHR/AIRH symposium on transport and reactive processes in Aquifers, Zürich. 469-474.
- GRIFOLL, M., SELIFONOV, S. A., CHAPMAN, P. J. (1994): Evidence for a novel pathway in the degradation of Fluorene by *Pseudomonas* sp. strain F274. - *Appl. Environ. Microbiol.* 60: 2438-2449.
- GRIFOLL, M., SELIFONOV, S. A., GATLIN, C. V., CHAPMAN, P. J. (1995): Actions of a versatile Fluorene-degrading bacterial isolate on polycyclic aromatic compounds. - *Appl. Environ. Microbiol.* 61: 3711-3723.
- HADDOCK, J. D., GIBSON, D. T. (1995): Purification and characterization of the oxygenase component of Biphenyl 2,3-dioxygenase from *Pseudomonas* sp. strain LB400. - *J. Bacteriol.* 177: 5834-5839.
- HAJAJI, S. (1998): Freisetzung organischer Schadstoffe aus Bitterfelder Braunkohlen und deren Adsorption in Aktivkohlefiltern. Diplomarbeit am Lehrstuhl für Angewandte Geologie, Geologisches Institut der Universität Tübingen.
- HAMMER, E., KROWAS, D., SCHÄFER, A., SPECHT, M., FRANCKE, W., SCHAUER, F. (1998): Isolation and characterization of a Dibenzofuran-degrading yeast: identification of ring cleavage products.- *Appl. Environ. Microbiol.* 64: 2215-2219.
- HATHEWAY, A. B. (1997): The office of remediation of former manufactured gas plants & other coal-tar sites.- Center for Environmental Science and Technology (CEST), University of Missouri-Rolla.
- HATHEWAY, A. B. (1999): Remediation of manufactured gas plants & coal-tar sites. Marcel Dekker Publishers, New York.
- HERFORT, M., PTAK, T., LIEDL, R. & TEUTSCH, G. (1999): Das Gaswerk Gaisburg als Testfeld eines DFG-Forschungsprojektes.- Schriftenreihe des Amtes für Umweltschutz, 4/1999:130-152, Stuttgart, DFG-Publ.Nr. 74.
- HERFORT, M. (1999): Characterization of Contaminant Transport in a Heterogeneous Porous Aquifer. PhD Dissertation at the Geological Institute, University of Tübingen. (in preparation).
- HOLDER, TH. (1999): Orientierende Erkundung E12 - Gaswerke der Neckarwerke Stuttgart AG Talstraße 117. Analytische Auswertung der Immissionspumpversuche. - Bericht am Lehrstuhl für Angewandte Geologie der Universität Tübingen.

- HOLDER, TH., TEUTSCH, G., PTAK, TH., SCHWARZ, R. (1998): A new approach for source zone characterization: the Neckar Valley study. in: Herbert, M., Kovar, K. (Eds.) (1998): Proc. GQ '98 Conf., Tübingen, Germany, September 1998. IAHS Publ. no. 250. 49-55.
- IMHOFF, P. T., MILLER, C. T. (1996): Dissolution fingering during the solubilization of nonaqueous phase liquids in saturated porous media. 1. Model predictions. *Water Resour. Res.*, 32:1919-1928.
- IMHOFF, P. T., THYRUM, G. P., MILLER, C. T. (1996): Dissolution fingering during the solubilization of nonaqueous phase liquids in saturated porous media. 2. Experimental observations. *Water Resour. Res.*, 32:1929-1942.
- JOHANSEN, S. S. (1996): Heteroaromatic compounds and their biodegradation products in creosote-contaminated groundwater.- PhD Dissertation, Department of Environmental Science and Engineering, Technical University of Denmark, Lyngby. 119.
- JOHNSON and TRATNYEK (1995): Dechlorination of Carbon Tetrachloride by iron metal: The role of competing corrosion reactions. Preprint extended abstract presented before the Division of Environmental Chemistry, American Chemical Society, Anaheim CA, April 2-7 1995.
- JUNGBAUER UND PARTNER (1994): Historische Erkundung und Erhebung des Sachstandes auf dem Gaswerksgelände der TWS AG in Stuttgart-Gaisburg. 46.
- KÄSTNER, M., MAHRO, B., WIENBERG, R. (1993): Biologischer Schadstoffabbau in kontaminierten Böden. *Economica Verlag, Bonn*. 180.
- KELLER, A., FROINES, J., KOSHLAND, C., REUTER, J., SUFFET, I. M., LAST, J. (1998): Health & environmental assessment of MTBE. - Report to the Governor and Legislature of the State of California.
- KIM, H., HEMOND, H. F., KRUMHOLZ, L. R., COHEN, B. A. (1995): In-situ biodegradation of Toluene in a contaminated stream. 1. Field studies. - *Environ. Sci. Technol.* 29: 108-116.
- KLEINEIDAM, S. (1998): Der Einfluß von Sedimentologie und Sedimentpetrographie auf den Transport gelöster organischer Schadstoffe im Grundwasser. - *Tübinger Geowissenschaftliche Arbeiten (TGA) Reihe C*, 41, 1998. 82.
- KROPP, K. G., GONCALVIS, J. A., ANDERSSON, J. T., FEDORAK, P. M. (1994): Microbially mediated formation of benzonaphthothiophenes from benzothiophenes. *Appl. Environ. Microbiol.* 60: 3624-3631.
- LANE, W. F., LOEHR, R. C. (1992): Estimating the equilibrium aqueous concentrations of polynuclear aromatic hydrocarbons in complex mixtures. *Environ. Sci. Technol.* 26: 983-990.
- LANTZ, S. E., MONTGOMERY, M. T., SCHULTZ, W. W., PRITCHARD, P. H., SPARGO, B. J., MUELLER, J. G. (1997): Constituents of an organic wood preservative that inhibit the Fluorathene-degrading activity of *Sphingosomonas paucimobilis* strain EPA505. - *Environ. Sci. Technol.* 31: 3573-3580.
- LEVINE, A. D., LIBELO, E. L., BUGNA, G., SHELLEY, T., MAYFIELD, H., STAUFFER, T. B. (1997): Biogeochemical assessment of natural attenuation of JP-4-contaminated ground water in the presence of fluorinated surfactants. - *Sci. Tot. Environ.* 208: 179-195.
- LOYEK, D. (1998): Die Löslichkeit und Lösungskinetik von polyzyklischen aromatischen Kohlenwasserstoffen (PAK) aus der Teerphase. - Dissertation am Lehrstuhl für Angewandte Geologie der Universität Tübingen.
- LOYEK, D., GRATHWOHL, P. (1998): Ermittlung und Reduzierung der Schadstoffemission bei teer- und teerölkontaminierten Böden. - Abschlußbericht zum PWAB-Projekt PD 94.159, Lehrstuhl für Angewandte Geologie der Universität Tübingen. 62.
- LUTHY R. G., DZOMBAK, D. A., PETERS C. A., ROY, S. B., RAMASWAMI, A., NAKLES, D. V., NOTT, B. R. (1994): Remediating tar-contaminated soils at manufactured gas plant sites.- *Environ. Sci. Technol.* 28: 266A-276A.
- LYMAN, W. J., REEHL, W.F., ROSENBLATT, D. H.(1990): Handbook of chemical property estimation methods: environmental behaviour of organic compounds. - 2nd ed., McGraw - Hill, New York.
- MACKAY, D., SHIU, W.-Y. (1977): Aqueous solubility of polynuclear aromatic compounds. -*Jour. Chem. Eng. Data* 22: 399-402.

- MACKENBROCK, U., KOPP-HOLTWIESCHE, BLANK, W. (1994): Zur biologischen Abbaubarkeit von Industriechemikalien. - *TerraTech* 4: 41-51.
- MAIER, U. (1998) - Schadensherderkundung anhand von Bodenluftanomalien - Feldmessungen und numerische Modellierung.- Diplomarbeit am Lehrstuhl für Angewandte Geologie, Geologisches Institut der Universität Tübingen.
- MAK- und BAT-Werte Liste 1995. - Deutsche Forschungsgemeinschaft. Senatkommission zur Prüfung gesundheitsschädlicher Arbeitsstoffe. Mitteilung 31. 177.
- MAYER A. S., MILLER, C. T. (1996): The influence of mass transfer characteristics and porous media heterogeneity on nonaqueous phase dissolution. - *Water Resour. Res.* 26: 2783-2796.
- MCALISTER, P. M., CHIANG, C. Y. (1994): A practical approach to evaluating natural attenuation of contaminants in ground water. - *GWMR*, 14 :161-173.
- MCGRODDY, S. E., FARRINGTON, J. W. (1995): Sediment pore water partitioning of polycyclic aromatic hydrocarbons in three cores from Boston Harbour, Massachusetts. - *Environ. Sci. Technol.* 29: 1542-1550.
- MERKEL, P. (1996): desorption and release of polycyclic aromatic hydrocarbons (PAH) from contaminated aquifer materials. - Tübinger Geowissenschaftliche Arbeiten (TGA) Reihe C, 45. 76.
- MILLER, C. T., POIRIER-MCNEIL, M. M., MAYER, A. S. (1990): Dissolution of trapped nonaqueous phase liquids: Mass transfer characteristics. - *Water Resour. Res.* 26: 2783-2796.
- MÜLLER, J. G., MIDDAUGH, D. P., LANTZ, S. E., CHAMPAN, P. J. (1991): Biodegradation of creosote and Pentachlorophenol in contaminated groundwater: Chemical and biological assessment. - *Appl. Environ. Microbiol.* 57: 1277-1285.
- MÜLLER, (1989): Creosote contaminated sites. Their potential for bioremediation. - *Environ. Sci. Technol.* 23: 1197-1201.
- NELSON, E. C., GHOSHAL, S., EDWARDS, J. C., MARSH, G. X., LUTHY, R. G. (1996): Chemical characterization of coal tar-water interfacial films. - *Environ. Sci. Technol.* 30:1014-1022.
- NENITESCU, C. D. (1966): Chimie Organica. I. Ed. Didactica si Pedagogica, Bucuresti. 895.
- NEUMANN et al. (1998): Changes in the classification of carcinogenic chemicals in the work area (Section III of the German List of MAK and BAT values).- *Journal of Cancer Research and Clinical Oncology* 124: 661-669.
- NEWELL, CH. J., MCLEOD, R. K., GONZALES, J. R., WILSON, J. T. (1996) - BIOSCREEN 4.1. Natural Attenuation Decision Support System. U.S. Environmental Protection Agency/600/R-96/087, Office of Research and Development Washington DC. 72.
- NIELSEN, P. H., BJARNADOTTIR, H., WINTER, P. L., CHRISTENSEN, TH. H. (1995): In situ and laboratory studies on the fate of specific organic compounds in an anaerobic landfill leachate plume, 2. Fate of aromatic and chlorinated aliphatic compounds.- *J. Cont. Hydrol.* 20: 51-66.
- NYER, E.K.; DUFFIN, M. E. (1997): The state of art of bioremediation. *Ground Water Monitoring and Remediation* 17 (2). 64-69.
- OTTEN, A., TONNAER, M. H., ALPHENAAR, C. R. (1998): - Extensive remediation concepts based on natural attenuation. - in: Wickramanayake, G. B., Hinchee, R. E. (Eds.) (1998): Natural attenuation. Chlorinated and recalcitrant compounds. Battelle Press, Columbus, Ohio. 105-110.
- POWERS, S. E., ABRIOLA, L. M., DUNKIN, J. S., WEBER W. J. JR. (1994): Phenomenological models for transient NAPL-water mass-transfer processes. - *J. Cont. Hydrol.* 16: 1-33.
- PYKA, W. (1994): Freisetzung von Teer Inhaltsstoffen aus residualer Teerphase in das Grundwasser: Laboruntersuchungen zur Lösungsrate und Lösungskinetik. - Tübinger Geowissenschaftliche Arbeiten (TGA) Reihe C, 45. 76.
- REICHERT, B., HÖTZL, H., WEBER, K., EISWIRTH, M. (1998): Factors controlling the natural attenuation of BTEX. - in: Herbert, M., Kovar, K. (Eds.) (1998): Proc. GQ '98 Conf., Tübingen, Germany, September 1998. IAHS Publ. no. 250. 237-244.
- RHEE, S.-K., CHANG, J. H., CHANG, Y. K., CHANG, H. N. (1998): Desulfurization of Dibenzothiophene and Diesel oils by a newly isolated *Gordona* strain, CYKS1. - *Appl. Environ. Microbiol.* 64: 2327-2331.

- RIES, J. (1998): Beprobung gaswerkspezifischer Schadstoffe im Abstrom des 'Testfeld Süd'.- Diplomarbeit am Lehrstuhl für Angewandte Geologie, Geologisches Institut der Universität Tübingen.
- SALANITRO, J. P. (1993): The role of bioattenuation in the management of aromatic hydrocarbon plumes in aquifers. - Fall *GWMR*:150-161.
- SATO, S. I., NAM, J. W., NOJIRI, H., YAMANE, H., OMORI, T. (1997): Identification and characterization of genes encoding Carbazole 1,9a-dioxygenase in *Pseudomonas* sp. strain CA10. - *J. Bacteriol.* 179: 4850-4858.
- SCHETTLER, I. (1998): Tiefenhorizontierte Schadstoffverteilung im Grundwasser eines Gaswerkstandorts (Testfeld Süd): Felderprobung von Multilevelpackersystemen und Laborversuche zur Eignung von Probenahmeschläuchen.- Diplomarbeit am Lehrstuhl für Angewandte Geologie, Geologisches Institut der Universität Tübingen.
- SCHIEDEK, TH., GRATHWOHL, P., TEUTSCH, G.(1998): Natural attenuation and plume length of organic contaminants. in: E.G.S.: Annales Geophysicae, Part II: Hydrology, Oceans & Atmosphere. 16(II): C489.
- SCHMID, A., ROTHE, B., ALTENBUCHNER, J., LUDWIG, W., ENGESSER, K. H. (1997): Characterization of three distinct extradiol dioxygenases involved in mineralization of Dibenzofuran by *Terrabacter* sp. strain DPO360.- *J. Bacteriol.* 179: 53-62.
- SCHWARZ, R., Ptak, Th.,Holder, Th., Teutsch , G. (1998): Groundwater risk assessment at contaminated sites: a new approach for the inversion of contaminant concentration data measured at pumping wells. - in: Herbert, M., Kovar, K. (Eds.) (1998): Proc. GQ '98 Conf., Tübingen, Germany, September 1998. IAHS Publ. no. 250. 68-71.
- SCHWARZENBACH, R. P., GSCHWEND, P. M., IMBODEN, D. M. (1996): Environmental organic chemistry. John Wiley & Sons, New York. 681.
- SELIFONOV, S. A., CHAPMAN, P. J., AKKERMAN, S. B., GURST, J. E., BORTIATYNSKI, J. M., NANNY, M. A., HATCHER, P. G. (1998): Use of ¹³C nuclear magnetic resonance to assess fossil fuel biodegradation: Fate of [¹³C]Acenaphthene in creosote polycyclic aromatic compound mixtures degraded by bacteria. - *Appl. Environ. Microbiol.* 64: 1447-1453.
- SIMS, R. C., OVERCASH, M. R. (1983): Fate of polynuclear aromatic compounds (PNAs) in soil-plant systems. - *Residue Reviews*, 88, Springer, New York. 1-68.
- SONTHEIMER, H., CORNEL, P., SEYM, M. (1983): Untersuchungen zur Sorption von aliphatischen Chlorkohlenwasserstoffen durch Böden aus Grundwasserleitern. - *Veröffentl. des Ber. und Lehrstuhls für Wasserchemie und DVGW-Forschungsstelle am Engler-Bunte Institut*, 21: 1-46, Karlsruhe.
- STARKE, U., HERBERT, M., EINSELE, G.(1991): Polyzyklische aromatische Kohlenwasserstoffe (PAK) in Boden und Grundwasser. - in: Rosenkranz, D., Einsele, G., Harreß, H.-M. (Hsg.) (1991): Bodenschutz. Ergänzbare Handbuch der Maßnahmen und Empfehlungen für Schutz, Pflege und Sanierung von Böden, Landschaft und Grundwasser. - Erich Schmidt Verlag, 1-37.
- STEINER, D., BURTSCHER, H. K. (1994): Desorption of Perylene from combustion, NaCl and carbon particles. - *Environ, Sci. Technol.* 28: 1254-1259.
- STUART-KEIL, K. G., HOHNSTOCK, A. M., DREES, K. P., HERRICK, J. B., MADSEN, E. L. (1998): Plasmids responsible for horizontal transfer of Naphthalene catabolism genes between bacteria at a coal tar-contaminated site. - *Appl. Environ. Microbiol.* 64: 3633-3640.
- STUMM, W., MORGAN, J.J. (1996): Aquatic chemistry. Chemical equilibria and rates in natural waters. Wiley Interscience. 1022.
- STURMANN, P. J., STEWART, P. S., CUNNINGHAM, A. B., BOUWER, E. J., WOLFRAM, J. H. (1995): Engineering scale-up of in situ bioremediation processes: a review. - *J. Cont. Hydrol.* 19: 171-203.
- TAY, S. T.-L., HEMOND, H. F., POLZ, M. F., CAVANAUGH, C. M., DEJESUS, I., KRUMHOLZ, L. R. (1998): Two New *Mycobacterium* strains and their role in Toluene degradation in a contaminated stream. - *Appl. Environ. Microbiol.* 64: 1715-1720.

- TEUTSCH, G.; HOLDER, TH., PTAK, TH., SCHWARZ, R. (1998): Ein neues Verfahren zur Grundwasser-Immissionsbestimmung an kontaminierten Standorten. *Grundwasser*.
- TSAO, C.-W., SONG, H.-G., BARTHA, R. (1998): Metabolism of Benzene, Toluene and Xylene hydrocarbons in soil. - *Appl. Environ. Microbiol.* 64: 4924-4929.
- UMVELTMINISTERIUM (1993): Gemeinsame Verwaltungsvorschrift des Umweltministeriums und des Sozialministeriums über Orientierungswerte für die Bearbeitung von Altlasten und Schadensfälle. - GABI vom 30. November. 1115-1123.
- U.S. EPA, Office of Solid Waste and Emergency Response (1999): Use of monitored natural attenuation at superfund, RCRA corrective action, and underground storage tank sites. - Directive 9200.-17P, April 1999. 32.
- VERHAAR, H. K. M., BUSSER, F. J. M., HERMENS, J. L. M. (1995): Surrogate parameter for the baseline toxicity content of contaminated water: simulating the bioconcentration of mixtures of pollutants and counting molecules.- *Environ. Sci. Technol.* 29: 726-734.
- VERSCHUEREN, K. (1996): Handbook of environmental data on organic chemicals. Van Nostrand Reinhold, New York.
- WALTHERS, R. W., LUTHY, R. G. (1984): Equilibrium adsorption of polycyclic aromatic hydrocarbons from water onto activated carbon. - *Environ. Sci. Technol.* 30: 1589-1595.
- WEIB, H. (1998): Säulenversuche zur Gefahrenbeurteilung für das Grundwasser an PAK-kontaminierten Standorten. - Tübinger Geowissenschaftliche Arbeiten (TGA) Reihe C, 45. 111.
- WELTY, J. R., WICKS, C. E., WILSON, R. E. (1969): Fundamentals of momentum, heat and mass transfer. John Wiley, New York.
- WORLD WILDLIFE FUND (1999): Persistent organic pollutants: hand-me-down poisons that threaten wildlife and people.

Internet sites and databases:

ChemFinder: <http://www.chemfinder.com>

Environmental Science Center of Syracuse Research Corporation (SRC), Experimental log Kow database: <http://esc.syrres.com>

Greenpeace International Toxic Campaign: <http://www.greenpeace.org/ctox.html>

Occupational Health and Safety - Material Safety Data Sheets: <http://www.msdssearch.com>

United Nations Environmental Programme' POP (persistent organic pollutants) page: <http://irpct.unep.ch/pops>

U.S. National Library of Medicine, Hazardous Substances Database: <http://toxnet.nlm.nih.gov>

World Wildlife Fund's Global Toxic initiative: <http://www.worldwildlife.org/toxics>

Appendices

Appendix I: Main organisations involved in reviewing or evaluating toxicological data on organic chemicals

International organizations

- European Centre for Ecotoxicology and Toxicology of Chemicals (ECETOC)
- European Community (EC)
 - Classification and Labelling of Dangerous Substances
 - Occupational Exposure Limit Values
 - Ad-Hoc Group on Dangerous Chemicals, Carcinogens
- International Agency for Research on Cancer (IARC)
- International Programme on Chemical Safety (IPCS)
- Nordic Expert Group for Documentation of Occupational Exposure Limits (NEG)

Federal Republic of Germany

- Berufsgenossenschaft der Chemischen Industrie (BG Chemie)
- Beratergremium für Umweltrelevante Altstoffe (BUA)
- Senatskommission der Deutschen Forschungsgemeinschaft zur Prüfung Gesundheitsschädlicher Arbeitsstoffe (MAK Kommission)
- Verband der Chemischen Industrie (VCI)

Netherlands

- Gezondheidsraad (GR)
- Rijksinstituut voor Volksgezondheid en Milieuhygiene (RIVM)
- Werkgroep van Deskundigen (WGD)

Sweden

- Kriterigruppen for Hygieniska Gransvarden (KHG)

United Kingdom

- The British Industrial Biological Research Association (BIBRA)
- Health and Safety Executive (HSE)

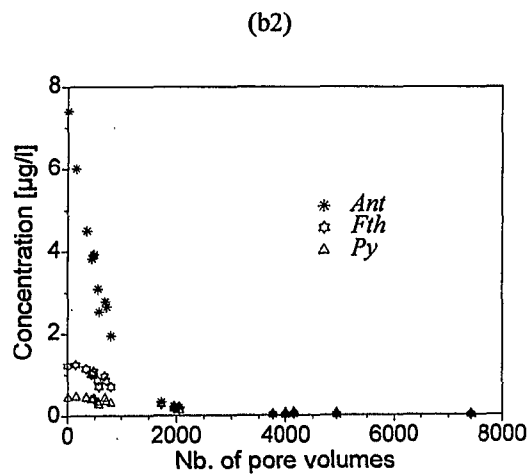
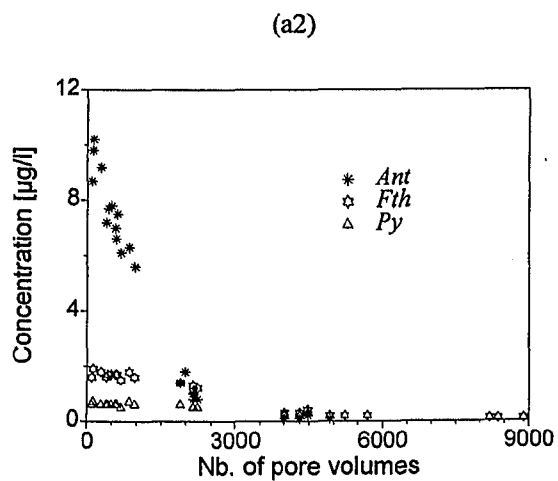
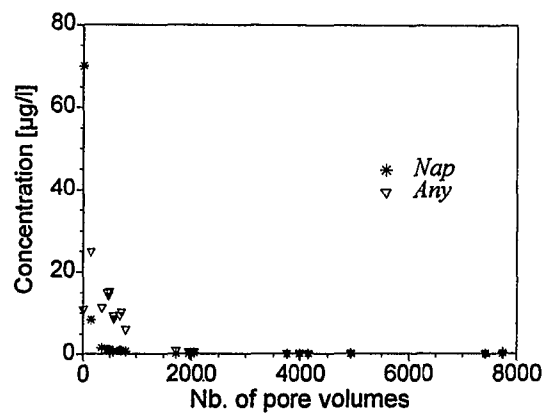
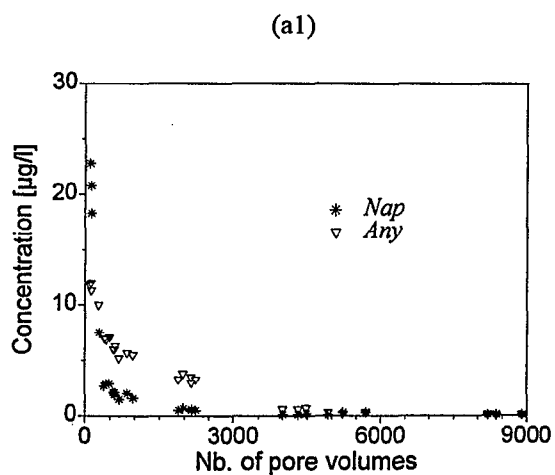
United States of America

- American Conference of Governmental Industrial Hygienists (ACGIH)
- Agency for Toxic Substances and Disease Registry (ATSDR)
- Environmental Protection Agency (EPA)
 - Office of Toxic Substances (OTS)
 - Environmental Criteria and Assessment Office
- National Institute for Occupational Safety and Health (NIOSH)
- Cosmetic Ingredient Review (CIR)

Appendix II: Substances identified at 'Testfeld Süd'

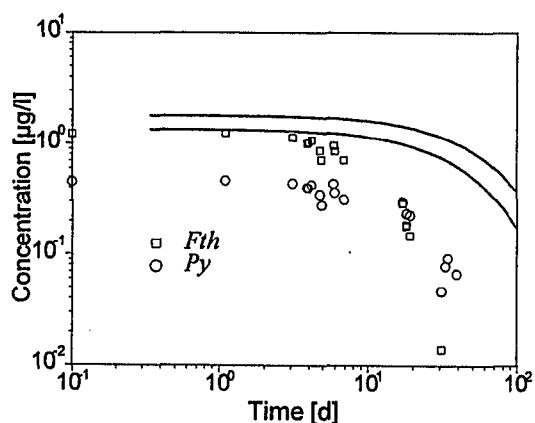
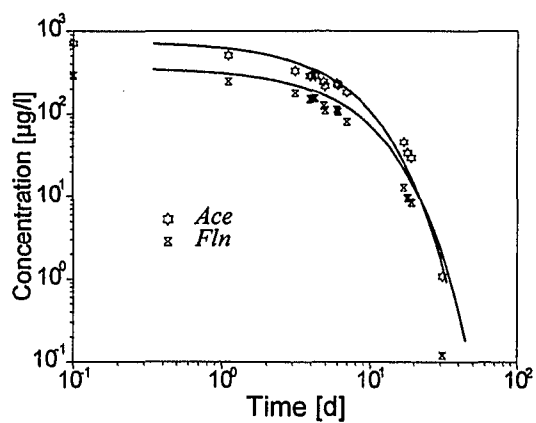
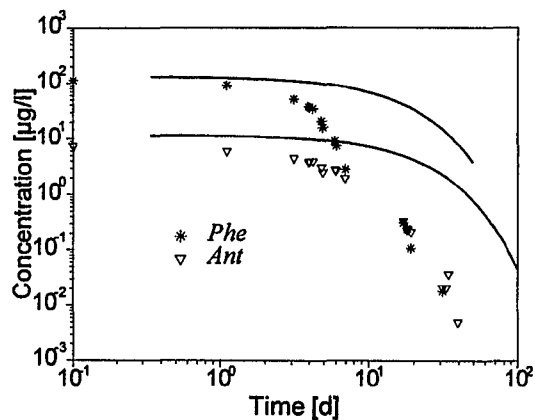
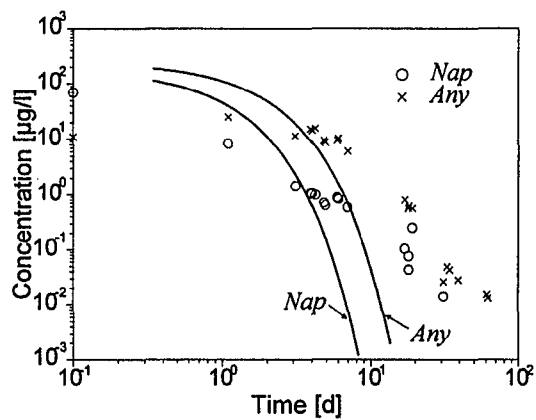
Substance	m/z ⁺ (Target Ion)	Nb. of isomers
Polycyclic aromatic hydrocarbons (16 EPA)		
Naphthalene	128	1
Acenaphthylene	152	1
Acenaphthene	154	1
Fluorene	166	1
Phenanthrene	178	1
Anthracene	178	1
Fluoranthene	202	1
Pyrene	202	1
Benzo(a)anthracene	228	1
Chrysene	228	1
Benzo(b)fluoranthene	252	1
Benzo(k)fluoranthene	252	1
Benzo(a)pyrene	252	1
Dibenzo(a,h)anthracene	278	1
Indeno(1,2,3-cd)pyrene	276	1
Benzo(g,h,i)perylene	276	1
Other PAH		
Indane	117	1
Methylindane	117	2
Dimethylindane	131	5
Indene	115	1
Methylindene	130	2
Dimethylindene	129	5
1- and 2-Methylnaphthalene	142	1+1
Dimethylnaphthalene	142	3
Ethyl-naphthalene	141	1
Trimethylnaphthalene	155	5
Monoaromatic hydrocarbons		
Benzene	78	1
Toluene	91	1
o- and p-Xylene	106	1+1
Ethylbenzene	106	1
Propylbenzene	105	1
Isopropylbenzene	105	1
1,2,3-Trimethylbenzene	120	1
1,2,4- Trimethylbenzene	120	1
1,3,5- Trimethylbenzene	120	1
Heterocyclic aromatic compounds		
Thiophene	84	1
Trimethylthiopene	126	1
Benzofuran	118	1
Methylbenzofuran	131	3
Dimethylbenzofuran	145	2
Dibenzofuran	168	1
Methyl-dibenzofuran	182	1
Benzo-thiophene	134	1
Carbazole	167	1
Acridine	179	1
Xanthene	182	1
Thioxanthene	197	1
Other (presumably metabolites)		
Methylindanol	133	1
Tetramethylindanone	173	1
Methylnaphthol	158	2
Dihydro-trimethyl-naphthalenone	173	2
Acridone	195	1
Methylquinolinol/-one	159	3

Appendix III: PAHs concentrations in the column leachate, samples B55C1 (a) and B55C2 (b).

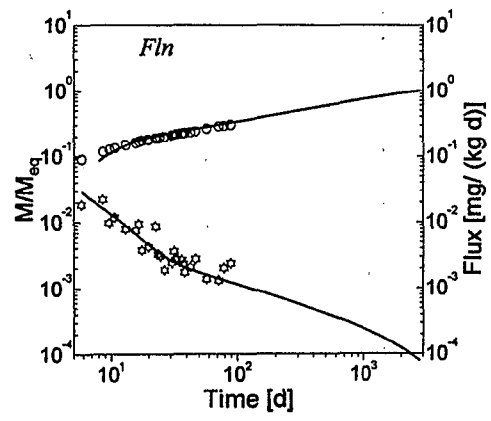
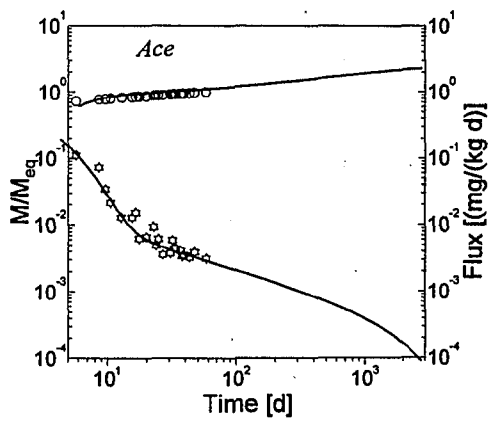


(b1)

Appendix IV: Measured (symbols) versus calculated concentrations (curves) during dissolution for the column B55C2. The calculated curves are those shown for all PAHs in Fig. 5.8 (b).



Appendix V: Desorption kinetics modelling for Ace and Fln out of disturbed aquifer material from 'Testfeld Süd' (B56 8.05 m - 8.4 m)



Appendix VI: Sampling points in the multilevel groundwater wells at 'Testfeld Süd' (after SCHETTLER, 1998)

Groundwater Well	Sampling Point	Depth [m]	Groundwater Well	Sampling Point	Depth [m]
B44	1	7.90	B54	1	7.48
	2	7.25		2	7.13
	3	6.25		3	6.53
	4	5.46		4	6.13
				5	5.53
				6	5.13
				7	4.53
				8	4.13
B47	1	6.82	B55	1	8.04
	2	6.37		2	7.59
	3	5.87		3	7.09
	4	5.37		4	6.44
	5	4.82		5	5.69
		6		5.09	
		7		4.59	
		8		4.04	
B49	1	6.99	B56	1	8.16
	2	6.19		2	7.61
	3	5.29		3	7.11
	4	4.49		4	6.71
		5		6.11	
		6		5.61	
		7		5.06	
B53	1	7.18	B57	1	7.52
	2	6.68		2	7.07
	3	6.18		3	6.57
	4	5.68		4	6.07
	5	5.18		5	5.57
	6	4.63		6	5.02

In der Reihe C der Tübinger Geowissenschaftlichen Arbeiten (TGA) sind bisher erschienen:

- Nr. 1: Grathwohl, Peter (1989): Verteilung unpolarer organischer Verbindungen in der wasserungesättigten Bodenzone am Beispiel der leichtflüchtigen aliphatischen Chlorkohlenwasserstoffe. 102 S.
- Nr. 2: Eisele, Gerhard (1989): Labor- und Felduntersuchungen zur Ausbreitung und Verteilung leichtflüchtiger chlorierter Kohlenwasserstoffe (LCKW) im Übergangsbereich wasserungesättigte/wassergesättigte Zone. 84 S.
- Nr. 3: Ehmann, Michael (1989): Auswirkungen atmogener Stoffeinträge auf Boden- und Grundwasser sowie Stoffbilanzierungen in drei bewaldeten Einzugsgebieten im Oberen Buntsandstein (Nordschwarzwald). 134 S.
- Nr. 4: Irouschek, Thomas (1990): Hydrogeologie und Stoffumsatz im Buntsandstein des Nordschwarzwaldes. 144 S.
- Nr. 5: Sanns, Matthias (1990): Experimentelle Untersuchungen zum Ausbreitungsverhalten von leichtflüchtigen Chlorkohlenwasserstoffen (LCKW) in der wassergesättigten Zone. 122 S. **(Vergriffen!)**
- Nr. 6: Seeger, Thomas (1990): Abfluß- und Stofffrachtseparation im Buntsandstein des Nordschwarzwaldes. 154 S.
- Nr. 7: Einsele, Gerhard & Pfeffer, Karl-Heinz (Hrsg.) (1990): Untersuchungen über die Auswirkungen des Reaktorunfalls von Tschernobyl auf Böden, Klärschlamm und Sickerwasser im Raum von Oberschwaben und Tübingen. 151 S.
- Nr. 8: Douveas, Nikon G. (1990): Verwitterungstiefe und Untergrundabdichtung beim Talsperrenbau in dem verkarsteten Nord-Pindos-Flysch (Projekt Pigai-Aoos, NW-Griechenland). 165 S.
- Nr. 9: Schlöser, Heike (1991): Quantifizierung der Silikatverwitterung in karbonatfreien Deckschichten des Mittleren Buntsandsteins im Nordschwarzwald. 93 S.
- Nr. 10: Köhler, Wulf-Rainer (1992): Beschaffenheit ausgewählter, nicht direkt anthropogen beeinflusster oberflächennaher und tiefer Grundwasservorkommen in Baden-Württemberg. 144 S.
- Nr. 11: Bundschuh, Jochen (1991): Der Aquifer als thermodynamisch offenes System. – Untersuchungen zum Wärmetransport in oberflächennahen Grundwasserleitern unter besonderer Berücksichtigung von Quellwassertemperaturen (Modellversuche und Geländebeispiele). 100 S.
- Nr. 12: Herbert, Mike (1992): Sorptions- und Desorptionsverhalten von ausgewählten polyzyklischen aromatischen Kohlenwasserstoffen (PAK) im Grundwasserbereich. 111 S.
- Nr. 13: Sauter, Martin (1993): Quantification and forecasting of regional groundwater flow and transport in a karst aquifer (Gallusquelle, Malm, SW-Germany). 150 S.
- Nr. 14: Bauer, Michael (1993): Wasserhaushalt, aktueller und holozäner Lösungsabtrag im Wutachgebiet (Südschwarzwald). 130 S.
- Nr. 15: Einsele, Gerhard & Ricken, Werner (Hrsg.) (1993): Eintiefungsgeschichte und Stoffaustag im Wutachgebiet (SW-Deutschland). 215 S.

- Nr. 16: Jordan, Ulrich (1993): Die holozänen Massenverlagerungen des Wutachgebietes (Süd-schwarzwald). 132 S.
- Nr. 17: Krejci, Dieter (1994): Grundwasserchemismus im Umfeld der Sonderabfalldeponie Billigheim und Strategie zur Erkennung eines Deponiesickerwassereinflusses. 121 S.
- Nr. 18: Hekel, Uwe (1994): Hydrogeologische Erkundung toniger Festgesteine am Beispiel des Opalinustons (Unteres Aalenium). 170 S.
- Nr. 19: Schüth, Christoph (1994): Sorptionskinetik und Transportverhalten von polyzyklischen aromatischen Kohlenwasserstoffen (PAK) im Grundwasser - Laborversuche. 80 S.
- Nr. 20: Schlöser, Helmut (1994): Lösungsgleichgewichte im Mineralwasser des überdeckten Muschelkalks in Mittel-Württemberg. 76 S.
- Nr. 21: Pyka, Wilhelm (1994): Freisetzung von Teerinhaltsstoffen aus residualer Teerphase in das Grundwasser: Laboruntersuchungen zur Lösungsrate und Lösungsvermittlung. 76 S.
- Nr. 22: Biehler, Daniel (1995): Kluftgrundwässer im kristallinen Grundgebirge des Schwarzwaldes – Ergebnisse von Untersuchungen in Stollen. 103 S.
- Nr. 23: Schmid, Thomas (1995): Wasserhaushalt und Stoffumsatz in Grünlandgebieten im württembergischen Allgäu. 145+ 92 S.
- Nr. 24: Kretzschmar, Thomas (1995): Hydrochemische, petrographische und thermodynamische Untersuchungen zur Genese tiefer Buntsandsteinwässer in Baden-Württemberg. 142 S. **(Vergriffen!)**
- Nr. 25: Hebestreit, Christoph (1995): Zur jungpleistozänen und holozänen Entwicklung der Wutach (SW-Deutschland). 88 S.
- Nr. 26: Hinderer, Matthias (1995): Simulation langfristiger Trends der Boden- und Grundwasser- versauerung im Buntsandstein-Schwarzwald auf der Grundlage langjähriger Stoffbilanzen. 175 S.
- Nr. 27: Körner, Johannes (1996): Abflußbildung, Interflow und Stoffbilanz im Schönbuch Waldgebiet. 206 S.
- Nr. 28: Gewalt, Thomas (1996): Der Einfluß der Desorptionskinetik bei der Freisetzung von Trichlorethen (TCE) aus verschiedenen Aquifersanden. 67 S.
- Nr. 29: Schanz, Ulrich (1996): Geophysikalische Untersuchungen im Nahbereich eines Karstsystems (westliche Schwäbische Alb). 114 S.
- Nr. 30: Renner, Sven (1996): Wärmetransport in Einzelklüften und Kluftaquiferen – Untersuchungen und Modellrechnungen am Beispiel eines Karstaquifers. 89 S.
- Nr. 31: Mohrlök, Ulf (1996): Parameter-Identifikation in Doppel-Kontinuum-Modellen am Beispiel von Karstaquiferen. 125 S.
- Nr. 32: Merkel, Peter (1996): Desorption and Release of Polycyclic Aromatic Hydrocarbons (PAHs) from Contaminated Aquifer Materials. 76 S.
- Nr. 33: Schiedek, Thomas (1996): Auftreten und Verhalten von ausgewählten Phthalaten in Wasser und Boden. 112 S.

- Nr. 34: Herbert, Mike & Teutsch, Georg (Hrsg.) (1997): Aquifersysteme Südwestdeutschlands - Eine Vorlesungsreihe an der Eberhard-Karls-Universität Tübingen. 162 S.
- Nr. 35: Schad, Hermann (1997): Variability of Hydraulic Parameters in Non-Uniform Porous Media: Experiments and Stochastic Modelling at Different Scales. 233 S.
- Nr. 36: Herbert, Mike & Kovar, Karel (Eds.) (1998): GROUNDWATER QUALITY 1998: Remediation and Protection - Posters -.- Proceedings of the GQ'98 conference, Tübingen, Sept. 21-25, 1998, Poster Papers. 146 S.
- Nr. 37: Klein, Rainer (1998): Mechanische Bodenbearbeitungsverfahren zur Verbesserung der Sanierungseffizienz bei In-situ-Maßnahmen. 106 S.
- Nr. 38: Schollenberger, Uli (1998): Beschaffenheit und Dynamik des Kiesgrundwassers im Neckartal bei Tübingen. 74 S.
- Nr. 39: Rügner, Hermann (1998): Einfluß der Aquiferlithologie des Neckartals auf die Sorption und Sorptionskinetik organischer Schadstoffe. 78 S.
- Nr. 40: Fechner, Thomas (1998): Seismische Tomographie zur Beschreibung heterogener Grundwasserleiter. 113 S.
- Nr. 41: Kleineidam, Sybille (1998): Der Einfluß von Sedimentologie und Sedimentpetrographie auf den Transport gelöster organischer Schadstoffe im Grundwasser. 82 S.
- Nr. 42: Hückinghaus, Dirk (1998): Simulation der Aquifergenese und des Wärmetransports in Karstaquiferen. 124 S.
- Nr. 43: Klingbeil, Ralf (1998): Outcrop Analogue Studies – Implications for Groundwater Flow and Contaminant Transport in Heterogeneous Glaciofluvial Quaternary Deposits. 111 S.
- Nr. 44: Loyek, Diana (1998): Die Löslichkeit und Lösungskinetik von polyzyklischen aromatischen Kohlenwasserstoffen (PAK) aus der Teerphase. 81 S.
- Nr. 45: Weiß, Hansjörg (1998): Säulenversuche zur Gefahrenbeurteilung für das Grundwasser an PAK-kontaminierten Standorten. 111 S.
- Nr. 46: Jianping Yan (1998): Numerical Modeling of Topographically-closed Lakes: Impact of Climate on Lake Level, Hydrochemistry and Chemical Sedimentation. 144 S.
- Nr. 47: Finkel, Michael (1999): Quantitative Beschreibung des Transports von polyzyklischen aromatischen Kohlenwasserstoffen (PAK) und Tensiden in porösen Medien. 98 S.
- Nr. 48: Jaritz, Renate (1999): Quantifizierung der Heterogenität einer Sandsteinmatrix (Mittlerer Keuper, Württemberg). 106 S.
- Nr. 49: Danzer, Jörg (1999): Surfactant Transport and Coupled Transport of Polycyclic Aromatic Hydrocarbons (PAHs) and Surfactants in Natural Aquifer Material - Laboratory Experiments. 75 S.
- Nr. 50: Dietrich, Peter (1999): Konzeption und Auswertung gleichstromgeoelektrischer Tracerversuche unter Verwendung von Sensitivitätskoeffizienten. 130 S.
- Nr. 51: Baraka-Lokmane, Salima (1999): Determination of Hydraulic Conductivities from Discrete Geometrical Characterisation of Fractured Sandstone Cores. 119 S.

Nr. 52: M^cDermott, Christopher I. (1999): New Experimental and Modelling Techniques to Investigate the Fractured System. 170 S.



ATTEMPTO SERVICE GmbH
Wilhelmstraße 7 · 72074 Tübingen